Aus der Abteilung für Klinische Pharmakologie
Leiter: Prof. Dr. med. S. Endres

Medizinischen Klinik und Poliklinik IV
Klinikum der Universität
Ludwig-Maximilians-Universität München

Direktor: Prof. Dr. med. M. Reincke

The Influence of the Chemokine CCL22 on Tumor Development and Growth

Dissertation

zum Erwerb des Doktorgrades
der Naturwissenschaften
an der Medizinischen Fakultät
der Ludwig-Maximilians-Universität München

vorgelegt von
Moritz Rapp
aus Rosenheim

2013

Gedruckt mit Genehmigung der Medizinischen Fakultät
der Ludwig-Maximilians-Universität München

Betreuerin: Prof. Dr. med. Dr. rer. nat. Carole Bourquin

Zweitgutachter: Prof. Dr. Peter Nelson

Mitbetreuung durch die promovierten Mitarbeiter:

Dr. med. David Anz und Prof. Dr. med. Stefan Endres

Dekan: Prof. Dr. med. Dr. h.c. M. Reiser, FACR, FRCR

Tag der mündlichen Prüfung: 13.12.2013

Dedicated to Anna, my parents Sybille and Eugen,

my sister Genoveva and my brother-in-law Attila.

Erklärung nach § 7 Abs. 4 der Promotionsordnung vom 16. Juli 2010

Hiermit versichere ich, dass diese Dissertation selbstständig angefertigt wurde, ich mich außer den angegebenen Hilfsmitteln keiner weiteren bedient habe und alle Erkenntnisse, die aus dem Schrifttum ganz oder annähernd übernommen wurden, als solche kenntlich gemacht und nach ihrer Herkunft unter Bezeichnung der Fundstelle einzeln nachgewiesen sind.

Des Weiteren versichere ich, dass die hier vorgelegte Dissertation nicht in gleicher oder in ähnlicher Form bei einer anderen Stelle zur Erlangung eines akademischen Grades eingereicht wurde.

München, 28.01.2013

.....
Moritz Rapp

Table of Contents

Introduction

1. Introduction

1.1 Tumor immunology

According to the World Health Organization, cancer was the third leading cause of death in high-income countries in 2008 (source: WHO, list of leading causes of death 2008). The first and second leading cause of death were cardiovascular and cerebrovascular diseases, respectively. In recent years the therapy of infectious diseases and cardiovascular diseases strongly improved, thereby increasing remarkably the average life expectancy in countries with modern medical care. In contrast, the incidences of nearly all types of cancer dramatically increased in the last decades in these countries. According to the American Cancer Society, the increase in cancer incidences is mostly due to the demographic changes in Western countries (source: American Cancer Society, cancer facts & figures 2012). Therefore, efficient treatment of cancer has become one of the most important challenges for modern medicine.

Cancer always derives from a single initially harmless cell. After accumulating several mutations, this cell can give rise to a tumor, a process called malignant transformation. In order to become a tumor, tumor cells must gain certain abilities such as the independence from growth factors and immortalisation. In the past decades it became clear that in addition the tumor cells must acquire mechanisms to circumvent immune surveillance in order to develop to a clinically relevant tumor. Cancer development is thought to be a dynamic process which is accompanied by immunoediting. This process is divided in the three phases: elimination, equilibrium and escape (Dunn *et al.,* 2002, 2004). In the first phase, also called immune surveillance (Burnet, 1970), potential tumor cells are recognized and killed by the immune system. The second phase, the equilibrium, follows if some degenerated cells survived the first phase. As a consequence of selection imposed by the immune system these cells accumulate mutations and intracellular changes that promote their survival and suppress their killing. If one of these cells has gathered enough mutations to escape immune surveillance, the final phase is reached. In this phase the selected tumor cell can grow and cause clinically apparent cancers (Shankaran *et al.,* 2001).

One of the major difficulties of cancer therapy is that all tumor cells must be removed and destroyed to cure a patient because even one remaining tumor cell can grow again to a lethal tumor. The standard treatment of cancer today is surgery, chemotherapy and radiation. Although these clinical methods became more effective in the last decades, a complete tumor remission and thereby associated long time survival of the patients is usually not guaranteed.

In the last few years cancer immunotherapy has become more and more promising as fourth possibility of treating tumor patients. The fundamental idea of immunotherapy is to reprogram the immune system in order to induce an effective immune response against an established tumor.

In untreated tumor-bearing patients, T cells specifically directed against tumor cells can be found. These T cells express T cell receptors (TCRs) that recognize certain tumor-specific tumor-associated antigens (TAAs). TAAs are antigens that generally are expressed exclusively by cancer cells and not by other healthy tissue cells. Such antigens develop in tumor cells due to inappropriate protein expression or mutated proteins that generate novel epitopes (Williamson *et al.,* 2006). For example, in many tumors a mutation of the cell cycle molecule p53 generates a novel antigen epitope which in turn is only presented by these tumor cells (Mayordomo *et al.,* 1996). Indeed, cytotoxic T cells, specific for certain TAAs and thereby capable of tumor cell killing, can be found in the tumor tissue of many patients. High tumor infiltration rates of these cells are often associated with better survival rates of the patients (Naito *et al.,* 1998).

Nevertheless, since immune-mediated spontaneous rejections of established tumors are rare, TAA specific cytotoxic T cells generally fail to eliminate the tumor. This implies that the tumor can develop mechanisms to evade an effective immune response. Today, there are many mechanisms known to contribute to this evasion. For example, tumors can produce immunosuppressive cytokines such as transforming growth factor-beta (TGF-β) that suppresses cell-mediated immunity (Tada *et al.,* 1991). Another way in which the tumor can block an anti-tumor immune response is by recruiting regulatory T cells (Tregs). These cells are known to suppress the function of other

immune cells such as cytotoxic T cells and thereby block anti-cancer immunity (Betts *et al.,* 2006). Increased numbers of Tregs have been found in the blood and the lymph nodes of tumor patients (Colombo *et al.,* 2007) as well as in the tissue of several human tumors (Betts *et al.,* 2006). In the last years it was shown that high numbers of tumor-infiltrating Tregs are associated with poor prognosis for tumor patients (Curiel *et al.,* 2005; Gobert *et al.,* 2009). Thus, manipulating the balance between intratumoral Tregs and cytotoxic T cells seems to be a promising new target for cancer therapy.

The advantage of using the host immune system for destroying cancer cells in patients is the potential detection and elimination of even single tumor cells in almost every part of the human body. In contrast to chemotherapy, an immune system mediated tumor cell killing could be very specific and side effects could be reduced. However, the human immune system is very complex and manipulating its mode of action is challenging and could be dangerous. One prominent example, demonstrating the risks of immune therapy, is the phase 1 clinical trial of the anti-CD28 monoclonal antibody TGN1412. This antibody was intended for the treatment against B cell chronic lymphocytic leukemia and rheumatoid arthritis. After successful trials in mice and monkeys the antibody was used for a phase 1 trial in human volunteers. Instead of mild effects in healthy donors, as predicted, strong side effects caused by a cytokine storm were observed in all test persons (Suntharalingam *et al.,* 2006).

Nevertheless, exploiting immune regulation is very promising and has great potential for treating many human diseases including tumors. Currently, there are many immune regulating drugs in clinical trials or even on the market. One example are antibodies directed against cellular receptors that regulate cell proliferation such as cetuximab, a monoclonal antibody directed against epidermal growth factor receptors (EGFR). This antibody is used to treat colorectal cancer (Karapetis *et al.,* 2008) and head and neck cancer (Bonner *et al.,* 2010). CTLA-4 blocking antibody is another example for generating an effective anti-tumor immune response in patients. It inhibits Treg function and prevents inactivation of activated effector T cells. Thereby, anti-CTLA-4 antibody treatment reduced cancer progression in

patients with metastatic melanoma (Hodi *et al.,* 2011; Phan *et al.,* 2003).

Another approach of clinically applied immunotherapy is the adoptive transfer of T cells. Therefore, T cells from tumor-bearing patients are isolated, selected for tumor-specific cytotoxic T cells, expanded *ex vivo* and finally re-injected into the patient (Rosenberg *et al.,* 1994; June, 2007).

1.2 Regulatory T cells and tumor immunity

1.2.1 Regulatory T cell subsets and function

In general, there are two main subtypes of regulatory T cells (Tregs) in mice and humans. These two subtypes are natural Tregs (nTregs) and induced Tregs (iTregs). Both express forkhead box p3 (FOXP3), a transcription factor that is required for suppressive function. Natural Tregs develop in the thymus from CD4+ thymocytes. In contrast to conventional T cells, nTregs are selected in the thymus by high-affinity binding to a self antigens. Thus, nTregs express TCRs against self antigens. On the other hand, iTregs develop in the periphery from uncommitted conventional CD4+ T cells. This second Treg subset is a heterogeneous group that consists of at least three distinct subgroups. Most of the iTregs found in the periphery belong to the first subgroup. These cells develop through the conversion of conventional T cells into iTregs induced by TGF-β, IL-2 and APCs that express low dose of antigen in the absence of co-stimulatory molecules. The second subgroup of iTregs, the T_R1 cells, are induced by high concentrations of IL-10 and secrete TGF-β and IL-10 after differentiation. T_H3 cells represent the third subgroup. These cells seem to be induced by TGF-β and can be found in the mucosal immune system.

To differentiate Tregs from other T cell subsets, many cell surface markers as well as intracellular markers have been identified in the last decade. In mice the most important Treg marker is the transcription factor FOXP3 (Hori *et al.,* 2003). Human Tregs also express FOXP3, but in contrast to mice many human conventional T cells without suppressive function up-regulate FOXP3 upon activation (Allan *et al.*, 2007). Beside the intracellular marker FOXP3, Tregs are also defined by high expression of the surface marker interleukin-2 receptor

α-chain (CD25), cytotoxic T lymphocyte-associated antigen 4 (CTLA-4), glucocorticoid-induced tumor necrosis factor receptor family-related gene (GITR) and lymphocyte activation gene-3 (LAG-3) as well as low expression of CD127.

By definition the main function of Tregs is to regulate the function of other immune cells. Tregs are needed to prevent autoimmunity by eliminating self reactive T cells that survived thymic selection, a process called peripheral tolerance (Sakaguchi, 2005). In addition, Tregs are required to prevent overwhelming immune responses against invading pathogens. To execute all these tasks, Tregs have a variety of mechanisms to control other immune cells.

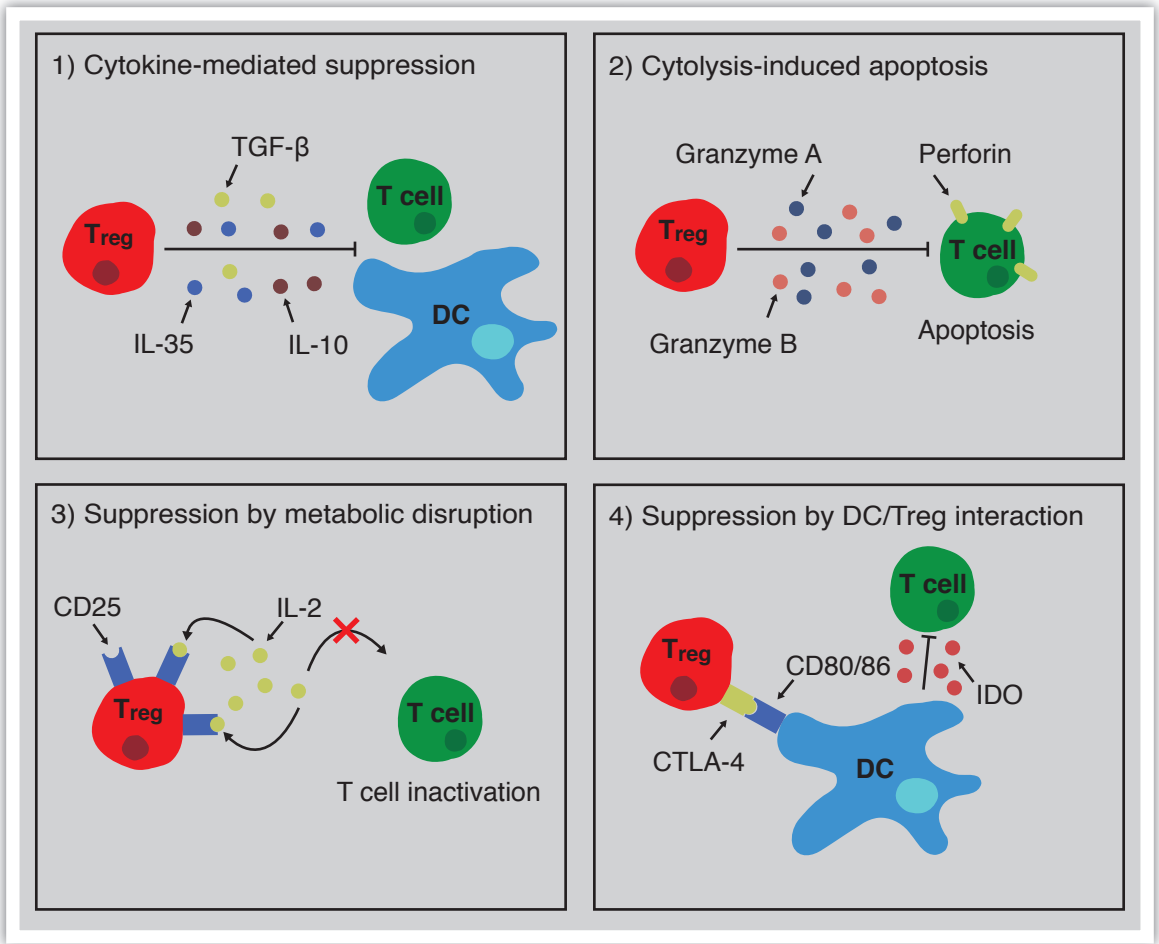

Figure 1: Mechanisms of Treg suppression. The illustration shows the modes of Treg suppression. First, Tregs can suppress DCs and T cells by secreting inhibitory cytokines. Second, Tregs release granzyme A and B as well as perforin to induce apoptosis in target cells. Third, CD25 expressed on the surface of Tregs can bind IL-2 and thereby deplete IL-2. Since IL-2 is needed by activated T cells for survival depletion of IL-2 leads to T cell inactivation. Fourth, Tregs mediate suppression by interaction with activated DCs. CTLA-4 expressed on the surface of Tregs binds with high affinity to the DC co-stimulatory receptors CD80 and CD86. Thereby T cells activation by CD80 and CD86 is blocked. In addition, CTLA-4 binding induces IDO expression by DCs which in turn suppresses T cells. [Figure is adapted from an illustration published by Vignali *et al.*, 2008]

The mechanisms of Treg action can be divided in four categories (*Figure 1*). First, Tregs can suppress immune cells such as dendritic cells (DCs), CD4+ and CD8+ effector cells by secreting inhibitory cytokines such as IL-10, IL-35 and TGF-β (Collison *et al.,* 2007; Letterio and Roberts, 1998; Hara *et al.,* 2001). The second mechanism of Treg-mediated immune regulation is the induced apoptosis via cytolysis. Such as cytotoxic T cells Tregs can express granzyme A and B as well as perforin (Grossman *et al.,* 2004). Suppression by metabolic disruption is the third mode of Treg action. For example, Tregs express high amounts of interleukin-2 receptor α-chain (CD25). CD25 can bind and thereby deplete local IL-2. This cytokine is needed by activated effector T cells for survival. Thus, depleting IL-2 leads to effector T cell inactivation (Thornton and Shevach, 1998). Finally, suppression by targeting dendritic cells is the fourth mode of Treg function. Unlike the other three mentioned mechanisms, this mechanism requires direct cell contact between Tregs and DCs. To interact with DCs, Tregs express high levels of CTLA-4. This surface molecule binds with high affinity to the co-stimulatory molecules CD80 and CD86, both being expressed by mature DCs. Thereby, Tregs prevent T cell activation by blocking and suppressing these co-stimulatory molecules (Read *et al.,* 2000; Cederbom *et al.,* 2000) and induce indoleamine 2,3-dioxygenase (IDO) release by DCs, which in turn initiates apoptosis in activated T cells (Fallarino *et al.,* 2003).

1.2.2 Regulatory T cells in murine and human tumors

In healthy persons Tregs are crucial for preventing autoimmune diseases and limiting immune responses against invading pathogens. Deficiency of FOXP3, a transcription factor essential for Treg development and function, induces a profound autoimmune-like lymphoproliferative disorder in mice and humans. Mice that lack FOXP3 are known as scurfy mice (Brunkow *et al.*, 2001). Humans carrying a loss-of-function mutation on the FOXP3 gene suffer from a disease called immune dysregulation, polyendocrinopathy, enteropathy, X-linked syndrome (IPEX) (Bennett *et al.*, 2001), a rare X-linked recessive genetic disorder. Since FOXP3 deficiency results in Treg defects, this severe disorders illustrate the importance of Tregs for maintaining immune homeostasis.

Nevertheless, due to their immune suppressive function, Tregs are often harmful for tumor-bearing patients. Regulatory T cells can be coopted by

tumor cells to escape immune surveillance. Thereby, an effective anti-tumor immune response is blocked and tumor development is promoted (Betts *et al.*, 2006). Since more and more Treg-specific markers were found (see above) in the last years, a reliable identification of these cells has become possible. With these markers a lot of progress has been made in investigating the role of Tregs in cancer patients. For instance, in many tumor-bearing patients increased amounts of Tregs were found in the blood and the lymph nodes (Colombo *et al.*, 2007) as well as in the tumor tissue itself (Betts *et al.*, 2006). In further experiments the functionality of these tumor-infiltrating Tregs was confirmed. By isolating these cells from freshly dissected murine and human tumors, their suppressive nature in regard to blocking effector T cell proliferation *in vitro* was clearly shown (Curiel *et al.*, 2004; Zhou *et al.*, 2006). These findings were also confirmed *in vivo*. As shown by Yu and colleagues in murine tumors, CD4+CD25+ Tregs actively suppress the proliferation of CD8+ cytotoxic T cells at the local tumor site and thereby promote tumor growth especially in later stages of tumor progression (Yu *et al.*, 2005). Consistent with the previous findings, high amounts of tumor-infiltrating Tregs are associated with poor prognosis and predict poor survival in human ovarian carcinoma and breast cancer (Curiel *et al.*, 2005; Gobert *et al.*, 2009).

1.2.3 Regulatory T cells as therapeutic target

According to the previously discussed findings Tregs seem to be a very promising target for anticancer therapy. Indeed, by reducing Treg function and/or intratumoral accumulation, therapeutic effects in tumor-bearing mice were observed. The therapeutic benefits of Treg depletion in tumor-bearing mice were first demonstrated by adoptive T cell transfer experiments in BALB/c athymic nude mice. Adoptively transferred CD25-depleted CD4+ cells, considered as non-Treg cells, into RL male 1 (BALB/c-derived radiation leukemia) tumor-bearing nude mice resulted in tumor regression. In contrast, nude mice treated with a non-depleted CD4+ T cell adoptive transfer died due to rapid tumor progression (Shimizu *et al.*, 1999). Similar results were observed in tumor-bearing mice treated with an anti-CD25 monoclonal antibody. In these experiments, antibody-mediated CD4+CD25+ Treg depletion induced tumor growth retardation in murine sarcoma and melanoma (Tanaka *et al.*, 2002). IL-2 immunotoxin-mediated Treg depletion is another approach

in mouse tumor models. This toxin mediates the depletion of all CD25+ T cells. Breast tumor growth of tumor-bearing mice treated with IL-2 immunotoxin was markedly inhibited (Knutson *et al.*, 2006). Another approach for reducing intratumoral accumulation of Tregs is to block the function of the surface receptor CCR4. The specific expression of CCR4 on Tregs makes this chemokine receptor a promising target for anti-tumor therapy. Indeed, CCR4 monoclonal antibody has the potential to inhibit tumor-directed Treg migration and thereby promote anti-tumor immunity (Ishida and Ueda, 2006).

In humans, Treg depletion can be achieved by the FDA-approved fusion protein Ontak (denileukin diftitox). Ontak is the human equivalent to murine IL-2 immunotoxin. This protein is a toxin consisting of IL-2 fused to diphtheria toxin. Ontak binds to all CD25+ cells via IL-2. After receptor binding the protein is internalized, inhibits protein synthesis and thereby induces apoptosis in all CD25+ cells (Foss, 2000). In patients with renal cell carcinoma (RCC) Ontak significantly reduced blood Treg numbers and improved tumor-specific T cell activation (Dannull *et al.*, 2005). However, a significant correlation of Treg depletion and tumor regression was not observed. This could be due to the fact that activated effector T cells up-regulate CD25 expression and thereby become susceptible for Ontak depletion. In conclusion the Ontak effectiveness for tumor therapy is still uncertain.

CTLA-4 blocking antibody is another approach for generating an effective anti-tumor immune response in human (Hodi *et al.*, 2011). This antibody has a dual effect. On the one hand it inhibits Treg function and on the other hand it prevents inactivation of activated effector T cells. In patients with metastatic melanoma anti-CTLA-4 antibody treatment reduced cancer progression. However, CTLA-4 blockade also induced potent autoimmune diseases such as dermatitis, hepatitis and hypophysitis (Phan *et al.,* 2003).

In contrast to anticancer therapy in mice, most therapies in humans show only slight effects for tumor regression and overall survival. Precise intratumoral Treg targeting is one of the major problems in boosting anti-tumor immunity in humans. In most approaches not only intratumoral Tregs are depleted, but also all other Tregs, which in turn evoke autoimmunity.

Another issue is the specificity of Treg targeting. Since precise human Treg markers are still missing, Treg depletion always involves the depletion of other anti-tumor immunity promoting immune cells. In conclusion, new therapeutic approaches must be found. Beside total Treg depletion, preventing tumor infiltration of these cells appears to be a very promising therapeutic approach. In contrast to Treg depletion, blockade of Treg tumor infiltration would avoid side effects such as autoimmunity in treated cancer patients.

1.2.4 Migration pattern of regulatory T cells

The trafficking of Tregs, as for all T cell subsets, is controlled by chemokines and chemokine receptors. The expression of chemokines and the appropriate chemokine receptors are tightly regulated. The chemokine receptor expression profile of immune cells is depending on the current cellular activation and differentiation stage (Lanzavecchia and Sallusto, 2000). The receptor profile of a certain immune cell determines whether it circulates through the secondary lymphoid tissue and blood cycle, encounters with antigen presenting cells (APCs), or migrates to sites of inflammation (Rossi and Zlotnik, 2000; Zlotnik and Yoshie, 2000).

Compared to other immune cells, murine and human Tregs express high levels of the chemokine receptors CCR4 and CCR8 (Iellem *et al.,* 2001). The ligands of CCR4 are the macrophage-derived chemokine (MDC) CCL22 and the thymus and activation regulated chemokine (TARC) CCL17. CCL1, also a member of the CC chemokines, as well as the virokine vMIP-I are the ligands for CCR8. Consistently with the chemokine receptor expression, Tregs show high chemotactic response to the chemokines CCL22, CCL17, CCL1 and vMIP-I (Iellem *et al.,* 2001).

1.3 The chemokine CCL22

1.3.1 Molecular and biologic characteristics of CCL22

In general, all chemokines carry four cysteine motifs in conserved protein domains. These four cysteines are essential for the 3-dimensional protein

shape. The word chemokine is derived from **chemo**tactic cyto**kines**. The name chemokine indicates the function of these proteins which is mediating specific cell migration along a certain chemotactic gradient.

The chemokine CCL22 was first described in humans by Godiska and colleagues in 1997 (Godiska *et al.,* 1997). One year later the murine equivalent was found by Schaniel and colleagues (Schaniel *et al.*, 1998). Murine CCL22 shares 64% identity and 86% similarity with human CCL22 according to protein align analysis (www.ebi.ac.uk). The total length of murine CCL22 is 92 amino acids (aa) whereas human CCL22 consists of 93 amino acids. The first 24 N-terminal amino acids of murine and human CCL22 represent a signal peptide that mediates protein secretion after ribosomal translation. In the process of chemokine secretion this signal peptide is cleaved off the protein and mature CCL22 (69 aa long in human and 68 aa in murine) with a molecular mass of 7.8 kDa is released (Godiska *et al.,* 1997; Schaniel *et al.,* 1998). Beside the full length CCL22 protein truncated forms can be found in mice and humans. The serine protease CD26/dipeptidyl-peptidase IV (CD26/DPP IV) can remove two or four N-terminal peptides of CCL22. The shorter forms of CCL22 can no longer bind to CCR4, the exclusive receptor of CCL22. Thus, CCL22 cleavage mediates CCL22 inactivation which in turn could represent a feedback mechanism of negative regulation (Proost *et al.,* 1999).

Initially, CCL22 was called macrophage-derived chemokine (MDC) because macrophages appeared to be the specific source of this chemokine. Beside macrophages CCL22 is expressed by monocyte-derived dendritic cells (Godiska *et al.*, 1997; Schaniel *et al.*, 1998). Expression of murine and human CCL22 was observed mainly in the thymus, lymph nodes, lung and spleen (Godiska *et al.*, 1997; Schaniel *et al.*, 1998; Tang *et al.*, 1999). The highest chemotactic index among all T cells was observed for Tregs. The chemotactic index indicates the number of cells migrated in response to a certain chemokine divided by the number of spontaneously migrated cells. Thus, Tregs represent the major subset of immune cells that respond to CCL22 (Iellem *et al.*, 2001).

The DC-specific expression of CCL22 is regulated by the DC activation status. Immature DCs express moderate CCL22 levels. However, after maturation the

expression of the chemokine is up-regulated (Sallusto *et al.*, 1999). Iellem *et al.* postulated that this Treg specific chemokine could mediate Treg recruitment to APCs in order to prevent autoimmunity against self-antigens and inhibit overwhelming inflammatory immune reactions against invading pathogens (Iellem *et al.*, 2001). Since chemokines mediate the migration of T cells, Treg tumor infiltration is also chemokine-dependent. The Treg specific chemokine CCL22 is an abundantly expressed chemokine in many human tumors such as breast cancer and ovarian carcinoma (Curiel *et al.*, 2004; Gobert *et al.*, 2009; Ishida *et al.*, 2006; Yang *et al.*, 2006). Blockade of CCL22 prevents the migration of human Tregs into primary human ovarian tumors of nonobese diabetic/severe combined immunodeficiency (NOD/SCID) mice (Curiel *et al.*, 2004). Thus, CCL22 seems to mediate Treg tumor infiltration and thereby represents a promising target for anti-tumor immune therapy.

1.3.2 Characteristics of CCR4, the receptor of CCL22

Like all chemokine receptors, the CC chemokine receptor CCR4 is an integral protein and consists of seven helical trans-membrane domains (*Figure 2*).

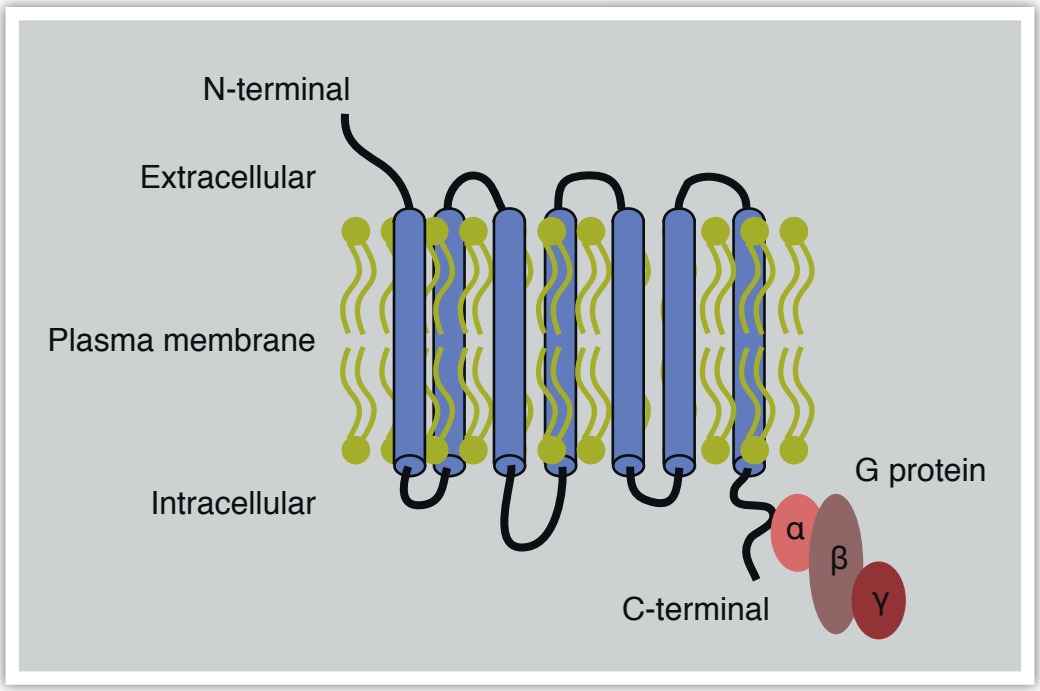

Figure 2: Chemokine receptor structure. Chemokine receptors consist of seven trans-membrane domains that form three extracellular and three intracellular loops. The extracellular N-terminal end binds with high specificity certain chemokines whereas the intracellular C-terminal end is G protein-coupled and mediates signal transduction after ligand binding [Figure is adapted from an illustration published by Savarin-Vuaillat and Ransohoff, 2007]

The helical receptor structure is achieved by three intracellular and three extracellular loops. The extracellular N-terminal end of the receptor protein determines chemokine binding specificity whereas the intracellular C-terminal end enables G protein binding and mediates signal transduction after ligand binding. In general, all chemokine receptors are very similar in size and bind chemokines with high selectivity (Power *et al.*, 1995).

Shortly after the identification of CCL22 as a new chemokine Imai and colleagues identified CCR4 as the exclusive receptor of CCL22 (Imai *et al.*, 1998). Beside CCL22, the chemokine CCL17 binds to CCR4. However, the binding affinity of CCL17 to CCR4 is 3-fold lower than the binding affinity of CCL22 (Imai *et al.*, 1998). CCR4 is specifically expressed by Tregs. Consistent with these data the highest chemotactic response towards CCL22 as well as CCL17 among all leukocytes was observed for Tregs (Iellem *et al.*, 2001).

1.4 Toll-like receptors

Toll-like receptors (TLRs) play a crucial role in the activation of the innate and adaptive immune system. TLRs belong to the receptor superfamily of pattern recognition receptors (PRRs). These receptors recognize highly conserved molecules derived from invading pathogens, also known as pathogen-associated molecular pattern (PAMPs). PAMPs are essential for pathogen survival and function. Thus, PAMPs are highly conserved, and pathogens with mutations in these molecular structures are usually not viable, making PAMPs an ideal target for pathogen recognition. Another subfamily of the PRR superfamily is represented by the RIG-I-like receptors (RLR). Intracellularly expressed retinoic-acid-inducible gene I (RIG-I) and melanoma-differentiation-associated gene 5 (MDA-5) are receptors of this family.

The TLR family was identified in 1997 due to their sequence similarities with the *Drosophila melanogaster* receptor protein Toll (Medzhitov *et al.,* 1997). After antigen encounter the *Drosophila* Toll receptor activates the production of antimicrobial proteins. Mutations of this protein lead to high susceptibility to fungi and Gram-positive bacteria (Lemaitre *et al.*, 1996). In most

vertebrates ten to twelve functional TLRs can be found (Roach *et al.*, 2005).

1.4.1 Toll-like receptors and their ligands

In human at least ten functional TLRs (TLR1 to 10) are expressed. TLR1 to TLR9 are conserved between humans and mice although murine TLR8 and TLR10 are not functional. Additionally, mice express TLR11, 12 and 13 which are missing in humans (Akira *et al.*, 2006). The receptors TLR1, 2, 4, 5, 6, 10 and 11 are located on the cell surface of immune cells such as macrophages and dendritic cells. Due to their location these receptors recognize extracellular PAMPs from microbial membranes such as the endotoxin lipopolysaccharide (LPS) or lipoproteins and lipids from fungal cell walls.

TLR	PAMP	Pathogen	Synthetic ligand	Location
TLR1	Dimers with TLR2			extracellular
TLR2	Triacyl lipopeptides Diacyl lipopeptides Zymosan	Bacteria Mycoplasma Fungus	n.d.	extracellular
TLR3	dsRNA	Virus	poly (I:C); poly (A:U)	intracellular
TLR4	LPS Envelope proteins	Bacteria Virus	monophosphoryl lipid A	extracellular
TLR5	Flagellin	Bacteria	n.d.	extracellular
TLR6	Dimers with TLR2			extracellular
TLR7	ssRNA, siRNA	RNA virus	adenosine and guanosine derivative	intracellular
TLR8	ssRNA	RNA virus	adenosine and guanosine derivative	intracellular
TLR9	CpG DNA Malaria hemozoin	Bacteria DNA virus Parasites	unmethylated CpG motifs	intracellular
TLR10	n.d.		n.d.	extracellular
TLR11	Profilin-like molecule	Parasites	n.d.	extracellular
TLR12	n.d.		n.d.	n.d.
TLR13	n.d.		n.d.	n.d.

Table 1: Overview of all known physiologic and synthetic TLR ligands as well as cellular TLR locations. TLR 11, 12 and 13 is missing in humans, whereas TLR9 and TLR10 are not functional in mice (n.d. indicates none described). References: Alexopoulou *et al.,* 2001; Coban *et al.,* 2005; Hayashi *et al.,* 2001; Heil et *al.,* 2004; Hemmi *et al.,* 2002; Kurt-Jones *et al.,* 2000; Lund *et al.,* 2003; Ozinsky *et al.,* 2000; Poltorak *et al.,* 1998; Takeuchi *et al.,* 1999; Yarovinsky *et al.,* 2005.

In contrast to the surface TLRs the receptors TLR3, 7, 8 and 9 are located intracellularly in endosomal and lysosomal vesicles as well as in the membrane of the endoplasmatic reticulum (Roach *et al.*, 2005). The intracellular TLRs recognize nucleic acids such as bacterial unmethylated CpG motifs or viral single-stranded RNA (ssRNA) and double-stranded RNA (dsRNA) (Akira *et al.*, 2006). In table 1 natural occurring and synthetic TLR ligands as well as cellular TLR locations are summarized.

1.4.2 Immune activation by Toll-like receptor ligands

After a pathogen invasion for example during bacterial infection, pathogen specific molecules (PAMPs) are recognized by TLRs. Ligand binding leads to TLR activation and thereby induces patterns of gene expression which in turn activate the hosts innate immune system and subsequently instructs the rise of an antigen specific immune reaction mediated by the adaptive immune system. TLR ligand binding is the first step of this signal cascade. This binding causes conformational changes of the receptors and dimerization with other activated TLRs. Thereby, adaptor proteins such as myeloid differentiation primary response gene 88 (MyD88) which are crucial for signal transduction are recruited. All TLRs except TLR3 utilize MyD88 for intracellular signal transduction. Beside MyD88 three other adaptor proteins are used for TLR signal transduction, the TIR-containing adapter inducing IFN-β (TRIF), the TRIF-related adapter molecule (TRAM) and the TIR domain-containing adapter molecule (TIRAP) (Kawai and Akira, 2007; Gay *et al.*, 2006). Signal transduction via these adaptor proteins leads to the activation of mitogen-activated protein (MAP) kinase complex and nuclear factor-κB (NF-κB). The transcription factor NF-κB in turn activates the transcription of a variety of pro-inflammatory cytokines such as IL-1, IL-6, IL-10 and IL-12 as well as tumor necrosis factor alpha (TNF-α) (Meylan *et al.*, 2006; Moynagh, 2006).

In addition to the MAP kinase and NF-κB signal pathway, intracellular TLRs can utilize a second discrete pathway for signal transduction. In this pathway adaptor protein recruitment leads ultimately to IFN regulatory factor (IRF) activation such as IRF-3, IRF-5 and IRF-7 which in turn induces type I IFN production (*Figure 3*). The IRF pathway is primarily induced after viral infection (Doyle *et al.*, 2002; Schoenemeyer *et al.*, 2005).

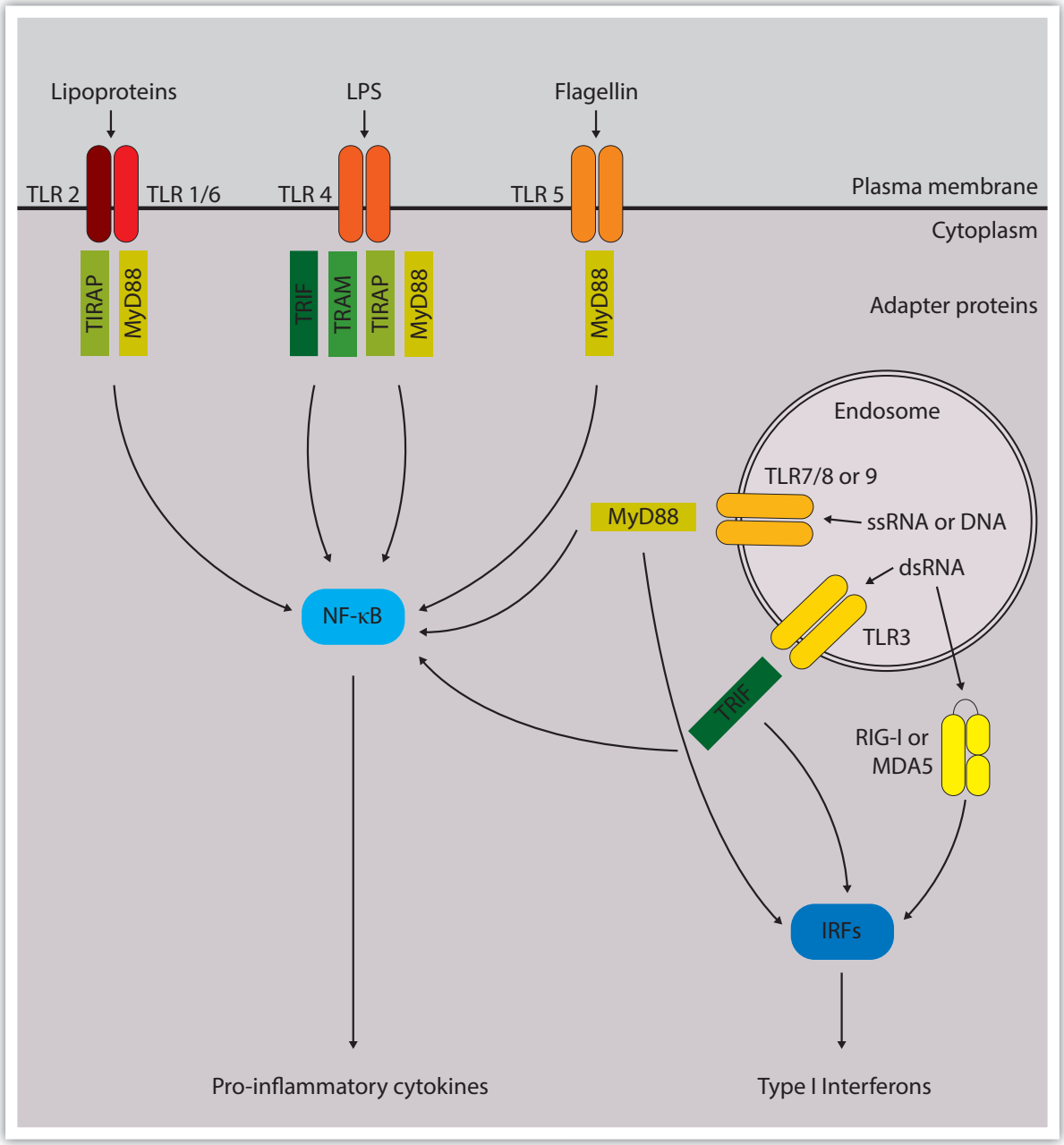

Figure 3: Schematic diagram of pattern-recognition receptors. The diagram shows the toll-like receptor and RIG-I-like receptor family. Examples of receptor ligands, cellular receptor localization, adapter proteins and relevant transcription factor are illustrated. Selected relevant references can be found in the text [Figure is based on an review of Kanzler *et al.*, 2007].

The amount and type of secreted mediators after TLR activation determine the type and magnitude of the subsequent immune reaction. This in turn is dependent on the type and amount of invading pathogen as well as the cell type that is activated by a certain pathogen. Secreted cytokines such as IL-1, IL-6, IL-10 and IL-12 recruit other innate immune cells such as neutrophils and macrophages to the site of inflammation in order to potentiate an ongoing immune response. In addition, TLR activation is a crucial step in

the activation of the adaptive immune system. For instance, immature DCs that recognize pathogens by TLRs start to maturate, produce co-stimulatory molecules such as CD80/86 and migrate to the lymph nodes where they initiate an antigen specific adaptive immune reaction by activating T cells (Shortman and Heath, 2001).

1.4.3 Toll-like receptor ligands and anti-cancer immunotherapy

Manipulating the innate immune system could affect the progress of many diseases. Several different TLR ligands show promising effects for the treatment of certain diseases and are used in the clinic already. TLR ligands are utilized for cancer, allergy and viral infection treatments. By the use of synthetic TLR ligands the innate immune system can be activated and a tumor-induced immune suppression can be abolished (Kanzler *et al.*, 2007). Treating tumor-bearing mice with the TLR9 ligand CpG reduced tumor growth and increased overall survival (Heckelsmiller *et al.*, 2002; Houot and Levy, 2009; Krieg, 2008). Currently, the anti-tumoral effects of CpG in humans are tested in clinical trials (Weber *et al.*, 2009; Vollmer and Krieg *et al.*, 2009). The synthetic TLR7 agonist imiquimod is another example for effective TLR-mediated anti-cancer therapy. This TLR ligand is FDA approved and used in the clinic to treat superficial basal cell carcinoma and vulvar intraepithelial neoplasia (Chang *et al.*, 2005; van Seters *et al.*, 2008). In addition to TLRs other PRR members represent promising targets for anti-tumor therapy. For instance, the synthetic small RNA molecules poly (I:C) and triphosphate RNA activate the intracellular receptors MDA-5 and RIG-I, respectively (Gitlin *et al.*, 2006; Anz *et al.*, 2009). In tumor-bearing mice these ligands could block tumor development and increase overall survival (Tormo *et al.*, 2006; Poeck *et al.*, 2008).

In addition, there is an increasing interest in using TLR ligands as adjuvants for existing anti-tumor therapies such as radiation, anti-tumor antigen directed monoclonal antibodies or cytotoxic drugs (Kanzler *et al.*, 2007). In tumor-bearing mice CpG could be used as an adjuvant for boosting the efficiency of anti-cancer vaccines (Heckelsmiller *et al.*, 2002; Bourquin *et al.*, 2005; Tormo *et al.*, 2006; Speiser *et al.*, 2005). In human clinical trials for using PRR agonists in combination with anti-cancer vaccines are under way.

The mechanisms by which PRR agonists promote anticancer immunity are complex. Activation of the adaptive immune system subsequent of innate immune system activation is a very important step for inducing an efficient anti-tumor immune reaction by PRR ligands. For instance, PRR ligands can cause DC maturation. Mature DCs express co-stimulatory molecules. Thereby, these DCs can activate CD8+ cytotoxic T cells which in turn can generate a potent anti-tumor immune reaction (Haring *et al.*, 2006). Especially TLR7 and TLR9 activation induces high levels of IFN-α produced by plasmacytoid dendritic cells (pDCs). IFN-α in turn initiates MHC-I expression on tumor cells and thereby enhances detection and killing of these cells by activated cytotoxic T cells (Marley *et al.*, 1989). In addition to cytotoxic T cells natural killer cells seem to play an important role for PRR ligand-induced anti-tumor immunity (Berger *et al.*, 2009; Bourquin *et al.*, 2009; Sivori *et al.*, 2004). Nevertheless, the precise mechanisms of PRR agonist-mediated immunotherapy are still unknown. In particular the role of Tregs in this therapeutic setting is rarely investigated. Although it is reported that ligands for TLRs and RLRs abrogate the suppressive function of Tregs (van Maren *et al.*, 2008; Anz *et al.*, 2009), little is known about their precise effect on Tregs in tumor-bearing mice and humans. Moreover, it remains unclear how TLR and RLR ligands influence Treg tumor infiltration.

1.5 Objectives

During tumor development an immunosuppressive milieu is created by the tumor which prevents an efficient anti-tumor immune reaction. In the last decade the functions of Tregs were described in great detail, and Tregs were identified in several human tumors as one of the key mediators of this tumor-induced immune suppressive environment. In contrast to Treg function the knowledge of the mechanisms that recruit Tregs into the tumor tissue in order to mediate intratumoral immune suppression is still very limited.

In general, the migration of immune cells is mediated by chemokines. Thus, intratumoral Treg recruitment is presumably mediated by the increased expression of one or more chemokines. One very promising candidate is the

chemokine CCL22. This chemokine is a potent Treg attractor (Iellem *et al.*, 2001) and is highly expressed in many tumors (Curiel *et al.*, 2004; Gobert *et al.*, 2009; Ishida *et al.*, 2006; Yang *et al.*, 2006). From a therapeutic perspective, identifying the mechanisms that mediate Treg recruitment to the tumor tissue represents an attractive tool for manipulating the tumor-induced immune suppressive milieu. Previous experiments in our group have shown that TLR stimulation reduces the amount of intratumoral CCL22 and the number of Tregs in the tumor tissue. Since TLR ligands can induce tumor regression, CCL22 suppression could be an important part of this TLR ligand-mediated anti-tumor immune reaction.

Since little is known about the impact of intratumoral CCL22 on tumor-induced Treg recruitment, tumor development, disease outcome and TLR ligand-induced tumor therapy, this work was designed to answer the following questions:

❶ Which cell type produces CCL22 in the tumor tissue?

❷ What is the impact of intratumoral CCL22 on tumor growth and overall survival?

❸ What is the mechanism of TLR ligand-mediated intratumoral CCL22 suppression?

❹ Is TLR ligand-mediated intratumoral CCL22 suppression important for the TLR ligand-induced anti-tumor immune reaction?

The answer to these questions should allow a better understanding of the mechanisms of tumor development and growth. Thereby, promising novel targets for an efficient anti-cancer therapy may identified.

Materials & Methods

2. Materials & Methods

2.1 Materials

2.1.1 Technical equipment

Alpha Imager	Alpha Innotech, San Leandro, USA
Balance (LP 6209)	Sartorius, Göttingen, Germany
Cell culture CO2 incubator (BD 6220)	Heraeus, Hanau, Germany
Cell culture laminar flows	Heraeus, Hanau, Germany
Centrifuge 5424	Eppendorf, Hamburg, Germany
FACS Canto II	BD bioscience, Heidelberg, Germany
Gel electrophoresis systems	Bio-rad, Munich, Germany
LightCycler 2.0 System	Roche, Mannheim, Germany
MiniMACS, QuadroMACS	Miltenyi Biotec, Bergisch Gladbach, Germany
Mithras LB940 multilabel plate reader	Berthold Technologies, Bad Wildbad, Germany
Multifuge 3L-R	Heraeus, Hanau, Germany
Nanodrop ND-1000	NanoDrop, Wilmington, USA
Neubauer hemocytometer	Optik Labor Frischknecht, Balgach, Germany
pH meter	WTW, Weilheim, Germany
Power Supply 200/2.0	Bio-Rad, Munich, Germany
Refrigerators (4°C, -20°C)	Bosch, Gerlingen, Germany
Refrigerators (-80°C)	Thermo Scientific, Waltham , USA
Shaker	NeoLab, Heidelberg, Germany
Thermocycler T3	Biometra, Göttingen, Germany
Thermomixer	Eppendorf, Hamburg, Germany
Vortex	VF2 Janke & Kunkel, Staufen, Germany

2.1.2 Chemicals, reagents and buffers

Agarose LE	Biozym, Hess Oldendorf, Germany
Bovine serum albumine (BSA)	Sigma Aldrich, Steinheim, Germany
Chloroform	Sigma Aldrich, Steinheim, Germany
Collagenase	Sigma Aldrich, Steinheim, Germany
Dimethyl sulfoxide (DMSO)	Sigma Aldrich, Steinheim, Germany

DNase I	Sigma Aldrich, Steinheim, Germany
dNTP Mix, 10 mM	invitrogen, Carlsbad, USA
Donkey Serum	Millipore, Billerica, USA
Dulbecco's Phosphate buffered saline (PBS)	PAA, Pasching, Germany
Ethanol	Sigma Aldrich, Steinheim, Germany
Ethylenediaminetetraacetic acid (EDTA)	Sigma Aldrich, Steinheim, Germany
FACSFlow, FACSClean, FACSShutdown	BD bioscience, Heidelberg, Germany
Isoflurane (Forene®)	Abbott, Zug, Switzerland
Isopropanol (100 Vol%)	Sigma Aldrich, Steinheim, Germany
Isopropanol (70 Vol%)	Apotheke Innenstadt, LMU Munich
Lipofectamine™ 2000 Transfection Reagent	invitrogen, Carlsbad, USA
$MgCl_2$ 25mM	Fermentas, St. Leon-Rot, Germany
MolTaq DNA Polymerase	Molzym, Bremen, Germany
O'GeneRuler™ DNA Ladder Mix	Fermentas, St. Leon-Rot, Germany
Percoll, d=1,124 g/ml	Biochrome, Berlin, Germany
Pfu Ultra Fusion HS	Stratagene, Waldbronn, Germany
Sodium pyruvate	PAA, Pasching, Austria
Trizol reagent	invitrogen, Carlsbad, USA
Trypan blue	Sigma Aldrich, Steinheim, Germany
Trypsin (10x)	PAA, Pasching, Austria
Tween 20	Roth, Karlsruhe, Germany

MACS buffer	Fixation buffer for FACS samples
2 mM EDTA	2% PFA
2% FCS in PBS	in PBS

ELISA assay diluent	ELISA wash buffer
1% BSA	0.05% Tween 20
in PBS, pH 7.0	in PBS

2.1.3 Cell culture reagents, media and cytokines

2-Mercaptoethanol	Sigma-Aldrich, Steinheim, Germany
Dulbecco's modified Eagle´s medium (DMEM), high glucose	PAA, Pasching, Austria
Fetal calf serum (FCS)	GibcoBRL, Karlsruhe, Germany
L-glutamine 200mM	PAA, Pasching, Austria
MEM-NEAA (non-essential amino acids)	GibcoBRL, Karlsruhe, Germany
Roswell Park Memorial Institute (RPMI)	PAA, Pasching, Austria

1640 medium	
Penicillin/Streptomycin (100x)	PAA, Pasching, Austria
VLE RPMI 1640 medium (very low endotoxin)	Biochrom, Berlin, Germany

4T1 medium	B16, CT26, Panc02 medium
10% FCS	10% FCS
2 mM L-glutamine	2 mM L-glutamine
100 IU/ml penicillin	100 IU/ml penicillin
100 µg/ml streptomycin	100 µg/ml streptomycin
in RPMI	in DMEM

Meth-A medium	mGC8, DC2.4 medium
10% FCS	10% FCS
2 mM L-glutamine	2 mM L-glutamine
100 IU/ml penicillin	100 IU/ml penicillin
100 µg/ml streptomycin	100 µg/ml streptomycin
2 mM sodium pyruvate	2 mM sodium pyruvate
2 mM nonessential amino acids	2 mM nonessential amino acids
in RPMI	in DMEM

T cell and DC medium	Cryo medium
10% FCS	50% appropriate culture medium
2 mM L-glutamine	40% FCS
100 IU/ml penicillin	10% DMSO
100 µg/ml streptomycin	
2 mM sodium pyruvate	
2 mM nonessential amino acids	
0.0001% of 2-mercaptoethanol	
in RPMI 1640	

Cytokines and growth factors	
Granulocyte-macrophage colony-stimulating factor (GM-CSF)	PeproTech, Hamburg, Germany
IFN-α, mouse recombinant	R&D Systems, Wiesbaden, Germany
IFN-γ, mouse recombinant	R&D Systems, Wiesbaden, Germany
Interleukin-1b, mouse recombinant	PeproTech, Hamburg, Germany
Interleukin-2, mouse recombinant	PeproTech, Hamburg, Germany
Interleukin-4, mouse recombinant	PeproTech, Hamburg, Germany

Interleukin-6, mouse recombinant	PeproTech, Hamburg, Germany
Interleukin-10, mouse recombinant	PeproTech, Hamburg, Germany
Interleukin-12, mouse recombinant	PeproTech, Hamburg, Germany

Disposable plastic materials for cell culture experiments were purchased from Corning (Corning, USA), Eppendorf (Hamburg, Germany), Falcon (Heidelberg, Germany), Greiner (Frickenhausen, Germany) or Sarstedt (Nümbrecht, Germany).

2.1.4 Toll-like receptor ligands

CpG 1826 (CpG) 5'-TCCATGACGTTCCTGACGTT-3'	Coley, Massachusetts, USA
poly (I:C)	Amersham Bioscience, Little Chalfont, UK

2.1.5 Kits

Bio-Plex Cell Lysis Kit	Bio-Rad, Munich, Germany
Cell proliferation ELISA, BrdU	Roche, Mannheim, Germany
CCL22 murine Cytokine ELISA sets	BD Bioscences, San Diego, USA
CD11c MicroBeads MACS cell separation	Miltenyi Biotec, Bergisch Gladbach, Germany
CD4+CD25+ Regulatory T Cell Isolation Kit	Miltenyi Biotec, Bergisch Gladbach, Germany
CD4 Micro Beads MACS cell separation	Miltenyi Biotec, Bergisch Gladbach, Germay
FOXP3 Staining Buffer Set	eBioscience, San Diego, USA
GeneJET™ Plasmid Miniprep Kit 50 preps	Fermentas, St. Leon-Rot, Germany
JetQuick Gel Spin Kit	Genomed, Löhne, Germany
JetQuick PCR Purification Kit	Genomed, Löhne, Germany
Spin Universal RNA Mini Kit	Invitek, Berlin, Munich
Revert Aid First strand cDNA Synthesis Kit	Fermentas, St. Leon-Rot, Germany
Light Cycler 4800 Probes Master	Roche, Mannheim, Germany
LS, MS and LD columns	Miltenyi Biotec, Bergisch Gladbach, Germany

2.1.6 FACS antibodies

Description	Isotype	Clone	Company
B220 Pacific Blue a-mouse	Rat IgG2a,	RA3-6B2	BioLegend
CD3 FITC a-mouse	Ar Ham IgG	145-2C11	BioLegend
CD4 APC/Cy7 a-mouse	Rat IgG2b,	GK1.5	BioLegend
CD8a PerCp a-mouse	Rat IgG2a,	53-6.7	BioLegend
CD11b PE a-mouse	Rat IgG2b	M1/70.15	ImmunoTools
CD11c APC a-mouse	Ar Ham IgG	N418	BioLegend
CD25 PerCp a-mouse	Rat IgG1,	PC61	BioLegend
CD49b FITC a-mouse	Rat IgM,	DX5	BioLegend
FOXP3 eFlur®450 a-mouse	IgG2a,	FJK-16s	eBioscience
GR1 APC/Cy7 a-mouse	Rat IgG2b,	RB6-8C5	BioLegend

2.1.7 Software

Adobe Creative Suite	Adobe Systems, San José, USA
BD FACSDiva	BD Biosciences, San Diego, USA
FlowJo	Tree Star, Ashland, USA
GraphPad	GraphPad Software, Inc., California, USA
Microsoft Office	Microsoft, Redmond, USA

2.2 Molecular biology methods

2.2.1 Polymerase chain reaction

The polymerase chain reaction (PCR) is a method to amplify a defined part of an extracted DNA sample. To define this part, two specific primers are needed that flank the region of interest, one upstream and one downstream primer. The general range of a primer is 15-30 bases, and the guanosine and cytosine amount should be 40-60%. The maximum size of the DNA fragment, which can be amplified with a standard PCR, is 10.000 bases. A PCR consists of several cycles. After each cycle the amount of amplified DNA is doubled.

The PCR method was used for the amplification of specific cDNA fragments or genomic DNA. If a PCR product was used for cloning, the PCR primers

were designed to introduce restriction endonuclease recognition sites to facilitate specific cloning into a certain target plasmid. For this purpose it was vital to prevent point mutations. Thus, the polymerase PfuUltra (Fermentas) was used. This enzyme has a 3' to 5' exonuclease activity and thereby provides a higher fidelity than normal polymerases. For pure analytical purposes it was sufficient to use Moltaq (Molzym) polymerase which lacks proofreading activity. The composition of a standard PCR reaction mix for both polymerases is shown below:

PfuUltra Polymerase

as required	DNA (100 pg to 500 pg)
1x	10x PfuUltra II Reaction Buffer
0.2 mM each dNTP	invitrogen™ dNTP Mix (10 mM each dNTP)
0.25 µM	upstream primer (10 µM)
0.25 µM	downstream primer (10 µM)
1.25 U	PfuUltra DNA Polymerase (5 U/µl)

Moltaq Polymerase

as required	DNA (100 pg to 500 pg)
1x	10x Moltaq Reaction Buffer
10%	PCR Enhancer Solution
1mM	$MgCl_2$ (25mM)
0.2 mM each dNTP	dNTP Mix (10 mM each dNTP)
0.25 µM	upstream primer (10 µM)
0.25 µM	downstream primer (10 µM)
1 U	Moltaq DNA Polymerase (5 U/µl)

Standard PCR cycling conditions:

Function	Duration	Temperature	
Initial DNA Denaturation	5 minutes	95°C	
DNA Denaturation	20 s	95°C	} 30 cycles
Primer Annealing	20 s	65°C	
Primer Extension	15 s	72°C	
Final Extension	3 minutes	72°C	
End	∞	4°C	

After PCR reaction 1x DNA loading dye (Fermentas) was added to each sample. It contains two different dyes (bromophenol blue and xylene cyanol FF) for visual tracking of DNA migration during electrophoresis. Samples mixed with

loading dye were loaded on an agarose gel for length separation by gel electrophoresis (see below).

2.2.2 Polymerase chain reaction purification

If PCR products were needed for further experiments, such as molecular cloning, PCR products were purified by JETQuick PCR Purification Kit. Purification was done according to manufacturer's protocol. In brief: 400 µl of solution H1 were added to each sample and pipetted into a JetQuick spin column. After centrifugation at 12,000 g for 1 minute the flow-through was discarded and the column washed with 500 µl H2 solution. The column was washed twice by centrifugation at 12,000 g for 1 minute, and the flow-through was discarded. For DNA elution 40 µl pre-warmed (65-70°C) water was added to the center of the column followed by a final centrifugation step at 12,000 g for 2 minutes.

2.2.3 Gel electrophoresis

Gel electrophoresis is a technique to separate and visualize DNA fragments of different sizes. This technique was used to analyze PCR samples. For the electrophoresis a 2% agarose gel (2% agarose; 1x TAE) was used. After boiling the gel, 0.003% ethidium bromide was added, and the gel was poured. While cooling down, the gel forms a crosslinked polymer. This polymer allows the separation of DNA fragments due to their size. DNA is negatively charged. Thus, the DNA moves in an electric field from the negative pole to the positive pole. The smaller a DNA fragment, the faster it moves through the gel. Hence, DNA fragments of different sizes are separated. For size determination of the separated PCR fragments a 1 kb DNA Ladder (Fermentas - GeneRuler™) was used.

2.2.4 DNA gel extraction

The JETQuick Gel Extraction Kit was used for double-stranded DNA fragment purification of PCR samples after gel electrophoresis. The kit purifies DNA fragments of a length of 40 bp up to 20 kb. 80-95% of the fragments are recovered with a maximal binding capacity of 20 µg. The DNA adsorbs to the silica-membrane of the JETQuick spin column in high-salt buffer while contaminants pass through the column. The DNA is eluted in low-salt buffer (Vogelstein and Gillespie, 1979).

JETQuick Gel Extraction was done according to manufacturer's protocol. In brief: The appropriate DNA band was excised from an agarose gel after gel electrophoresis and transferred into an suitable tube. For each 100 mg gel slice 300 µl solution L1 was added. To solubilize the gel, the tube was incubated at 50°C for 15 minutes. Then the solubilized gel was loaded into a JETQuick spin column and centrifuged at 12,000 g for 1 minute. The flow-through was discarded and the column washed by adding 500 µl of reconstituted solution L2. Followed by another centrifugation step (12,000 g for 1 minute) the flow-through was discarded again. Finally, the column bond DNA was eluted by adding 50 µl of sterile water onto the center of the silica matrix of the JETQuick spin column and centrifugation at 12,000 g for 2 minutes. Higher DNA concentration was obtained by using preheated water (65-75°C) as elution buffer.

2.2.5 Molecular cloning

Molecular Cloning is a technique to integrate a specific sequence into a certain vector for amplification in bacteria. In order to amplify the vector and the integrated sequence, the cloning vector must carry an origin of replication. Additionally, one or more antibiotic resistances are needed for selection. In general, each cloning involves four steps: fragmentation (digest), ligation, transformation and selection.

Restriction digests

For analytical purposes 0.2-2 µg of DNA were digested with 10-20 U of one or two restriction endonucleases in an appropriate 1× buffer. Restriction digests were carried out for 1 hour at 37°C. After digestion samples were separated by gel electrophoresis and extracted via gel extraction kit (see section *2.2.3*) or directly purified by JETQuick PCR Purification Kit (see section *2.2.2*). DNA amounts were measured by standard photometry.

Ligation

To insert a specific DNA fragment (insert) into a multiple cloning site (MCS) of a plasmid vector, both, the insert and the vector, were digested with one or two appropriate restriction endonucleases (see above). After digest and fragment purification the gained insert and vector were used for ligation.

An insert vector ratio of 3 to 1 was used. Calculation of required insert and vector amounts for ligation was done according following formula:

$$\frac{a}{b} \times \frac{3}{1} \times c = d$$

a: amount of vector (ng)
b: size of vector (bp)
c: size of insert (bp)
d: amount of insert (ng)

Ligation was performed with a T4 DNA Ligase (Fermentas) and 1x Ligation buffer in a total volume of 20 µl at 17°C overnight. Ligation efficiency was verified by bacteria transformation with 10 µl ligation product and subsequent antibiotic selection. To verify proper integration and correct orientation of the insert, control PCRs with appropriate primers were performed after positive clone amplification and subsequent vector purification by plasmid DNA purification (see below). Additionally, in some cases positive clones were analyzed by sequencing (done by mwg/operon).

Transformation

For transformation chemically competent DH5 *E.coli.* were used. After thawing the competent cells on ice, plasmid vector was added to the cells. Followed by heat shock at 42°C for 1 minute the cells were placed back on ice. Finally, the cells were plated out on LB-agarose plates. For positive cell selection LB-plates with an appropriate antibiotic in a concentration of 1:1000 were used (usually ampicillin). If transformation was successful, colonies were observed after incubating the plates at 37°C for 24 hours.

2.2.6 Plasmid miniprep

Plasmid DNA purification from bacteria was done with the GenJET™ Plasmid Miniprep Kit. The procedure is based on alkaline lysis of bacterial cells followed by adsorption of DNA onto silica in the present of high salt (Vogelstein and Gillespie, 1979). The GenJET™ columns contain a silica membrane that enables a selective absorption of plasmid DNA in high-salt buffer and an elution of plasmid DNA in low-salt buffer. This ensures that only DNA will be isolated while RNA, cellular proteins, and metabolites are discarded.

The kit guarantees a DNA recovery of 90-95% with an maximum DNA yield

of 50 µg. For Plasmid DNA miniprep bacteria were amplified on an antibiotic-containing LB-plate, positive clones picked and proliferated in 2 ml antibiotic containing LB-medium for 16 hours at 37°C. Bacteria were harvested by centrifugation at 12,000 g for 2 minutes. The pelleted cells were resuspended in 250 µl Resuspension Solution, and 250 µl Lysis Solution was added. After thoroughly mixing the solution by inverting the reaction tube, 350 µl Neutralization Solution was added. For pelleting cell debris and chromosomal DNA, centrifugation at 12,000 g for 5 minutes was performed. The obtained supernatant was loaded on a GeneJET™ spin column. After another centrifugation step at 12,000 g for 1 minute the flow-through was discarded and the column washed two-times with 500 µl Wash Solution. Each wash step was followed by centrifugation at 12,000 g for 1 minute. To remove residual wash solution, an additional centrifugation step (12,000 g, 1 minute) was performed before DNA was eluted by adding 50 µl pre-warmed water (70°C) to the center of the spin column and centrifuging the tube for 2 minutes at 12,000 g.

2.2.7 Genomic DNA isolation

Genomic DNA was extracted from small tissue pieces cut from the tip of the tail of five week old mice. The tissue was lysated at 56°C in 500 µl Laird's Buffer (200 mM NaCl, 100 mM Tris-HCl pH 8.3, 5 mM EDTA, 0.2% sodium dodecyl sulfate) containing 0.15 mg/ml proteinase K. After 24 hours the samples were centrifuged at 14.000 rpm for 5 minutes. The supernatants were mixed with the same volume of isopropanol. Through inverting 3-4 times DNA appeared as small white fibres. Finally, the samples were centrifuged again, the isopropanol was completely removed and the DNA dissolved in 100 µl water. The DNA was used for genotyping by PCR. Therefore, 1 µl of each lysate was used for a standard PCR (see methods *2.2.1*). Primarily, the quality and quantity of DNA in each sample was verified with two primers that detect a common gene. In the case of a positive result a second PCR was performed to screen for the desired transgene. For further analyses samples were stored at 4°C.

2.2.8 Generation of a Tet-On CCL22 expression construct

For the generation of an inducible CCL22 expression vector a Tet-On Gene Expression construct was used (HT1080 Cell Line & pTRE2 Vector, 1999). This construct enables the doxycycline-dependent expression of CCL22. It consists

of two elements. The first element is the activator rtTA. The expression of this activator is regulated by the cytomegalovirus promoter CMV. This promoter guarantees a strong constitutive expression of rtTA in all cells carrying the Tet-On Gene Expression construct. The second element contains the tet promoter that regulates the expression of CCL22. The whole system is doxycycline sensitive. Doxycycline is a member of the tetracycline antibiotics group. In the absence of doxycycline the activator rtTA cannot bind to the promoter tet. Thus, tet is silent, and the gene of interest is not expressed. In the presence of doxycycline the antibiotic binds to rtTA. That leads to a conformation change of rtTA and enables rtTA to bind to the promoter tet. Thereby, the promoter is activated and promotes the expression of CCL22 (*Figure 4*). After integrating CCL22 into the Tet-On Gene Expression construct, the newly generated rtTA-Tet-CCL22 construct was inserted into the genome of CT26 mouse tumor cells via lentiviral transduction.

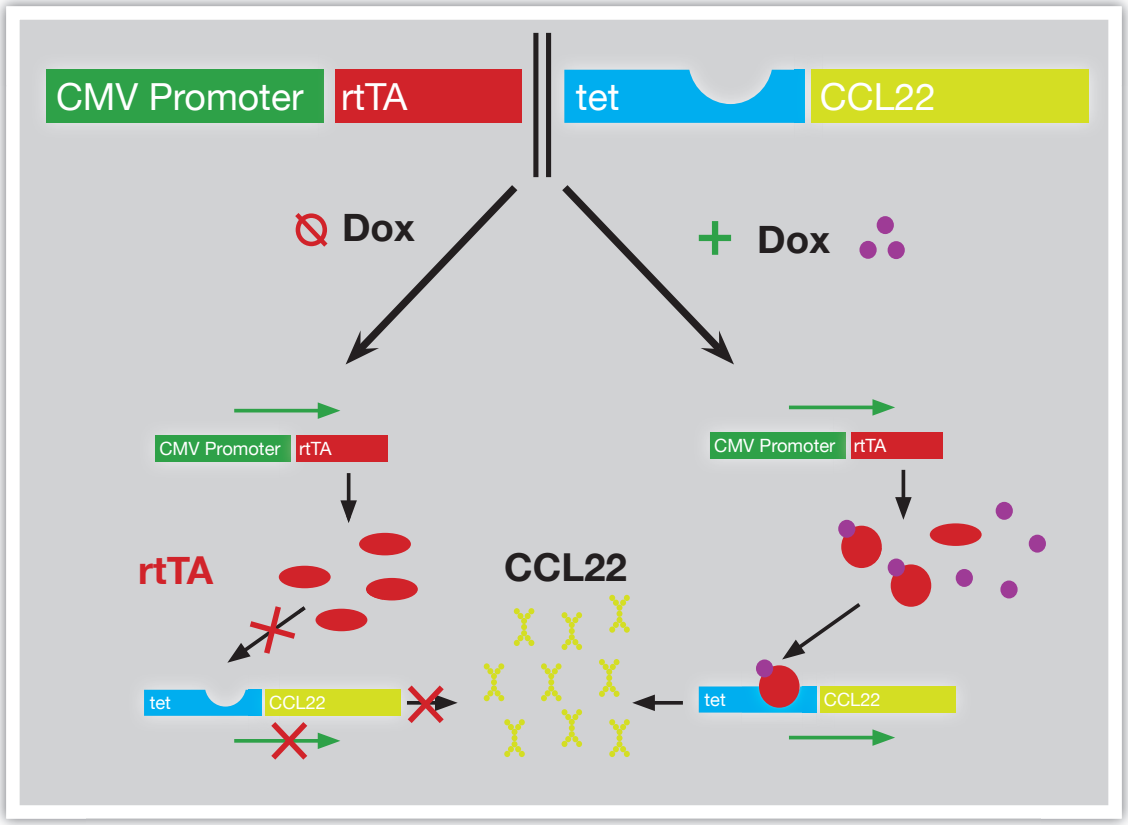

Figure 4: Doxycycline-dependent expression of CCL22. The construct consists of two elements. First, the constitutive promoter CMV that guarantees a strong expression of the activator rtTA. Second, the rtTA controlled tet promoter that regulates the expression of the gene of interest (CCL22). In the absence of doxycycline rtTA cannot activate the promoter tet. In the presence of doxycycline rtTA binds doxycycline. The conformation of rtTA changes. Thus, rtTA is able to bind to and thereby activate the promoter tet, that in turn promotes the expression of CCL22.

2.2.9 Lentiviral tumor cell transduction

To guarantee stable genomic integration of the rtTA-Tet-CCL22 construct (containing a puromycin selection marker) into the target cell, lentiviral transduction was used. Therefore, the transgene was packed into a lentivirus envelope.

The recombinant lentivirus was produced by transient transfection of HEK 293T cells using GeneJuice Transfection Reagent (Novagen). HEK 293T cells were transfected with a viral construct (containing rtTA under the control of a CMV promoter and CCL22 mRNA downstream of a Tet-responsive promoter, FugW backbone), VSV-G and delta 8.9 in a ratio of 10:1:10. Infectious lentiviruses were harvested at 72 hours post-transfection and filtered through a low-protein binding 0.45 µm filter flask. The filtered recombinant lentiviruses were packed on 20% sucrose solution and concentrated by ultracentrifugation (2 hours at 27,000 rpm). Subsequently, virus pellet was dissolved and used for CT26 cell transduction. 36 hours post-transduction cells were selected by puromycin (5 µg/ml) treatment for 72 hours. After 24 hours incubation with 2 µg/ml doxycycline inducible CCL22 expression of these novel generated puromycin selected rtTA-CCL22-CT26 cell lines were verified by ELISA.

2.2.10 RNA isolation

Single cell suspension RNA isolation

Total RNA was extracted from tumor-infiltrating immune cells and cultured cells with Trizol reagent. 0.5 to 2.0 x 10^6 cells per well of a 96 well plate were used for Trizol RNA isolation. All subsequently indicated volumes are optimized for lysing cells in a 96 well format. Initially, cells were lysed directly in a culture dish by adding 100 µl/well Trizol. After 5 minutes incubation at room temperature cell lysates were transferred into a 1,5 ml Eppendorf tube, and 20 µl chloroform was added per sample. Next, samples were mixed by hand, incubated for 5 minutes at room temperature and centrifuged at 12,000 g for 15 minutes at 4°C. After centrifugation the mixture separated into a lower red, phenol-chloroform phase, an interphase and a colorless upper phase that contained the extracted RNA. The upper phase of each sample was transferred into a new tube, and RNA was precipitated by adding 0.1 ml isopropyl alcohol. Subsequently, after 10 minutes incubation, samples were centrifuged

at 12,000 g for 15 minutes at 4°C, and supernatants were discarded. Finally, RNA pellets were washed with 0.2 ml 75% ethanol and dissolved in 25 µl RNase-free water.

Tissue RNA isolation

For total RNA isolation from tissue samples the InviTrap Spin Universal RNA Mini Kit from Invitek was used. 20 mg of fresh tissue was grounded under liquid nitrogen with a mortar and pestle. The powder was transferred into a 1.5 ml reaction tube and mixed with 900 µl lysis solution. To remove the genomic DNA the tube was centrifuged at maximum speed for 2 minutes. The supernatant was transferred in a new reaction tube, and 500 µl 100% ethanol was added. This mixture was loaded on a RTA Spin Filter, incubated for 1 minute and centrifuged for 1 minute at 10.000 g. After discarding the flow-through, two wash steps were performed. The first with 600 µl Wash Buffer R1 and the second with 700 µl Wash Buffer R2. The last washing step was repeated once. To eliminate any traces of ethanol, the tube was centrifuged at maximum speed for 5 minutes. Afterwards, total RNA was eluted by adding 40 µl RNase-free water onto the filter-membrane, incubating for 2 minutes and centrifuging for 1 minute at 10,000 g. RNA was stored at -20°C.

2.2.11 Quantitative real-time polymerase chain reaction

Quantitative real-time polymerase chain reaction (qRT-PCR) was used to quantify the relative amount of specific mRNAs in certain samples. Therefore, isolated total RNA was reverse transcribed in cDNA, amplified with specific primers and normalized to HPRT, a ubiquitous expressed gene in all cell types (HPRT probe-number and primer sequence: see appendices *8.2*).

For reverse transcription the RevertAid First Strand cDNA Synthesis Kit from Fermentas was used. Synthesis was done according to manufacturer's protocol. In brief:

cDNA Synthesis

as required	RNA (0.1 ng to 5 µg)
1 µl	oligo (dT) primer
to 12 µl	Water, nuclease-free

4 µl	5x Reaction Buffer
1 µl	RiboLock RNase Inhibitor (20 u/µl)
2 µl	10mM dNTP Mix
1 µl	RevertAidTM M-MuLV Reverse Transcriptase (200 u/µl)

After adding all components, the mixture was incubated for 60 minutes at 42°C. The reaction was terminated by heating at 70°C for 5 minutes. After this incubation all mRNA fragments of the sample were transcribed into cDNA. This cDNA was used for further analyses by qRT-PCR.

qRT-PCR was done with Roche LightCycler 488 Probes Master. With this kit the following standard reaction was prepared:

qRT-PCR

1.5 µl	Water, PCR-grade
0.2 µl	primer forward (10 µM)
0.2 µl	primer reverse (10 µM)
5 µl	Probes Master
0.1 µl	Probe
3 µl	cDNA

For specific primers and probes see appendix *8.2*. Relative gene expression of each gene was calculated as the ratio of gene of interest mRNA and hypoxanthine phosphoribosyltransferase (HPRT) mRNA, both determined in the same sample. qRT-PCR was performed with the LightCycler 480 Instrument. For all runs the standard Roche protocol Mono Color Hydrolysis Probes with 45 amplification cycles was used.

2.3 Immunological methods

2.3.1 CCL22 enzyme-linked immunosorbent assay (ELISA)

To measure the amount of CCL22 in different tissues, serum or the supernatant of cultured cells a CCL22 ”sandwich” ELISA (R&D System) was performed. Via ”sandwich” ELISA a sample with an unknown amount of CCL22 is immobilized

on a polystyrene microtiter plate using a CCL22 specific capture antibody. After the antigen is immobilized, the detection antibody is added forming a complex with the antigen. The detection antibody is covalently linked to the enzyme horseradish peroxidase (HRP). By adding an enzymatic substrate, a visible signal can be detected which indicates by comparing to the signal of a CCL22 standard dilution the quantity of CCL22 in the sample. Therefore, a standard dilution was prepared for each ELISA. The standard dilution consists of clearly determined amounts of CCL22 (from 500 pg/ml to 0 pg/ml). The CCL22 standard dilution was done according to *Figure 5*.

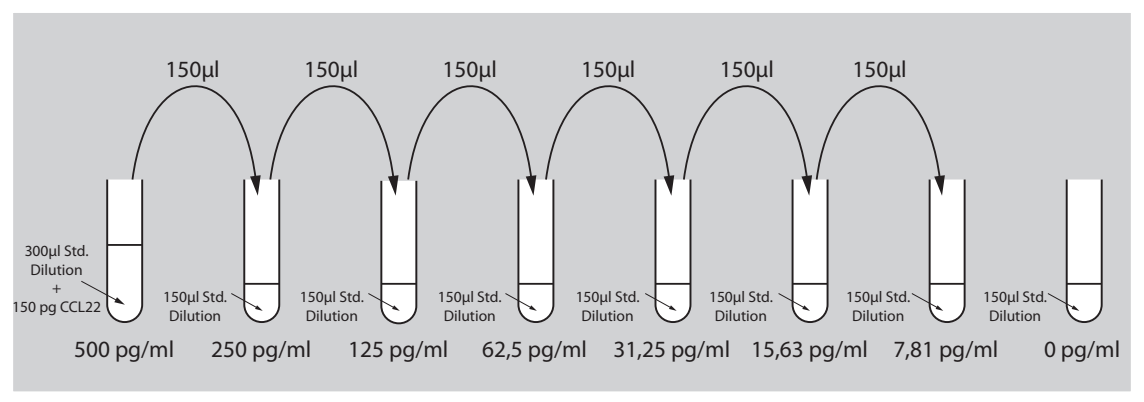

Figure 5: Standard dilution scheme. 500 pg/ml CCL22 was added to 300 µl standard dilution (donkey serum diluted 2:1 with PBS + 1% BSA). 150 µl of this first solution was mixed with 150 µl standard dilution. Then 150 µl of this second solution was mixed with another 150 µl standard dilution and so forth. At the end eight different CCL22 standard dilutions (500 pg/ml, 250 pg/ml, 125 pg/ml, 62.5 pg/ml, 31.25 pg/ml, 15.63 pg/ml, 7.81 pg/ml, and 0 pg/ml) were prepared. By comparing with this standard dilution, the unknown amount of CCL22 in a sample was verified.

At the beginning of each ELISA, CCL22 capture antibody was diluted in PBS to a final concentration of 2.0 µl/ml. 50 µl of this capture antibody solution per well was used to coat a 96 well microplate. The plate was sealed and incubated overnight at room temperature to enable binding of the antibody to the surface of the plate. On the next day the plate was washed three times with washing buffer (PBS + 0.05% Tween). To block any non specific binding sites on the surface of the plate, 150 µl blocking solution (PBS + 1% BSA) was added to each well. After 1 hour incubation the plate was washed again three times, and 50 µl sample (either pure or diluted with PBS + 1% BSA) or 50 µl standard dilution was added per well. 2 hours later the plate was washed again three times and incubated for 2 hours with 50 µl CCL22

detection antibody solution (diluted in PBS + 1% BSA to a final concentration of 50 ng/ml). By three times washing, all unbound detection antibody was removed. Afterwards, 50 µl enzyme solution (streptavidin HRP, diluted 1:200 with PBS + 1% BSA) was added to each well and incubated in the absence of light for 20 minutes. To eliminate all unbound enzymes, the plate was washed again three times. Finally, 50 µl substrate solution (H_2O_2 diluted 1:1 with tetramethylbenzidine) was added to each well. This substrate solution is converted by streptavidin HRP into a fluorescence signal. After 20 minutes the enzyme reaction was stopped by adding 25 µl per well stop solution (2 N H_2SO_4). Immediately after stopping the reaction, the optical density of each well was measured by using a microplate reader set to 450 nm + 570 nm as wavelength correction. The reference wavelength corrects for optical imperfections in the plate.

2.3.2 Cell proliferation BrdU ELISA

Tumor cell proliferation *in vitro* was measured by 5'-Bromo-2'-deoxyuridine (BrdU) cell proliferation ELISA kit from Roche. BrdU is a pyrimidine analogue that incorporates into the DNA of replicating cells instead of thymidine. By adding an anti-BrdU-peroxidase antibody and tetramethylbenzidin (TMB) as substrate the amount of incorporated BrdU can be measured with an ELISA reader. The obtained optical density (OD value) directly correlates with the cell proliferation rate. We used this technique to verify the proliferation rate of untreated and doxycycline-treated rtTA-CCL22-CT26 tumor cells. For this purpose, 40.000 tumor cells were cultured in a 96 well tissue-culture plate for 48 hours without or with different amounts of doxycycline in cell culture medium. 6 to 12 hours before analyzing the proliferation rate 7.5 µM BrdU was added to each well. After this labeling step the plate was centrifuged (400 g, 7 minutes) and the labeling medium was removed. Subsequently, the plate was dried at 60°C for one hour. Finally, the cells were fixated by adding FixDenat to each well, labeled with anti-BrdU antibody and incubated with TMB substrate solution according to the manufacturer's protocol. The reaction product was quantified in triplicates by measuring the absorbance at 370 nm (+ 492 nm as wavelength correction) using an ELISA reader.

2.3.3 Cytokine assays of tissue lysates

Tissue homogenates were resuspended in lysis buffer (BioRad Laboratories) and centrifuged. Total protein concentration was measured by Bradford assay

(BioRad Laboratories). All samples were diluted to a protein concentration of 10 to 30 mg/ml, and CCL22 concentration was measured by ELISA (R&D Systems). The cytokine concentration was calculated as ng cytokine/g protein in the respective lysate.

2.3.4 Flow cytometry

Flow cytometry is a technique for analyzing and counting cells suspended in a fluid due to their physical and chemical differences. To analyze each single cell, a hydrodynamically-focused stream of liquid is generated. By use of this liquid stream, each cell passes single file through a laser light. At the point where the liquid stream passes through the laser light several detectors are installed. The so-called Forward Scatter (FSC) is in line with the light beam and measures cell volume. Perpendicular to the beam several additional detectors are located that presents the Side Scatter (SSC). The SSC provides information about the granularity of a cell. Furthermore, different fluorescent detectors connected with optical filters can detect emitted light from fluorescent chemicals found attached or in the cytosol of a cell. These fluorescent dyes are conjugated with antibodies that binds to certain cell surface markers such as CD3 or cytosolic molecules such as the transcription factor FOXP3. The flow cytometer FACS Canto II is equipped with three different laser lights (405 nm, 488 nm and 633 nm) to illuminate cells tagged with a variety of different fluorescent dyes. All flow cytometry experiments were performed on this flow cytometer and analyzed with FlowJo software.

Analysis of cell surface antigens

Cells were diluted at 1 x 10^6 to 10 x 10^6 in 50 µl PBS. Flourochrome-conjugated monoclonal antibodies directed against the antigens of interest were added at a concentration of 10 µl/ml. After 30 minutes incubation at 4°C in the absence of light, cells were washed two times with PBS and finally re-suspended in PBS supplemented with 2% FCS for FACS analysis.

Analysis of intracellular antigens

For analyzing the intracellular transcription factor FOXP3, intracellular staining was performed by using the FOXP3 Staining Buffer Set (eBioscience). Initially, cell surface markers were labeled as described above. After surface

staining cells were centrifuged and re-suspended in fixation/permeabilization reagent. The fixation reagent guarantees the fixation of all bound surface antibodies, whereas the permeabilization reagent permeabilizes the cell membrane to enable the staining of intracellular antigens. Cells were incubated for 30 minutes at 4°C in fixation/permeabilization reagent and washed twice with Perm-Buffer. After washing the cells were re-suspended in 50 µl Perm-Buffer, and 10 µl/ml anti-FOXP3 antibody was added. Intracellular staining was performed for 30 minutes at 4°C in the absence of light. Finally, cells were washed two times with Perm-Buffer and re-suspended in PBS supplemented with 2% FCS for FACS analysis.

2.4 Cell culture

2.4.1 General culture conditions

All cell lines were cultured at 37°C and 5% CO_2 in tissue culture flasks. Cell culture procedures were executed with sterile reagents under a laminar flow hood. The concentration and viability of cells was determined by trypan blue staining. Trypan blue is a reagent that is not absorbed by viable cell. In dead cells, by contrast, the dye could pass the membrane and thereby stains cells blue. Thus, dead cells are visible in a distinctive blue color under the microscope and can be distinguished from viable cells. In order to stain death cells and count viable cells, 0,25% trypan blue in PBS was added in an appropriate dilution to cell suspensions. Cells were counted in a Neubauer hemocytometer under the microscope. The total number of cells per ml was calculated by multiplying the total cell number in one hemocytometer grid by the dilution factor and 10^4.

2.4.2 Murine tumor cell line

4T1 breast cancer (kindly provided by Dr. M. Wartenberg, Friedrich-Schiller-University, Jena, Germany) Colon-26 (CT26) (Cell Lines Service, Heidelberg, Germany), Colon-26 with inducible CCL22 expression (rtTA-CCL22-CT26), B16 melanoma F1 (LGC Promochem, Teddington, UK), mGC8 gastric cancer (kindly provided by Dr. med. J. Nöckel, LIFE-Center, University Clinic, Grosshadern, Germany) MethA sarcoma (kindly provided by Prof. W. Zimmermann,

LIFE-Center, University Clinic, Grosshadern, Germany) as well as Panc02 (kindly provided by Prof. C. Bruns, Department of Surgery, University of Munich, Germany) were maintained in complete DMEM or RPMI medium as described above. Tumor cells were split in a 1:10 dilution two times a week. Cells were detached with Trypsin-EDTA (0.25%), centrifuged (400 g, 7 minutes, 4°C), resuspended in fresh medium and transferred to culture flasks. All tumor cell lines were expanded for two to three passages upon receipt, stored in liquid nitrogen and freshly thawed prior each experiment.

2.4.3 Isolation of DC and T cells by magnetic cell separation

MACS (magnetic cell separation or magnetic-activated cell sorting) Technology from Miltenyi was used for the separation of magnetic labeled viable cells from lymphoid and non-lymphoid tissues.

For MACS separation cells are labeled with MACS MicroBeads which are superparamagnetic particles of approximately 50 nanometers in diameter and coated with antibodies against particular surface antigens. After cell labeling with these MicroBeads cells are applied on MACS columns. By a strong permanent magnet a high-gradient magnetic field is induced on the column matrix. Therefore, all labeled cells are retained in the column and all unlabeled cells pass through the column and can be collected. After removal of the column from the magnet, labeled cells can be released from the column and can also be collected. With MACS separation cells can be sorted by negative selection (= unbound fraction) and positive selection (= bound fraction).

Murine DC were separated from total spleen cells, lymphocytes or *ex vivo* tumor cell suspension with CD11c beads (= positive selection). Regulatory T cells were sorted from total spleen cells via a two-step procedure. First, non-CD4+ T cells were depleted by indirectly labeling with a cocktail of biotin-conjugated antibodies against CD8, CD14, CD16, CD19, CD36, CD56, CD123, TCR γ/δ and CD235a (glycophrin A) and Anti-Biotin MicroBeads (= negative selection). In a second step, the CD4+ flow-through fraction was labeled with CD25 MicroBeads for subsequent positive selection of CD4+CD25+ regulatory T cells.

In this study reagents from Miltenyi Biotec were used according to the manufacturer's instructions, and all cell separations were done according to manufacturer's protocol. In brief: Cells were labeled with the appropriate microbeads in MACS buffer for 15 minutes at 4°C and washed with MACS buffer. MS columns were placed in a magnet and equilibrated with 0.5 ml MACS buffer prior to loading the labeled cells in a volume of 0.5 ml. After washing the column with three times 0.5 ml MACS buffer, the column was removed from the magnet, and the bound fraction was eluted by flushing the cells in 1 ml MACS buffer through the column with the supplied plunger. If high purity of sorted cells was needed a second column purification step was performed. The purity of CD11c-sorted cells was 90% on average after one column purification. After a second column purification this purity was increased to more than 96%.

In the case of the two-step Treg separation procedure cells were incubated with a biotin antibody cocktail (including CD8, CD14, CD16, CD19, CD36, CD56, CD123, TCR γ/δ and CD235a). After 10 minutes at 4°C anti-biotin microbeads and CD25-PE antibody were added and incubated for another 15 minutes at 4°C. Afterwards, cells were washed with MACS buffer. A LD column was placed in a magnet and equilibrated with 2 ml MACS buffer prior to loading the labeled cells in a volume of 0.5 ml. The column was washed with three times 1 ml MACS buffer, and the flow through was collected. In the second separation step these CD4+ cells were incubated with anti-PE microbeads for 15 min at 4°C, washed with MACS buffer and applied in a volume of 0.5 ml onto a MS column (equilibrated with 0.5 ml MACS buffer). After washing the column, the column was removed from the magnet, and the bound fraction was eluted by flushing the cells in 1 ml MACS buffer through the column with the supplied plunger.

2.4.4 Toll-like receptor ligands treatment *in vitro*

For *in vitro* cultures murine tumor-infiltrating cells of CT26, B16 and Panc02 tumors were treated with 5 µg/ml CpG 1826 (Coley Pharmaceutical Group), 1000 U/ml murine interferon-alpha (IFN-α) (R&D Systems), 50 ng/ml murine interferon-gamma (IFN-γ) (Peprotech), 10 ng/ml murine IL-1β, IL-2, IL-6, IL-10 or IL-12 (all Peprotech), respectively.

2.4.5 Cell transfection

For cell transfection *in vitro* we cultured 1 to 4 x 10^4 cells per well in 96 well plates. For one well following transfection mixture was prepared: 2.0 to 5.0 µg plasmid was added to 10 µl Opti-MEM. The transfection reagent Lipofectamine 2000 was mixed with 10 µl Opti-MEM in a ratio of 5:1 to the amount of used plasmid DNA. Both mixtures were incubated for five minutes at room temperature, then combined and incubated for another 20 minutes. After 20 minutes the DNA and transfection reagent complex was added directly into the supernatant of cultured cells. Transfection efficiency was verified 24 hours post transfection.

2.4.6 Conditioned medium

Conditioned medium (CM) was produced by stimulating 5 x 10^5 splenocytes of C57BL/6 mice with 5 µg/ml CpG 1826 (Coley Pharmaceutical Group) for 2 hours, followed by extensive washing and culture in fresh medium for an additional 20 hours before removal and transfer of the supernatant into stimulation assays of murine tumor-infiltrating cells.

2.5 Animal experimental procedures

2.5.1 Animals

For this study female BALB/c and C57BL/6 mice were purchased from Harlan-Winkelmann (Borchen, Germany). IFN-I receptor (IFNAR)-deficient mice on C57BL/6 background were kindly provided by Dr. Z. Waibler (Paul-Ehrlich Institute, Langen, Germany). Mice were 6 to 10 weeks old at the onset of experiments. All mice were anesthetized with isoflurane for all interventions, but subcutaneous (s.c.) and intraperitoneal (i.p.) injections. Animal studies were approved by the local regulatory agency (Regierung von Oberbayern, Munich, Germany).

2.5.2 Organ and single cell preparation

Bone marrow-derived dendritic cell isolation: Femur and tibia were bilaterally dissected from sacrificed mice. Bones were cleaned with isopropanol, and bone marrow was extracted by flushing the bones with DC medium. The

obtained bone marrow was passed through a 40 µm cell strainer to gain a single cell suspension. Erythrocytes were lysed with ammonium chloride buffer, and remaining cells were cultured in DC medium supplemented with GM-CSF (20 ng/ml) and interleukin-4 (20 ng/ml). After seven days incubation differentiated DCs were harvested by gathering culture medium and rinsing culture flasks with cold PBS.

Spleen cell isolation: Mice were sacrificed by cervical dislocation, and spleens were removed. To get a single cell suspension, the obtained spleens were passed through a 40 µm cell strainer. Next, erythrocytes were lysed by resuspending the cells in red blood cell lysis buffer. After 2 minutes incubation the lysis was stopped by washing cells with PBS. Splenocytes were kept in T cell medium for further experiments.

Lymph node cell isolation: Mice were sacrificed. Brachial, axillary and inguinal lymph nodes were collected and passed through a 40 µm cell strainer. The through flow (= single cell suspensions) was centrifuged and resuspended in T cell medium.

Tumor-infiltrating leukocytes isolation: Tumors were removed from sacrificed mice, mechanically disrupted and incubated with 1 mg/ml collagenase and 0.05 mg/ml DNase (both Sigma Aldrich) at 37°C for 30 minutes. To obtain a single cell suspension, the tumors were passed through a 100 µm cell strainer followed by a 40 µm cell strainer. Suspended cells were layered on a gradient of 44% Percoll (upper phase) and 67% Percoll (lower phase) prior to centrifugation at 800 g for 30 minutes. The leukocytes from the interphase were collected and used for flow cytometry analysis or cell culture. These obtained tumor-infiltrating immune cells typically contained 1-2% B220+ cells (B cells), 17-20% CD11b+ cells (myeloid cells), 13-15% CD11c+ cells (DCs), 15% GR1+ cells (macrophages), 15% CD49b+ cells (NK cells), 5-6% CD3+CD4+ cells (Teffs) and 14% CD3+CD8+ cells (cytotoxic T cells). Defined by the expression of CD25 40% of the CD3+CD4+ fraction were Tregs (CD25+). The CD11c+ DC population can be subdivided in plasmacytoid DCs (pDCs) and conventional DCs (cDCs) according to the expression of B220. 20% of CD11c+ cells were pDCs (B220+) and 80% cDCs (B220-negative) (*Figure 6*).

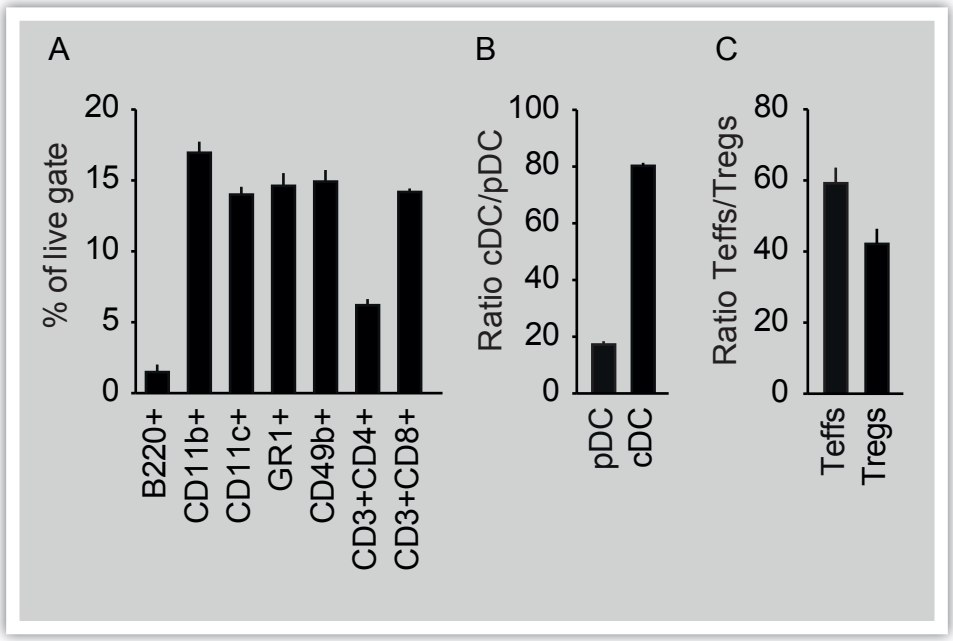

Figure 6: FACS analysis of tumor-infiltrating immune cells. To verify the composition of tumor-infiltrating immune cells three Panc02 tumors with a size of 100 mm^2 were dissected, immune cells isolated from the tumor tissue by Percoll density centrifugation and analyzed by FACS. (A) Cells were stained for different surface markers that define certain cell subsets of immune cells. The percentage indicates the amount of cells positive for a certain marker among all cells of the live gate. (B) The ratio of pDCs to cDCs was determined by the expression of B220. pDCs are the B220+ cells among all CD11c+ cells and cDCs are the B220-negative cells of all CD11c+ cells. (C) The ratio of Teffs to Tregs in tumor-infiltrating immune cells was calculated by the expression of the surface marker CD25. Teffs are the CD25-negative cells among CD3+CD4+ cells and Tregs are all CD25+ cells of the CD3+CD4+ cells. For CT26 and B16 tumors comparable cell distributions were observed among tumor-infiltrating immune cells. Error bars indicate SEM.

2.5.3 Toll-like receptor stimulation of mice

The fully PTO-modified CpG oligonucleotide 1826 (5'-TCCATGACGTT-CCTGACGTT-3') (Coley Pharmaceutical Group) was injected subcutaneously (100 µg CpG in PBS per mouse). Poly (I:C) (Amersham Bioscience) was applied intraperitoneally (250 µg in PBS per mouse).

2.5.4 Tumor experiments

For tumor induction 0.25 x 10^6 (CT26 and rtTA-CCL22-CT26) or 1.0 x 10^6 (B16 and Panc02) tumor cells were injected subcutaneously into the flank. Mice with subcutaneous rtTA-CCL22-CT26 tumors were fed with a normal or 25 mg/kg doxycycline-containing diet (provided by ssniff Spezialdiäten GmbH, Soest, Germany). The tumor size of individual tumors can be expressed as the product of the perpendicular diameters (= tumor area) or as the squared width divided by the bisected length

(= tumor volume) (Euhus *et al.*, 1986). All tumor sizes in this work were expressed as tumor area.

2.6 Statistical analysis

All data are presented as mean +/- SEM and were analyzed as appropriate by unpaired Student's t-test or by unpaired, one-way analysis of variance (ANOVA) with the Newman-Keuls multiple comparison test. Significance of survival time among different mouse groups was calculated by using the log-rank test. In all analyses $P < 0.05$ was set as point for significance. All statistic calculations were done with Prism GraphPad.

Results

3. Results

3.1 Source and impact of intratumoral CCL22

In this study we aimed to evaluate the impact of the chemokine CCL22 on anti-tumor immunity. To this aim we examined different mouse tumor models that allow evaluation of tumor progression in the presence or absence of CCL22.

3.1.1 CCL22 is expressed in murine tumors

As a first step we verified whether CCL22 is expressed in different subcutaneously established murine tumor entities *in vivo*. For this purpose six week old mice were subcutaneously injected with CT26 (colon carcinoma), B16 (melanoma), 4T1 (mammary cancer) or Panc02 (pancreatic cancer) tumor cells. After two weeks (approximate tumor size in length x width: 7 x 7 mm^2) tumors were dissected, and CCL22 levels were determined in tumor lysates by ELISA (*Figure 7*). In all tested murine tumors substantial intratumoral levels of CCL22 were observed. Serum CCL22 concentrations were used as reference.

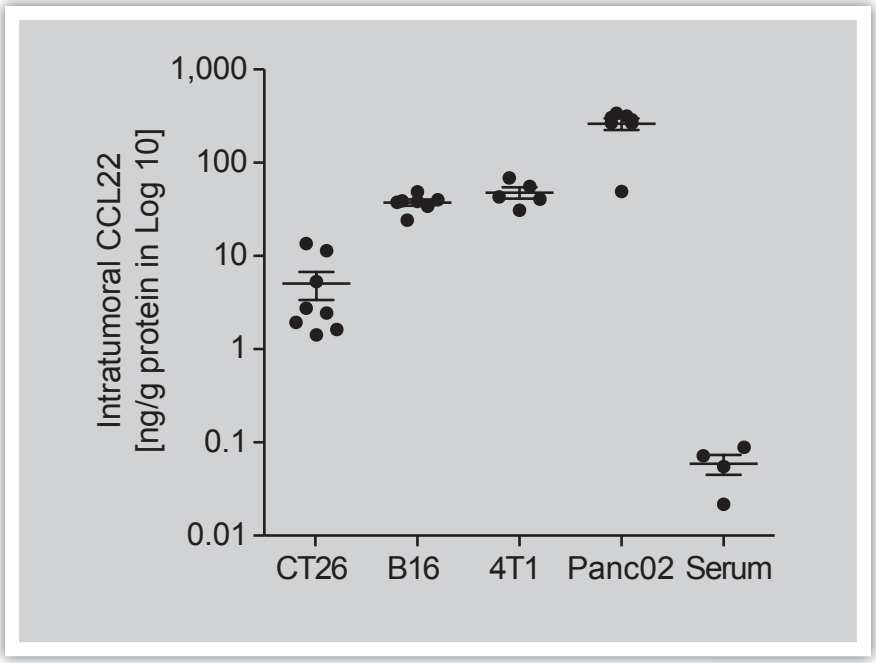

Figure 7: CCL22 levels in different murine tumor lysates. Intratumoral CCL22 levels of CT26 (n=5), B16 (n=7), 4T1 (n=5) and Panc02 (n=7) tumor homogenates were measured via ELISA. Intratumoral CCL22 levels are shown in comparison with serum CCL22 levels of tumor-bearing mice (n=4). Bars (—) indicate the mean CCL22 concentration per overall tumor protein.

The highest expression of CCL22 was observed in Panc02 tumors, whereas the lowest expression of all analyzed tumors was seen in CT26 tumors (100 times lower than in Panc02). In the spleen and the lymph nodes of tumor-bearing mice CCL22 levels were similar to the CCL22 levels measured in healthy wild-type mice. In the spleen we typically detected 50 to 60 ng CCL22 per g total protein and in the lymph node 300 to 500 ng CCL22 per g total protein.

3.1.2 Tumor cell lines do not secrete CCL22

Since CCL22 expression was observed in all tested murine tumor lysates, we aimed to identify the cellular source of intratumoral CCL22. In a first step we verified whether the tumor cells secrete CCL22. Therefore, we measured CCL22 levels in the culture supernatants of several different murine tumor cell lines. Strikingly, in all tested tumor cell supernatants no CCL22 expression was found (*Figure 8*). Thus, it is unlikely that the tumor cells themselves are the source of intratumoral CCL22.

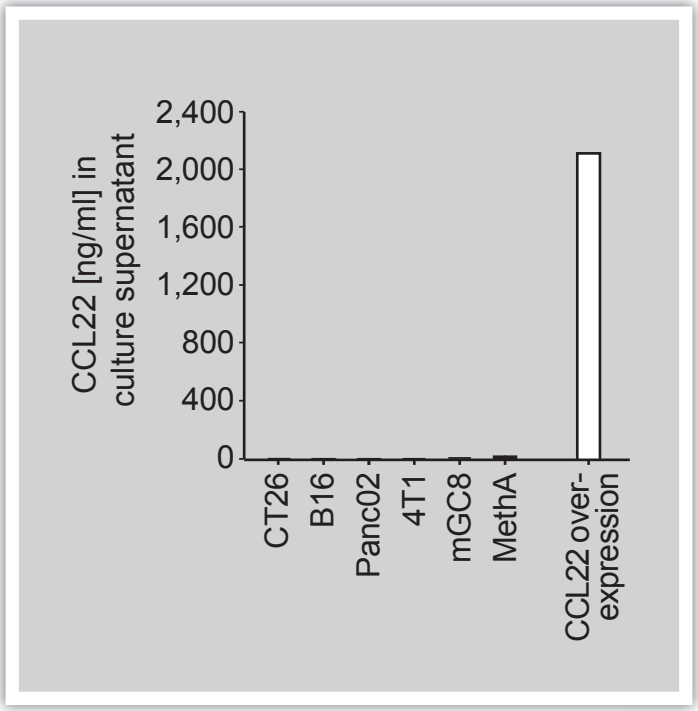

Figure 8: CCL22 levels in the culture supernatants of different tumor cell lines. Supernatants were analyzed for secretion of CCL22 by ELISA. CCL22 level in the supernatant of rtTA-CCL22-CT26 tumor cells was used as positive control (for rtTA-CCL22-CT26 cell line description see methods part *2.2.8*). Of each cell line 50.000 cells were cultured in triplicates in a 96 well plate. After two days CCL22 concentration in the culture supernatant was measured by ELISA. This experiment was repeated twice.

3.1.3 Intratumoral dendritic cells express CCL22

Since tumor cells are probably not the source of intratumoral CCL22, we hypothesized that tumor-infiltrating immune cells produce intratumoral CCL22. In murine tumors typically 2-4% of all cells are DCs, 2-3% are T cells, 4% are NK cells, 1% are NKT cells and 3% are B cells (source: dissertation Michaela Golic, Division of Clinical Pharmacology, LMU, Munich, 2010). In addition, Tang and Cyster described DCs as the main producer of CCL22 in lymph nodes of healthy mice (Tang and Cyster, 1999). To investigate whether DCs are also responsible for CCL22 expression in murine tumor tissue, we sorted single cell suspensions of subcutaneous murine tumors for CD11c+ cells. CD11c is a commonly used murine DC surface marker.

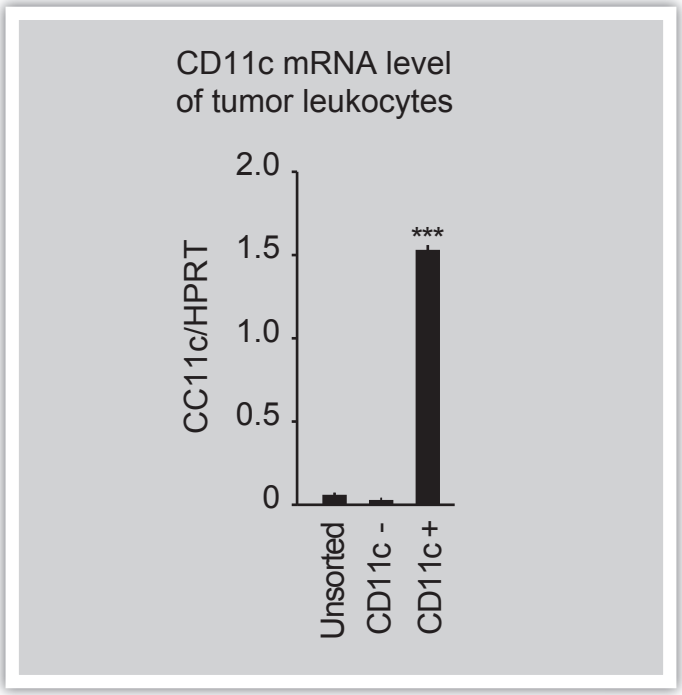

Figure 9: CD11c mRNA levels of sorted single cell suspensions of subcutaneous murine tumors. We used qRT-PCR to verify the CD11c expression of sorted single cell suspensions of subcutaneous murine tumors (n=5). For this purpose we measured CD11c mRNA levels of unsorted, CD11c-depleted and CD11c-enriched B16-infiltrating leukocytes. HPRT was used for normalization. The shown data are the result of two independently performed experiments. Error bars indicate SEM. P value of sorted CD11c+ cells was calculated relative to CD11c-depleted cells (***$p < 0.001$).

The purity of sorted single cell suspensions of subcutaneous murine tumors was confirmed by qRT-PCR and FACS analysis. We used qRT-PCR to measure CD11c mRNA levels of unsorted, CD11c-depleted and CD11c-enriched cells. As expected, low levels of CD11c were observed in unsorted tumor-infiltrating

leukocytes, whereas almost no CD11c was detected in CD11c-depleted leukocytes confirming the absence of CD11c-positive cells in this fraction. CD11c-enriched leukocytes showed high levels of CD11c mRNA (*Figure 9*).

The purity of the CD11c-enriched cells was further determined by FACS analysis. Therefore, isolated tumor leukocytes were stained with a CD11c antibody before and after CD11c MACS sort. More than 97% CD11c-positive cells were detected in the CD11c-enriched fraction confirming a high purity of this fraction. In unsorted tumor-infiltrating leukocytes 11.2% of the analyzed cells were positive for CD11c (*Figure 10*).

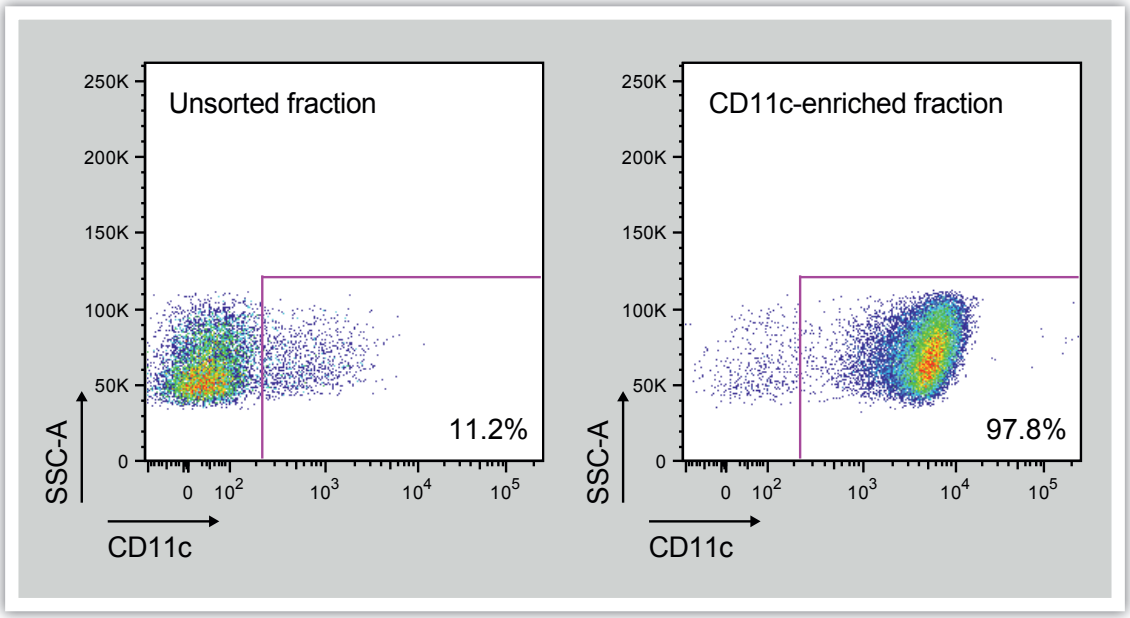

Figure 10: CD11c expression of unsorted and CD11c-sorted tumor-infiltration leukocytes. Left panel: 11.2% of unsorted cells were CD11c-positive. Right panel: 97.8% CD11c-positive cells were detected after a two column MACS sort in the fraction of CD11c-enriched cells. Shown is one representative FACS blot.

We measured CCL22 mRNA levels in freshly isolated CD11c-sorted cells of B16 tumors. In addition, CCL22 protein concentrations in the supernatants of *ex vivo* cultured sorted single cell suspensions of Panc02 tumors were determined by ELISA. Interestingly, CCL22 mRNA and protein were almost exclusively expressed by tumor-infiltrating CD11c+ cells (*Figure 11*), whereas almost no CCL22 was detectable in the CD11c-depleted fraction. In the unsorted condition only low CCL22 levels were observed. Thus, DCs appeared to be the exclusive producer of intratumoral CCL22.

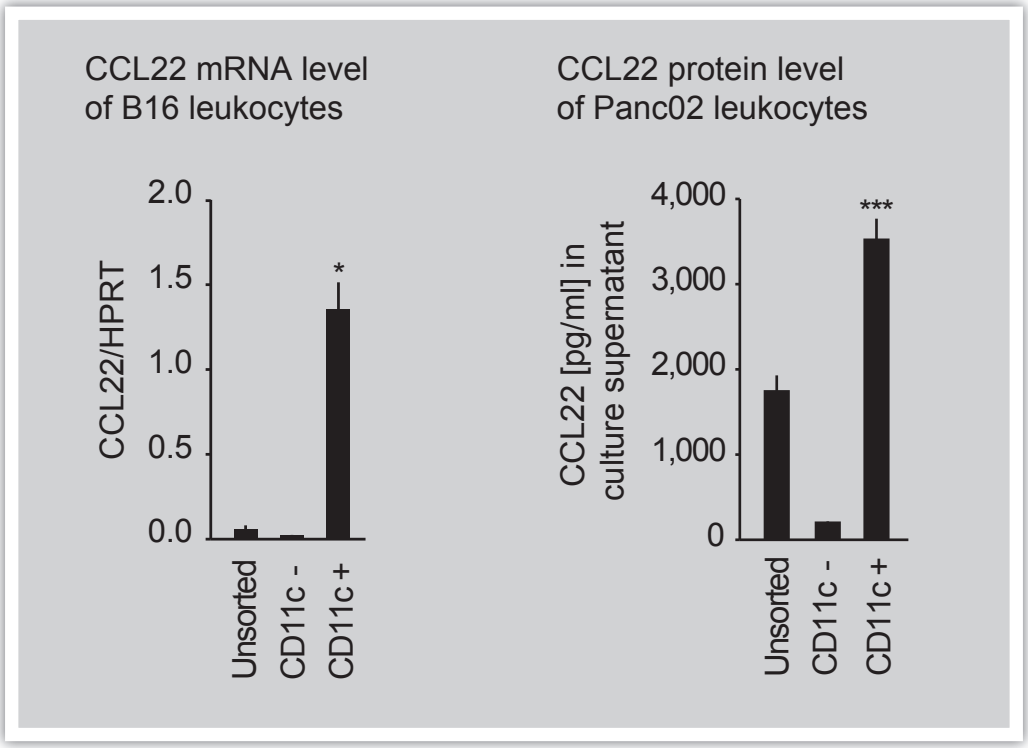

Figure 11: CCL22 mRNA and protein level of sorted single cell suspensions of subcutaneous B16 and Panc02 tumors. Mice received subcutaneously 1.0 x 10^6 B16 or Panc02 tumor cells (n=5, respectively). After tumors reached an average size of 100 mm^2 in length x width, tumors were resected, and single cell suspensions were prepared. Cells were sorted for CD11c+ cells (purity > 96%) and immediately used either for mRNA isolation (B16) or cell culture (Panc02). CCL22 mRNA level of B16-sorted single cell suspensions were analyzed by qRT-PCR and normalized to HPRT mRNA. Supernatants of cultured single cell suspensions of Panc02 tumors were collected after 72 hours, and CCL22 concentration was measured by ELISA. Overall mRNA levels and protein levels of three conditions were analyzed in triplicates: unsorted, CD11c-depleted (CD11c -) and CD11c-enriched (CD11c +) cells. The shown results were confirmed by repeating the experiment once. Error bars indicate SEM. P values of sorted CD11c+ cells were calculated relative to CD11c-depleted cells (*$p < 0.05$; ***$p < 0.001$).

3.1.4 CCL22 increases tumor growth and decreases survival

Since CCL22 is known to be a potent attractor of Tregs, a cell type described to promote tumor growth, we aimed to analyze the impact of intratumoral CCL22 levels on tumor growth and overall survival of tumor-bearing mice. For this purpose we generated a novel tumor cell line, specified as rtTA-CCL22-CT26 (see methods *2.2.8*. and *2.2.9)*. These tumor cells were transduced with a rtTA-CCL22 expression construct by lentiviral transduction. In cells that carry this construct, CCL22 expression is induced by doxycycline. In the presence of doxycycline the transactivator rtTA is active and promotes CCL22 expression, whereas in the absence of doxycycline rtTA is inactive, and induced CCL22 expression is blocked. The doxycycline-mediated inducibility

of CCL22 expression in rtTA-CCL22-CT26 tumor cells was verified *in vitro* and *in vivo*. After the administration of 2 µg/ml doxycycline, CCL22 expression was highly up-regulated in the supernatant of *in vitro*-cultured rtTA-CCL22-CT26 tumor cells. The same effect was observed *in vivo*. In rtTA-CCL22-CT26 tumor-bearing mice fed with a diet containing 25 mg/kg doxycycline, high intratumoral CCL22 levels were observed in comparison to rtTA-CCL22-CT26 tumor-bearing mice fed with normal diet (*Figure 12*).

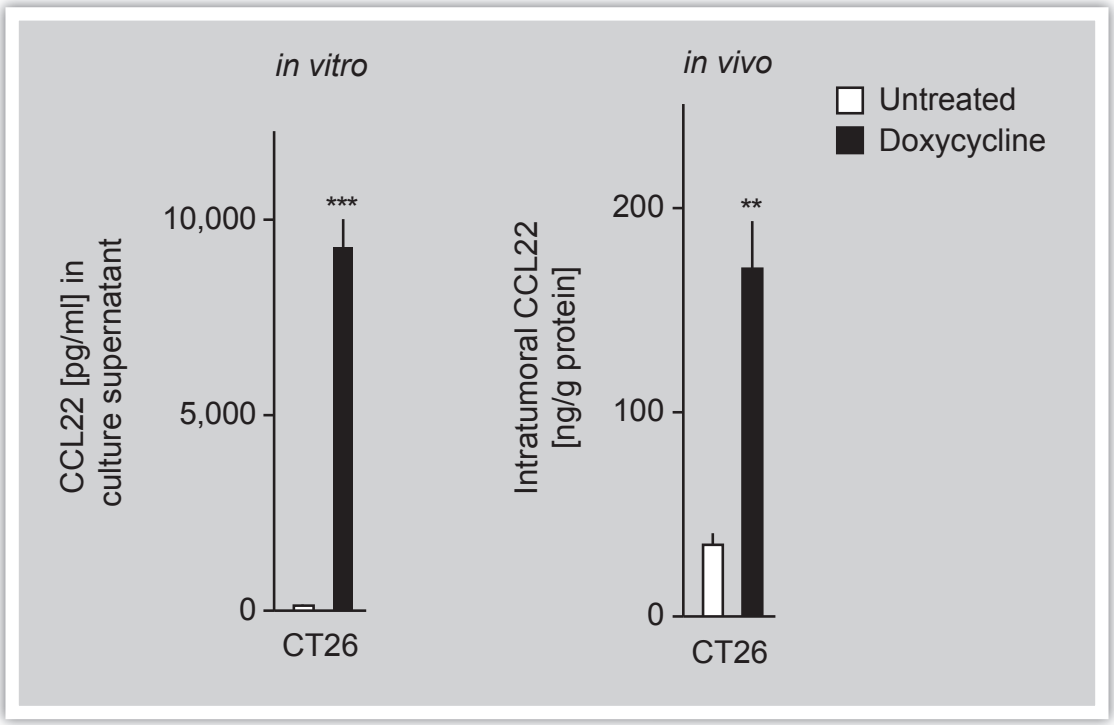

Figure 12: Doxycycline-dependent expression of CCL22 in vitro and in vivo. *Left figure:* 5 x 10^4 CT26 rtTA-CCL22-transduced tumor cells were cultured in a 96 well plate. 2 µg/ml doxycycline was added for 24 hours. CCL22 levels in the supernatant were measured in triplicates before and after doxycycline treatment. *Right figure:* Mice were subcutaneously injected with 1.0 x 10^5 rtTA-CCL22-CT26 tumor cells and divided into two groups. One group was fed with a normal diet (n=7) and the other group with doxycycline-containing (25 mg/kg) diet (n=7). After tumors reached a size of 225 mm^2 (length x width), mice were euthanized, tumors dissected, and CCL22 level was measured in the tumor lysates by ELISA. These experiments were repeated several times. Shown are the results of one representative experiment. Error bars indicate SEM (**p < 0.01; ***p < 0.001).

We aimed to investigate whether CCL22 affects tumor growth and disease outcome. Therefore, we compared the tumor growth and survival rate of rtTA-CCL22-CT26 tumor-bearing mice with and without doxycycline-induced CCL22 up-regulation. Strikingly, the over-expression of CCL22 had a clear impact on tumor growth. Mice treated with a doxycycline diet showed a significant faster tumor progression than mice fed with normal diet (*Figure 13*).

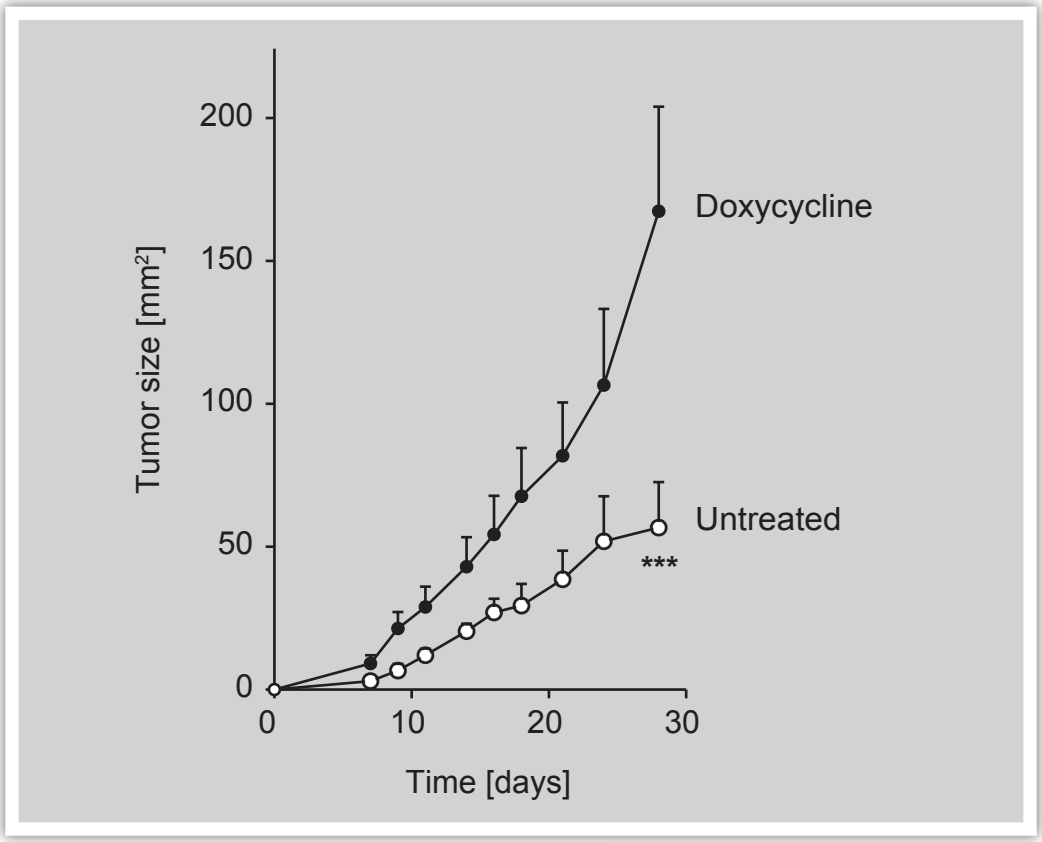

Figure 13: Tumor growth of rtTA-CCL22-CT26 tumors. Mice were subcutaneously injected with 1.0 x 10^5 rtTA-CCL22-CT26 tumor cells. Subsequently, mice were divided into two groups. One group was fed with a normal diet and the other group with doxycycline-containing (25 mg/kg) diet (n=7). Tumor size in length x width [mm^2] was measured every second day. Tumor growth was monitored for 30 days. These data were confirmed by repeating the experiment once. Error bars indicate SEM. P value of mice fed with normal diet was calculated according to mice fed with doxycycline diet (***$p < 0.001$).

In addition to tumor growth we determined the overall survival of rtTA-CCL22-CT26 tumor-bearing mice. Consistently with tumor progression mice with doxycycline-induced intratumoral CCL22 over-expression showed a lower survival rate compared to mice fed with normal diet (*Figure 14*).

Beside tumor growth we wanted to verify if CCL22 has also an impact on the ability of injected tumor cells to establish a solid tumor. Therefore, we used the same experimental model as described above, but injected only 5 x 10^4 rtTA-CCL22-CT26 tumor cells instead of 1.0 x 10^5 cells. This low dose of tumor cells is typically not sufficient to establish a tumor in the respective mouse. Indeed, five mice out of seven rejected the tumor one week after a small tumor was palpable and stayed tumor-free in the group fed with normal diet. However, in the group fed with doxycycline diet and thereby

induced CCL22 over-expression only one mouse out of seven stayed tumor-free and survived the monitored time period of 80 days (*Figure 15*). These results indicate that intratumoral CCL22 promotes tumor development.

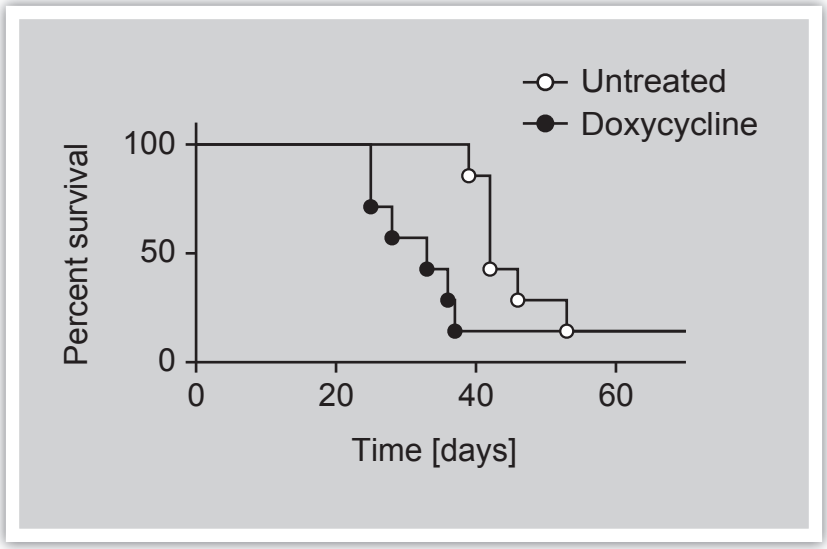

Figure 14: Overall survival of rtTA-CCL22-CT26 tumor-bearing mice. 14 mice were subcutaneously injected with 1.0 x 10^5 rtTA-CCL22-CT26 tumor cells. Seven mice were fed with a normal diet, and seven mice were fed with doxycycline-containing diet. Tumor size and health conditions of mice were monitored for 60 days. After a tumor reached a maximum size of 225 mm^2 in length x width, the corresponding mouse was euthanized. One mouse in each group rejected the induced tumor and survived the monitored time period of 60 days. In two follow-up experiments the same trend was observed.

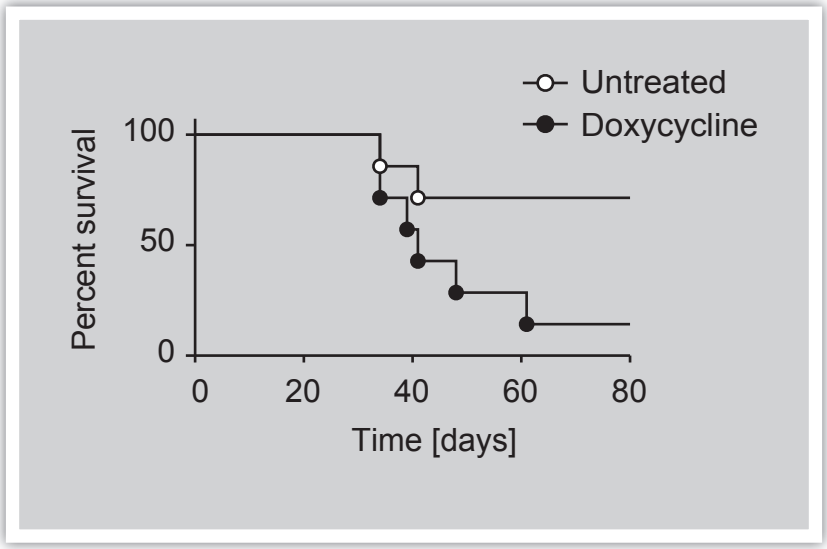

Figure 15: Overall survival of mice treated with a low dose of rtTA-CCL22-CT26 tumor cells. 14 mice were subcutaneously injected with 5 x 10^4 rtTA-CCL22-CT26 tumor cells. Seven mice were fed with a normal diet, and seven mice were fed with doxycycline-containing diet. Tumor size and health conditions of mice were monitored for 80 days. After a tumor reached a maximum size of 225 mm^2 in length x width, the corresponding mouse was euthanized. The shown results were confirmed in three follow-up experiments.

Next, we aimed to exclude that doxycycline itself contributes to the observed tumor progression. Therefore, we used untransduced CT26 tumor cells. Mice were subcutaneously injected with 1.0 x 10^5 CT26 tumor cells, and tumor growth was monitored for 30 days. In accordance with the previous experiment seven mice were fed with a doxycycline-containing diet, and seven mice received normal diet. We observed no differences in tumor growth between both groups indicating that doxycycline alone has no effect on tumor growth (*Figure 16*). Thus, the tumor-promoting effect is induced by CCL22 up-regulation and not by feeding mice with a doxycycline-containing diet.

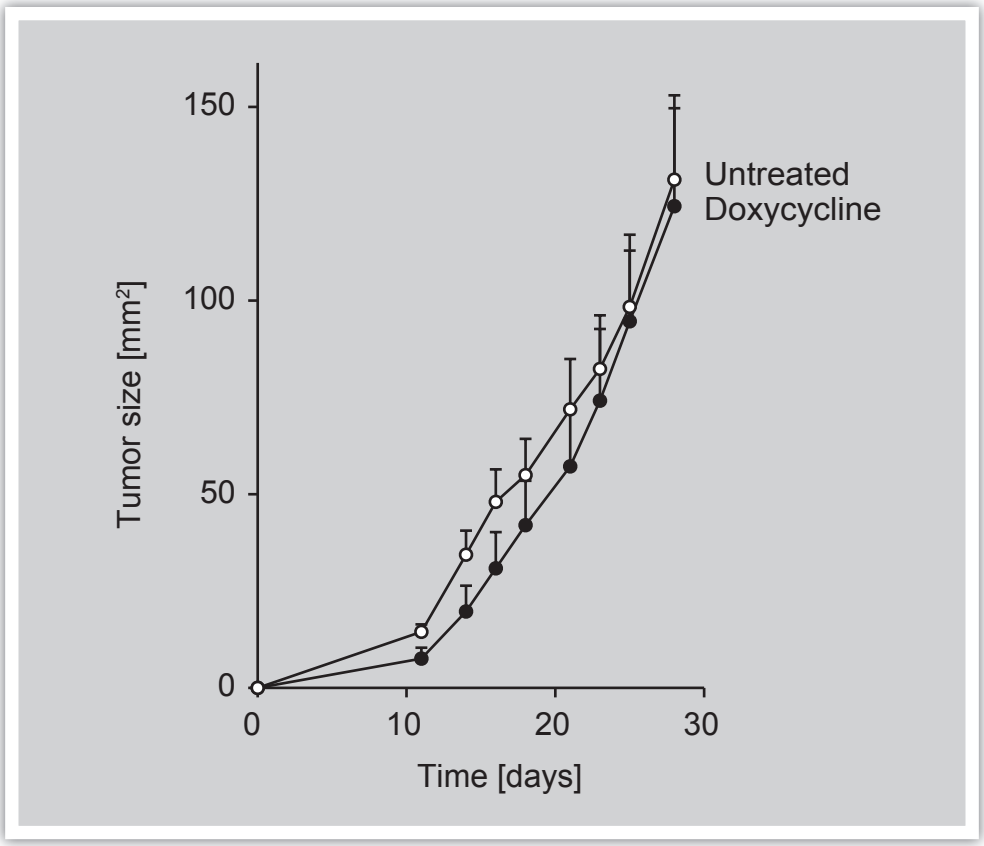

Figure 16: Tumor growth of CT26 tumors treated with doxycycline. Mice were subcutaneously injected with 1.0 x 10^5 CT26 tumor cells. Subsequently, mice were divided into two groups. One group was fed with a normal diet (n=7) and the other group with doxycycline-containing (25 mg/kg) diet (n=7). Tumor size in length x width [mm^2] was measured every second day. The experiment was repeated once. Error bars indicate SEM.

Finally, we verified if CCL22 has a direct effect on the replication of tumor cells. Therefore, the *in vitro* proliferation rate of untreated and doxycycline-treated rtTA-CCL22-CT26 tumor cells was measured by BrdU incorporation. No significant differences in cell replication were seen (*Figure 17*, left panel).

Additionally, the amount of induced CCL22 was confirmed by ELISA (*Figure 17*, right panel). In all conditions with doxycycline a high CCL22 expression was induced. Thus, CCL22 seems to have no direct effect on the proliferation rate of tumor cells. Only in the condition of tumor cells treated with the highest doxycycline dose a slight reduction of proliferation and CCL22 expression was observed indicating that high doxycycline levels could have a toxic effect.

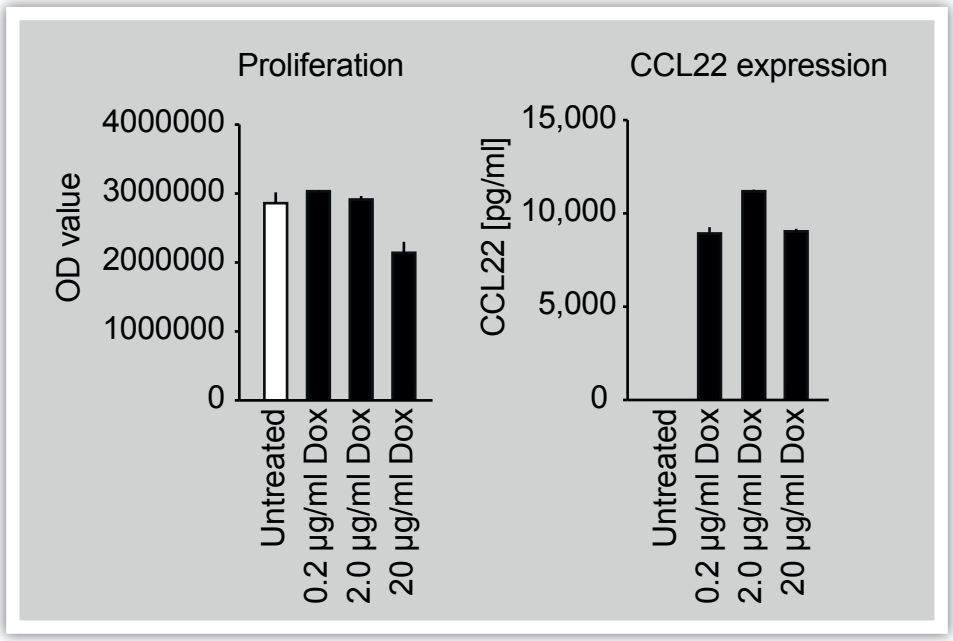

Figure 17: Proliferation rate and CCL22 expression of rtTA-CCL22-CT26 tumor cells treated with doxycycline. 40.000 rtTA-CCL22-CT26 tumor cells were cultured in triplicates without or with increasing amounts of doxycycline as indicated. Left panel: After 48 hours the cell proliferation rate was measured by BrdU ELISA. The optical density (OD) indicates the amount of incorporated BrdU into the DNA and thereby directly correlates with the replication rate of the analyzed cells (for further information see material and methods *2.3.2*). Right panel: The amount of produced CCL22 was quantified by ELISA in the supernatant of the cultured tumor cells collected prior BrdU ELISA. Shown is one of two performed experiments.

In conclusion, we identified DCs as the main producer of CCL22 in murine tumor tissue and showed here for the first time that CCL22 promotes tumor growth and reduces overall survival of tumor-bearing mice.

3.2 TLR-mediated intratumoral CCL22 regulation

In the previously described experiments we investigated the impact of intratumoral CCL22 on tumor growth and overall survival. Additionally, we

identified DCs as the main producer of intratumoral CCL22. Experiments done by Raffael Thaler and Dr. David Anz showed that the treatment of CT26 or B16 tumor-bearing mice with the synthetic TLR9 ligand CpG significantly reduces intratumoral CCL22 levels. CpG and other TLR agonists are known to suppress tumor growth and are currently investigated for their therapeutic potential in humans and mice.

TLR ligands such as CpG induce the secretion of inflammatory cytokines and thereby promote an anti-tumor immune response. For instance, the release of IFN-α after TLR activation enhances MHC-I expression on tumor cells. This in turn promotes cytotoxic T cell-mediated killing of these tumor cells. Overall, the precise mechanisms of TLR-induced tumor growth suppression are still not fully understood. Since CCL22 up-regulation promotes tumor growth and CCL22 down-regulation occurs during CpG-mediated tumor growth reduction, we hypothesized that CCL22 suppression is one of the major mechanisms that mediate TLR ligand-induced tumor regression. Therefore, the aim of the following experiments was to specify the mechanisms of TLR ligand-induced intratumoral CCL22 suppression and to verify the impact of this suppression on tumor immunity.

3.2.1 TLR ligands suppress intratumoral CCL22

First, we aimed to extend the previously in our group observed intratumoral CCL22 suppression to an additional experimental model. Since the measured CCL22 expression of Panc02 tumors is 10 times higher than in B16 tumors and even 100 times higher than in CT26 tumors, we wanted to verify if TLR ligands could also suppress Panc02 intratumoral CCL22 expression. Therefore, we treated B16, Panc02 or CT26 tumor-bearing mice with CpG. Consistent with the data from Raffael Thaler and Dr. David Anz a strong CCL22 down-regulation after CpG treatment in B16 and CT26 tumors was observed (*Figure 18*). Strikingly, although Panc02 tumors had the highest CCL22 expression of all screened subcutaneously tumor models (see *Figure 7*), TLR stimulation induced a significant suppression of intratumoral CCL22 in Panc02 tumors. Thus, CpG-mediated suppression was observed in all three tested tumor entities.

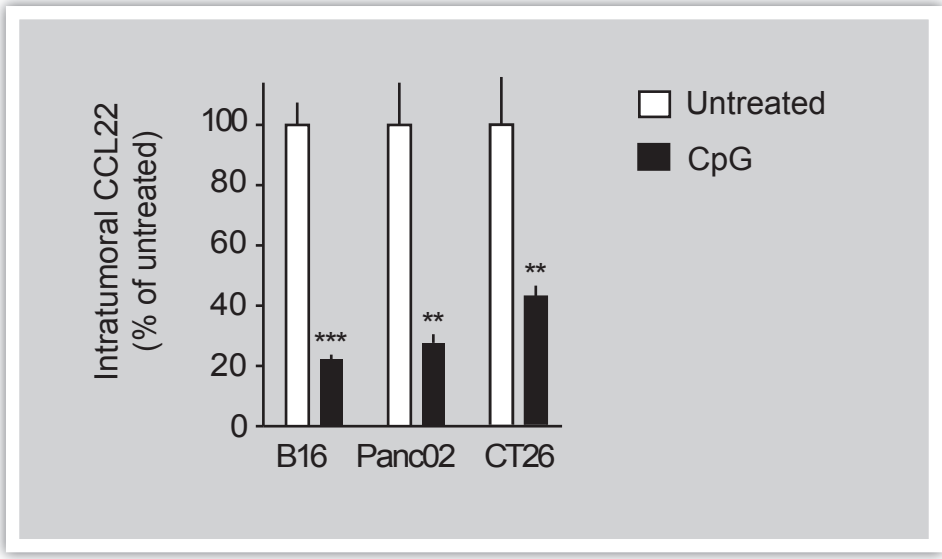

Figure 18: CCL22 levels in different murine tumor lysates after CpG treatment. Mice bearing established tumors (7 x 7 mm^2) received four injections of CpG (100 µg) at a four-day interval or stayed untreated. Two days after the last treatment B16 (n=6), Panc02 (n=5) and CT26 (n=10) intratumoral CCL22 levels of CpG-treated mice were measured by ELISA in the tumor homogenates (black bars). These levels were compared with CCL22 levels of B16 (n=7), Panc02 (n=7) and CT26 (n=11) tumor homogenates of untreated mice (white bars). Error bars indicate SEM. P values were calculated relative to untreated mice (**$p < 0.01$; ***$p < 0.001$).

We also verified whether intratumoral CCL22 expression is regulated by other TLR ligands than CpG. As shown in previous experiments by Raffael Thaler, the TLR3 and MDA-5 ligand poly (I:C) as well as the TLR7 ligand R848 suppress CCL22 in CT26 tumors. To evaluate whether other PRR ligands than CpG also suppress intratumoral CCL22 in murine tumors, we treated B16 tumor-bearing mice with the synthetic TLR3 and MDA-5 ligand poly (I:C). Therefore, mice with established B16 tumors received 250 µg poly (I:C). Two days after the injection of poly (I:C) tumors were dissected, and intratumoral CCL22 levels were measured by ELISA. Like CpG, poly (I:C) treatment resulted in a suppression of intratumoral CCL22 in B16 tumors (*Figure 19*). This indicates that the TLR ligand-mediated CCL22 suppression is a general phenomenon and not specific for a certain TLR ligand or tumor entity.

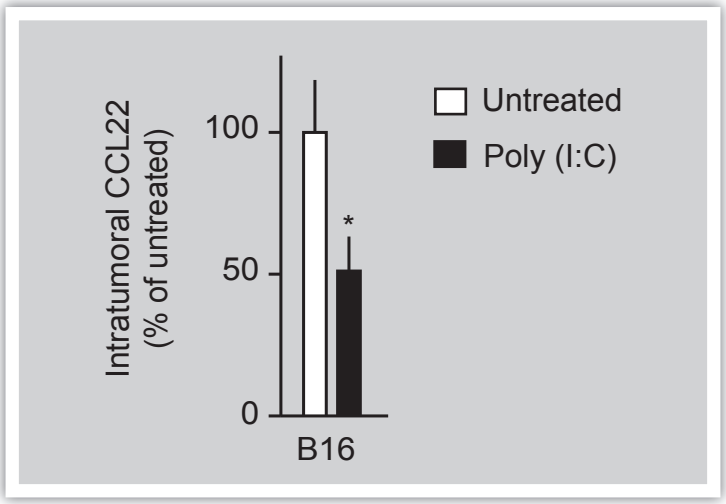

Figure 19: CCL22 levels in murine B16 tumor lysates after poly (I:C) treatment. Mice bearing established B16 tumors (7 x 7 mm^2) received one injection of poly (I:C) (250 µg) or remained untreated. Two days after treatment intratumoral CCL22 levels were measured by ELISA in the tumor homogenates of treated (n= 5; black bars) and untreated mice (n= 5; white bars). Error bars indicate SEM. P value was calculated relative to untreated mice (*p < 0.05).

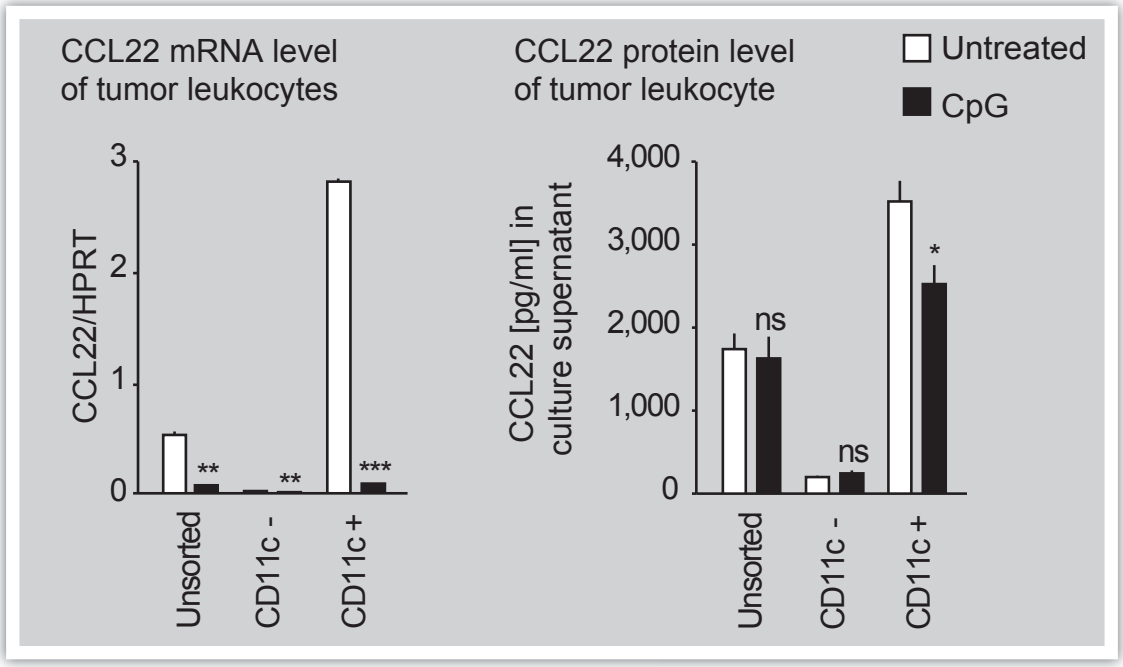

Figure 20: CCL22 mRNA and protein level of sorted single cell suspensions of subcutaneous Panc02 tumors after CpG treatment. Mice received subcutaneously 1.0 x 10^6 Panc02 tumor cells (n=5). After tumors reached an average size of 100 mm^2 in length x width, tumors were resected, and single cell suspensions were prepared. Subsequently, cells were sorted for CD11c (purity > 95%) and cultured in a 96 well plate. Triplicates of each fraction (unsorted, CD11c-depleted and CD11c-enriched cells) were either treated with 5 µg/ml CpG (black bars) or stayed untreated (white bars). After 72 hours supernatants were collected, and the remaining cells were used for mRNA isolation. Finally, CCL22 levels in the obtained supernatants were measured by ELISA, and qRT-PCR with the isolated mRNA was performed to verify CCL22 mRNA expression in the cultured cells. As a reference gene we used HPRT. The shown data were confirmed by repeating the experiment once. Error bars indicate SEM. P values of CpG-treated cells were calculated relative to untreated cells (*p < 0.05; **p < 0.01; ***p<0.001; ns indicates not significant).

Since we identified DCs as the main producer of intratumoral CCL22, we subsequently wanted to verify whether the treatment with TLR ligands can directly regulate the CCL22 secretion of tumor-infiltrating DCs. To answer this question, we used CD11c+ sorted single cell suspensions derived from subcutaneous Panc02 tumors. Unsorted, CD11c-depleted and CD11c-enriched intratumoral leukocytes were cultured either with 5 µg/ml CpG or without CpG. After 72 hours the levels of secreted CCL22 in the cell culture supernatants were measured by ELISA. The remaining cells were used for mRNA isolation and subsequent qRT-PCR.

On mRNA levels we observed a significant downregulation of CCL22 mRNA after CpG treatment for all fractions (unsorted, CD11c-depleted and CD11c-enriched). However, the most striking CCL22 mRNA suppression was observed in the CD11c-enriched fraction. A significant CCL22 downregulation also occurred on protein level for cultured CD11c-enriched cells, whereas no significant changes were observed in the unsorted and CD11c-depleted fractions (*Figure 20*). These data show that TLR ligands can directly suppress the CCL22 secretion of DCs.

3.2.2 CCL22 suppression is mediated by a soluble factor

Next, we wanted to know whether CCL22 suppression is mediated by a soluble factor that is released by DCs or if CpG has a direct intrinsic effect on DCs that suppresses CCL22 production. To answer this question, we stimulated splenocytes with or without CpG, removed CpG after two hours by extensive washing with PBS and harvested the supernatants after 24 hours. We termed these supernatants conditioned medium (CM) as they contain inflammatory factors induced by TLR stimulation, but not the TLR ligand itself. If CCL22 suppression is mediated by a soluble factor produced by DCs after TLR stimulation, this factor should be present in the conditioned medium of CpG-treated splenocytes. To verify this assumption, we cultured tumor-infiltrating immune cells with the conditioned medium of untreated and CpG-treated splenocytes (for cell composition of isolated tumor-infiltrating immune cells see Material and Methods part *2.5.2*). Interestingly, the CCL22 secretion of tumor-infiltrating immune cells cultured with conditioned medium of CpG-treated splenocytes was significantly reduced (*Figure 21*). This finding indicates that TLR ligand-mediated CCL22 suppression is induced by a soluble factor.

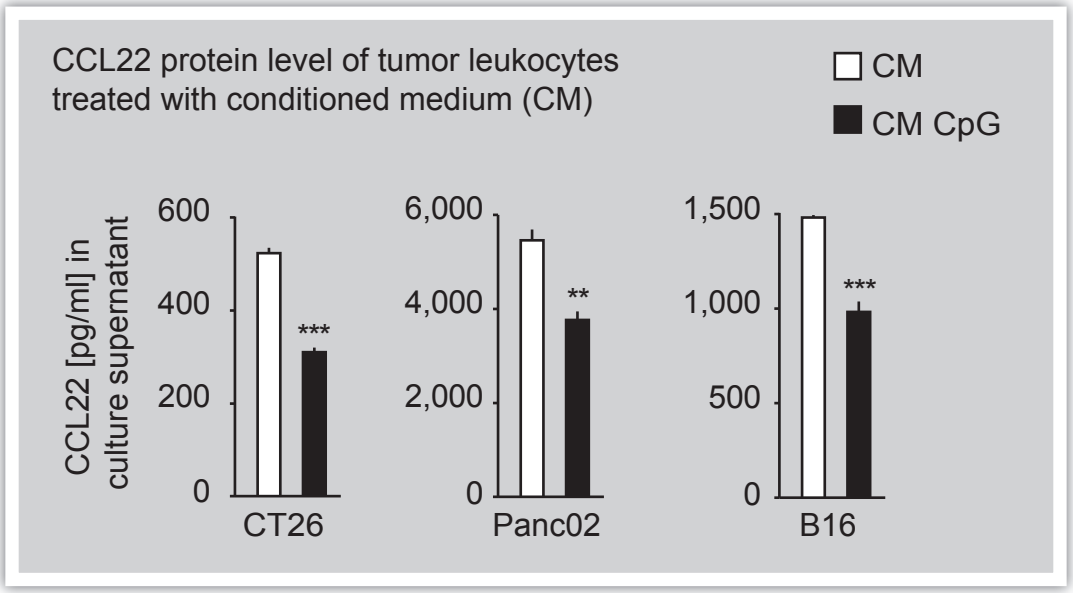

Figure 21: CCL22 levels of tumor-infiltrated leukocytes treated with conditioned medium. Tumor-infiltrating immune cells of subcutaneous CT26, Panc02 and B16 tumors (n=5, respectively) were isolated *ex vivo* by density centrifugation and cultured in triplicates for three days with conditioned medium gained from untreated splenocytes (CM) or conditioned medium obtained from CpG-treated splenocytes (CM CpG), respectively. Conditioned medium was obtained as described in the Material and Methods section. Subsequently, supernatant CCL22 levels were analyzed by ELISA. Shown are the representative results of two performed experiments. Error bars indicate SEM. P values of CM CpG-treated cells were calculated relative to CM-treated cells (**p < 0.01; ***p<0.001).

3.2.3 CCL22 suppression is mediated by IFN-α

Next, we performed stimulation experiments with several cytokines to identify the soluble factor that suppresses CCL22 secretion by tumor-infiltrating DCs. Therefore, we isolated tumor-infiltrating immune cells of freshly dissected subcutaneous Panc02 tumors by density centrifugation. After isolation these cells were cultured for three days with different recombinant cytokines that are typically released upon TLR stimulation. The appropriate cytokine concentrations were chosen according to titration experiments done by Stephan Eiber (Department of Clinical Pharmacology, LMU). In these experiments splenocytes of wild-type mice were treated with different amounts of the respective cytokines and the extent of CCL22 suppression was verified by ELISA. A significant CCL22 suppression was observed at a dose of 1000 U/ml IFN-α, 50 ng/ml IFN-γ, or 10 ng/ml IL-1β, IL-2, IL-6, IL-10 or IL-12, respectively (unpublished data). We used these concentrations to stimulate tumor-infiltrating immune cells. IL-10, IL-12, IFN-γ and IFN-α stimulation induced a significant CCL22 suppression. However, of all tested cytokines IFN-α was the most potent suppressor of CCL22 production (*Figure 22*). Thus, we chose this cytokine for further investigations.

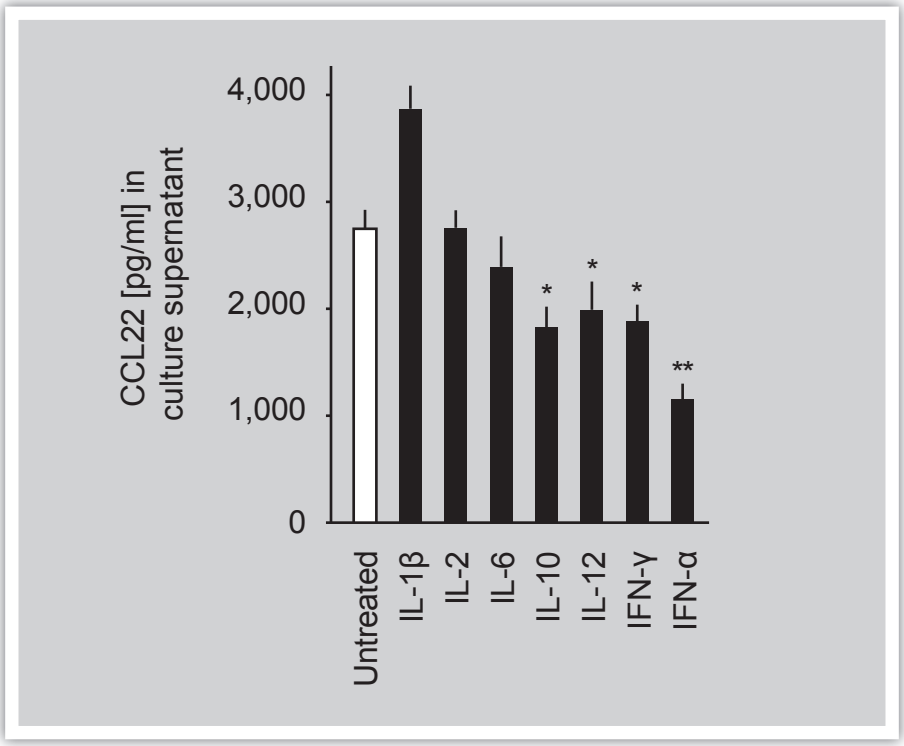

Figure 22: CCL22 protein level of tumor leukocytes treated with different soluble factors. Panc02-infiltrating immune cells of five tumor-bearing mice were treated *ex vivo* with different soluble factors as indicated or remained untreated. ELISA was used to measure CCL22 levels in the supernatants of triplicates after a three-day incubation. Error bars indicate SEM. P value of treated cells was calculated relative to untreated cells (*$p < 0.05$; **$p < 0.01$).

After identifying IFN-α as a potent CCL22 suppressor for Panc02 immune cells, we examined if IFN-α has the same effect on tumor-infiltrating immune cells of other tumor entities than Panc02. In analogy with the previous Panc02 experiment we cultured tumor-infiltrating immune cells from established subcutaneous CT26 and B16 tumors either in the presence or absence of IFN-α. As shown in *Figure 23* we observed a significant downregulation of CCL22 secretion after IFN-α treatment for both tumor entities.

Additionally, we investigated if IFN-α could also directly suppress the CCL22 secretion of intratumoral DCs. To answer this question, we sorted tumor-infiltrating immune cells of dissected Panc02 tumors for CD11c and cultured both CD11c-enriched and CD11c-depleted fraction with or without IFN-α. Strikingly, IFN-α treatment of CD11c+ cells caused a clear downregulation of CCL22 secretion. In contrast, untreated as well as IFN-α-treated CD11c negative cells secreted almost no CCL22 (*Figure 24*). In conclusion, these experiments showed that IFN-α directly suppresses CCL22 secretion of *ex vivo* obtained intratumoral DCs.

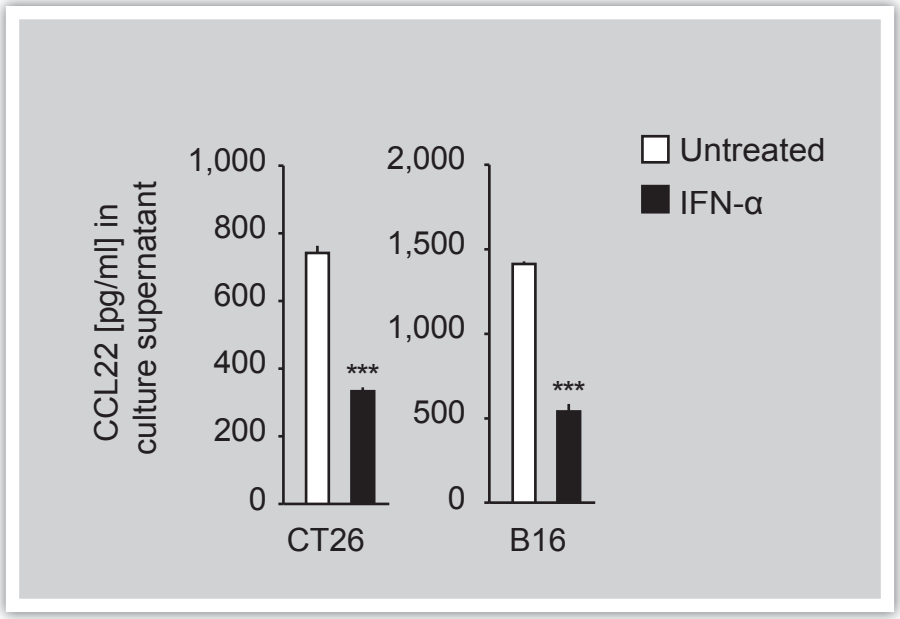

Figure 23: CCL22 protein level of tumor leukocytes treated with IFN-α. Freshly isolated tumor-infiltrating immune cells of subcutaneous CT26 (n=5) and B16 tumors (n=5) were either treated with IFN-α (black bar) or remained untreated (white bar). After three days of incubation, supernatants of triplicates were collected and CCL22 protein levels in the supernatants were measured by ELISA. Shown are the representative data of two independently performed experiments. Error bars indicate SEM. P value of IFN-α-treated cells was calculated relative to untreated cells (***$p < 0.001$).

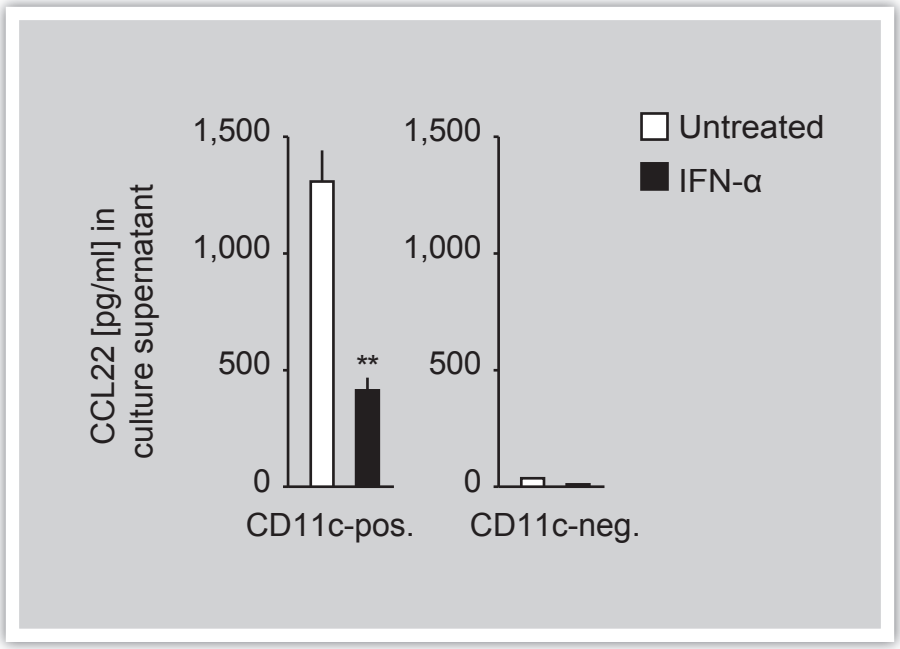

Figure 24: CCL22 protein level of CD11c-sorted tumor leukocytes treated with IFN-α. CD11c-sorted single cell suspensions (purity > 96%) of freshly isolated Panc02-infiltrating immune cells of five tumor-bearing mice were either treated with IFN-α (black bar) or remained untreated (white bar). After an incubation of three days, CCL22 protein levels in the supernatants were measured in triplicates by ELISA. Shown are the representative data of two independently performed experiments. The CD11c-negative fraction includes B cells, T cells, NK cells and macrophages (see also material and method part *2.5.2*). Error bars indicate SEM. P value of IFN-α-treated cells was calculated relative to untreated cells (**$p < 0.01$).

3.2.4 TLR-induced CCL22 suppression is abrogated in IFNAR mice

To test the impact of IFN-α on TLR-mediated intratumoral CCL22 downregulation, we performed *in vivo* tumor experiments with interferon-receptor-type-1 deficient (IFNAR) mice, kindly provided by Dr. Z. Waibler (Paul-Ehrlich Institute, Langen, Germany). IFNAR mice carry a knockout mutation in the coding region of the type-1-interferon-receptor. The knockout was achieved by integrating a neomycin cassette into exon 3 of the type-1-interferon-receptor gene. Since these mice cannot respond to IFN-α and IFN-β (Müller *et al.,* 1994), no suppression of intratumoral CCL22 should be induced by TLR stimulation.

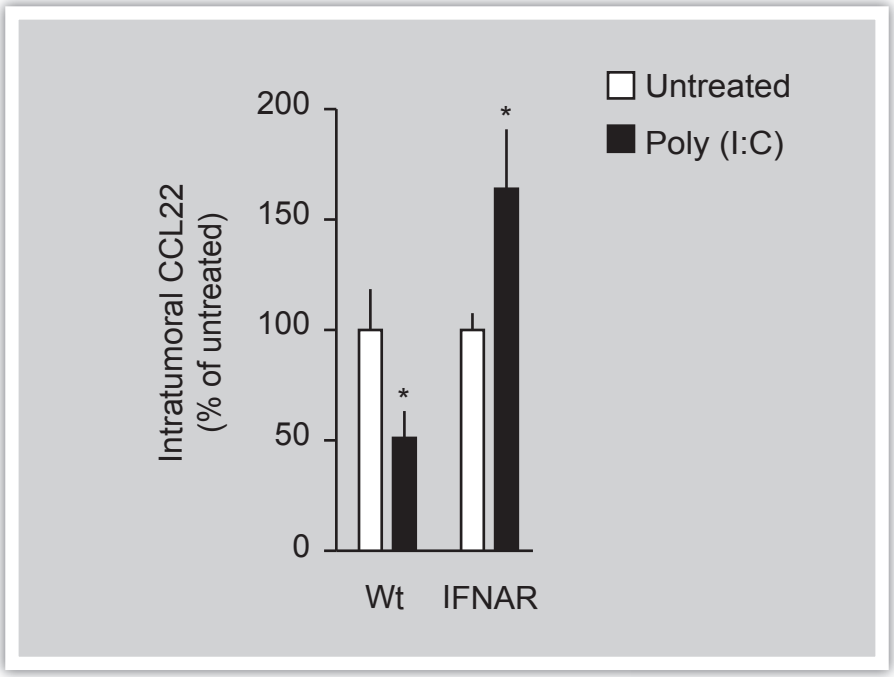

Figure 25: Intratumoral CCL22 levels of poly (I:C)-treated B16 tumor-bearing wild-type and IFNAR mice. Subcutaneous B16 tumors (1.0 x 10^6 cells per mouse) were induced in C57BL/6 (n=10) or type-I-interferon-receptor knockout (IFNAR) mice (n=10). On day nine after tumor induction both groups were either treated with poly (I:C) (250 µg per mouse) or remained untreated. Seven days after poly (I:C) injection, tumors were prepared, and CCL22 levels of homogenates were measured by ELISA. Also the tumor growth was monitored during the entire experiment (see next figure). Due to limited mouse availability this experiment was performed once. Error bars indicate SEM. P values of poly (I:C)-treated mice were calculated relative to untreated mice (*$p < 0.05$).

To verify this hypothesis, we subcutaneously injected B16 tumors into IFNAR and wild-type C57BL/6 mice. Both mice strains share the same genetic background. After a solid tumor was established, mice of both strains were either treated with the TLR3 and MDA-5 ligand poly (I:C)

or stayed untreated. We monitored tumor growth every second day and measured intratumoral CCL22 levels after dissecting the tumors 16 days after tumor induction.

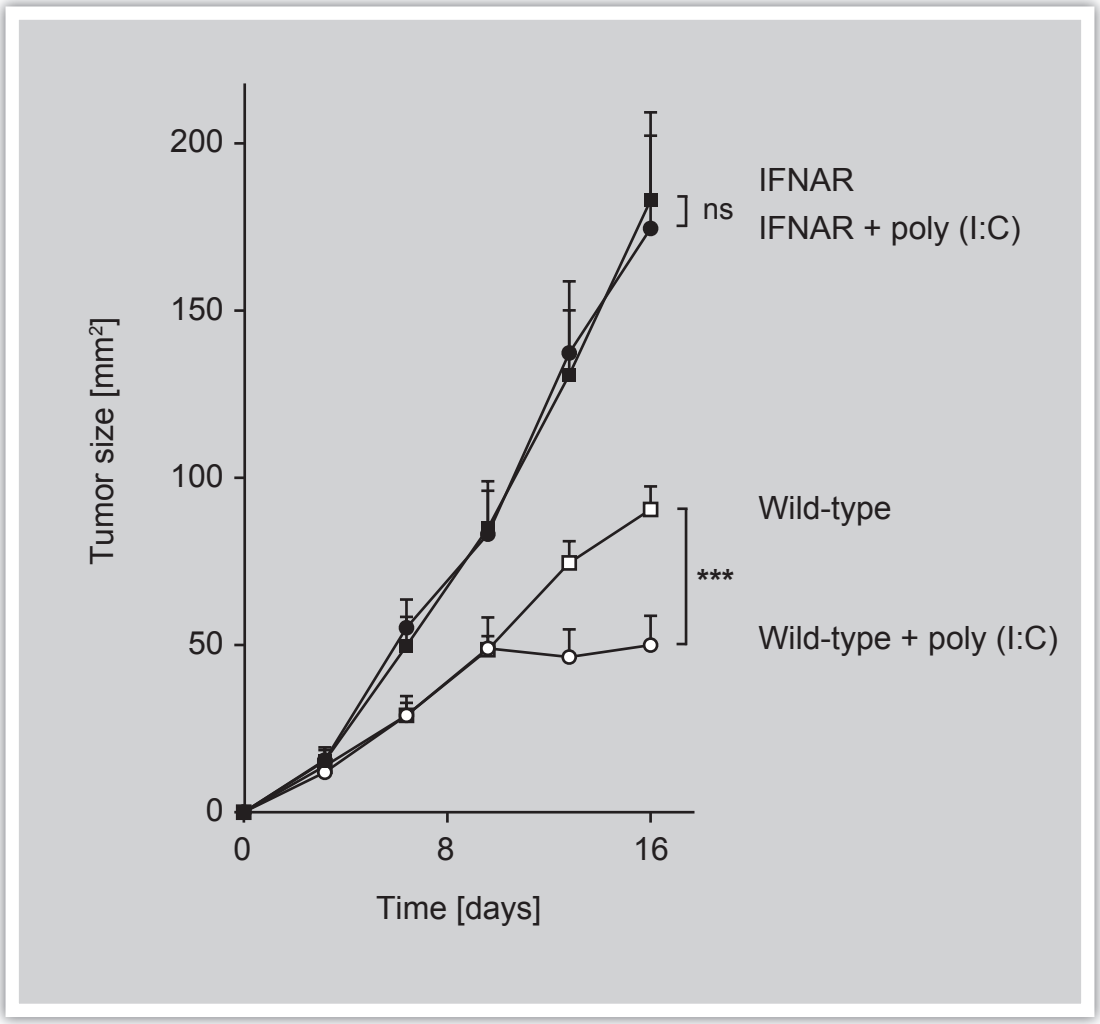

Figure 26: Tumor growth of poly (I:C)-treated B16 tumor-bearing wild-type and IFNAR mice. Subcutaneous B16 tumors were induced in C57BL/6 wild-type (n=10) as well as IFNAR mice (n=10), and poly (I:C) treatment was done as described above. Tumor growth in length x width [mm²] was measured continuously for 16 days after tumor injection. Error bars indicate SEM. P values were calculated relative to untreated mice (***p < 0.001, ns indicates not significant).

Consistent with previous reports, poly (I:C) leads to a significant tumor growth reduction in wild-type mice compared to untreated tumor-bearing wild-type mice. The tumor growth of IFNAR mice was accelerated compared to wild-type mice (*Figure 26*). However, this observation is a known effect in IFNAR mice. Since IFN-α is involved in many anti-tumoral immune regulations such as anti-angiogenesis, cell differentiation, tumor cell apoptosis as well as DC maturation, survival and antigen cross-presentation

IFN-α-unresponsiveness leads to increased tumor growth in IFNAR mice (Tarhini *et al.*, 2012; Kirkwood *et al.*, 2002; Wang *et al.*, 2007; Paquette *et al.*, 1998; Krown *et al.*, 1984).

Strikingly, the TLR ligand-mediated suppression of intratumoral CCL22 was not only abrogated in IFNAR mice, but even increased (*Figure 25*). Furthermore, no anti-tumoral therapeutic effect of TLR treatment was seen in tumor-bearing IFNAR mice (*Figure 26*). In summary, these results indicate that IFN-α is a key mediator in TLR ligand-induced intratumoral CCL22 suppression. Additionally, CCL22 suppression could contribute to the therapeutic effects of TLR ligands.

3.2.5 CCL22 contributes to TLR-mediated anti-tumor immunity

The previously described tumor experiment in IFNAR mice showed that IFN-α mediates the PRR-induced CCL22 suppression in tumor-bearing mice. In addition, the therapeutic effect of poly (I:C) treatment was abrogated in IFNAR mice. However, the contribution of CCL22 suppression blockade to this effect is very unclear since a type-1-interferon-receptor knockout influences many pathways in tumor-bearing mice. To evaluate the contribution of CCL22 suppression to the PRR-induced anti-tumor immune reaction, we performed an additional TLR stimulation tumor experiment with the novel generated rtTA-CCL22-CT26 tumor cell line (see Materials and Methods part *2.2.9*).

As shown in *Figure 12*, by feeding rtTA-CCL22-CT26 tumor-bearing mice with doxycycline, intratumoral CCL22 was up-regulated. We assumed that this up-regulation would abrogate TLR-mediated suppression of CCL22. Since in this experiment only the CCL22 suppression is blocked, the exclusive impact of CCL22 in CpG-induced tumor therapy could be elucidated.

We injected mice with 2.5 x 10^5 rtTA-CCL22-CT26 tumor cells subcutaneously. Overall 56 mice received tumors. 28 mice were fed with normal diet, and 28 mice were fed with doxycycline-containing diet. Three weeks after tumor induction 14 mice of each group were treated three times every third day with CpG. Tumor growth in length x width [mm^2] was monitored continuously for 32 days after tumor injection.

As expected in the group with no induced CCL22 over-expression (= fed with normal diet), CpG treatment resulted in a clear tumor growth reduction compared to untreated mice. Strikingly, in the group with doxycycline-induced CCL22 over-expression the CpG treatment had only a very poor therapeutic effect (*Figure 27*).

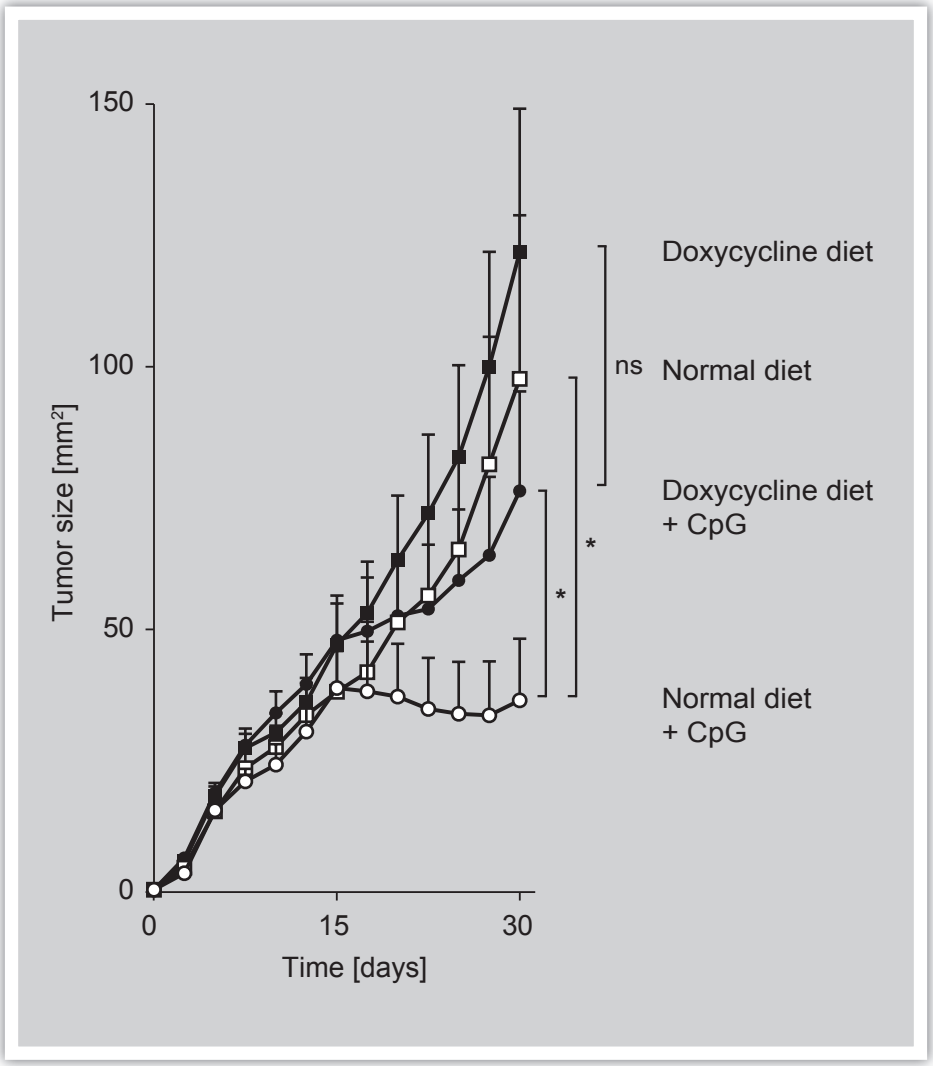

Figure 27: Tumor growth of CpG-treated rtTA-CCL22-CT26 tumor-bearing mice. BALB/c mice were inoculated with subcutaneous rtTA-CCL22-CT26 tumors and fed with a normal (n=28) or doxycycline-containing (n=28) diet. On day 21 after tumor induction both groups were either treated three times at a three-day interval with CpG (100 µg per mouse) or remained untreated. For each group the mean tumor growth of untreated and CpG-treated mice is shown. Tumor size [mm^2] was measured every second day. Shown are the combined data of three independently performed experiments. Error bars indicate SEM. P value of CpG-treated mice fed with normal diet was calculated relative to untreated mice fed with normal diet and CpG-treated mice fed with doxycycline diet (*$p < 0.05$, ns indicates not significant).

After the tumor growth of all mice was monitored for 32 days, we wanted to verify if the doxycycline-induced over-expression of CCL22 indeed blocked the CpG-mediated CCL22 suppression in the tumors. Therefore, the mice were sacrificed, tumors dissected and CCL22 levels were measured in the obtained tumor lysates. As expected in mice fed with a normal diet, CpG treatment significantly reduced intratumoral CCL22 expression (*Figure 28 A,* white and black bar on the left). However, in mice fed with doxycycline no significant difference in intratumoral CCL22 expression was observed between CpG-treated and untreated mice (*Figure 28 A,* white and black bar on the right). Thus, the doxycycline-induced CCL22 over-expression efficiently compensated the CpG-mediated CCL22 suppression in the tumor tissue. In summary, these results show that by blocking the TLR ligand-induced intratumoral CCL22 suppression, the TLR ligand-caused anti-tumor immunity is significantly reduced. Thus, the suppression of intratumoral CCL22 is important for TLR ligand-mediated anti-tumor immunity.

3.2.6 Suppression of intratumoral CCL22 reduces intratumoral Treg numbers

As mentioned above the chemokine CCL22 attracts Tregs. Consistent with the suppression of CCL22 after TLR stimulation previous experiments done by Dr. David Anz have shown that TLR stimulation also selectively reduces the amount of intratumoral Tregs. Since doxycycline-induced CCL22 over-expression compensates TLR ligand-induced CCL22 suppression, we hypothesized that thereby also the reduction in Treg tumor infiltration is abolished. To verify this assumption, we used flow cytometry to determine the amount of intratumoral Tregs. These levels were compared with the corresponding intratumoral CCL22 levels measured by ELISA. For this experiment we used the same mouse groups as described in the last result subsection (see part *3.2.5*).

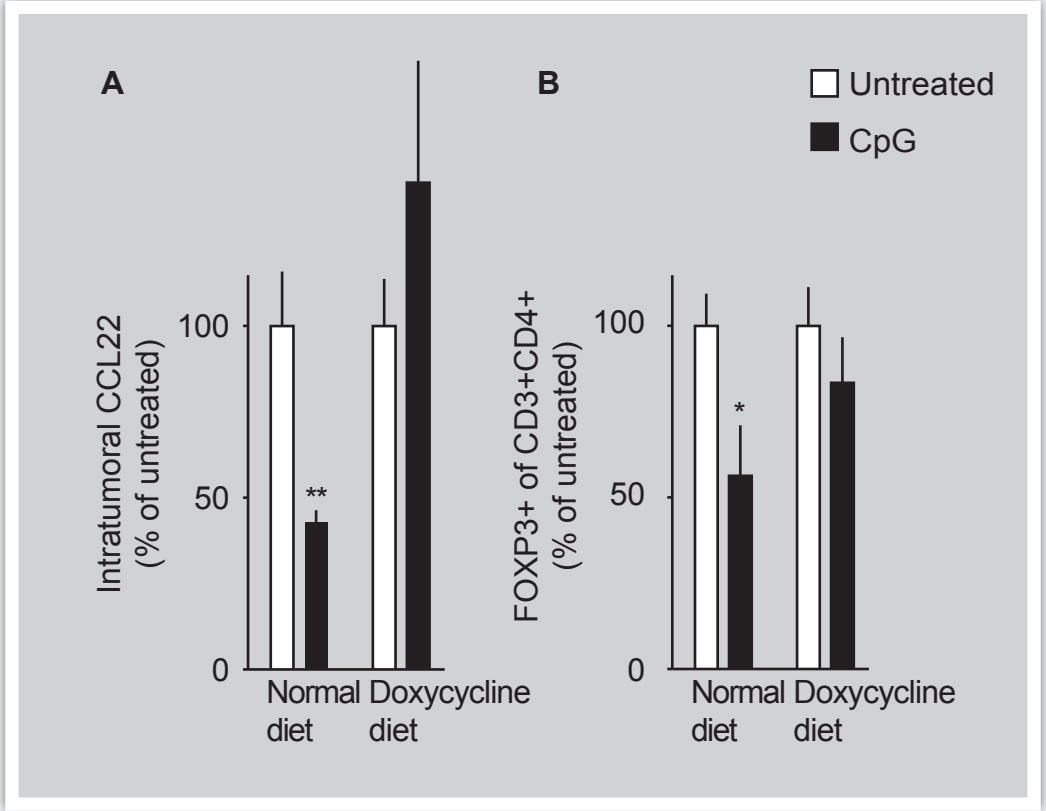

Figure 28: Intratumoral CCL22 and Treg levels of mice bearing rtTA-CCL22-transduced CT26 tumors. Mice with subcutaneous rtTA-CCL22-CT26 tumors were fed with a normal (n=28) or doxycycline-containing (25 mg/kg) diet (n=28). On day 21 after tumor induction both groups were either treated three times at a three-day interval with CpG or remained untreated. One day after the last injection, tumors were prepared. (A) CCL22 levels of homogenates were measured by ELISA, and (B) intratumoral levels of Tregs were analyzed by flow cytometry. Tregs were defined as FoxP3+ cells of CD3+CD4+ cells of the live gate. Shown are the combined data of three independently performed experiments. Error bars indicate SEM. P values were calculated relative to untreated mice (*$p < 0.05$; **$p < 0.01$).

As expected the CpG-mediated intratumoral CCL22 suppression (*Figure 28 A,* white and black bar on the left) led to a significant decrease of intratumoral Treg counts in tumor-bearing mice (*Figure 28 B,* white and black bar on the left). In contrast, the levels of other T cell subsets such as CD8+ cytotoxic T cells were not altered (*data not shown*). However, consistent with the unchanged intratumoral CCL22 levels of CpG-treated doxycycline fed mice, also the amount of intratumoral Tregs remained unchanged (*Figure 28 B,* white and black bar on the right). Thus, in mice fed with doxycycline CpG treatment failed to reduce intratumoral Treg numbers. *Figure 29* shows a representative FACS blot of each group. In conclusion, blockade of TLR ligand-mediated CCL22 suppression abolished the reduction of intratumoral Tregs and by this mean eventually abrogated the therapeutic effect of TLR stimulation.

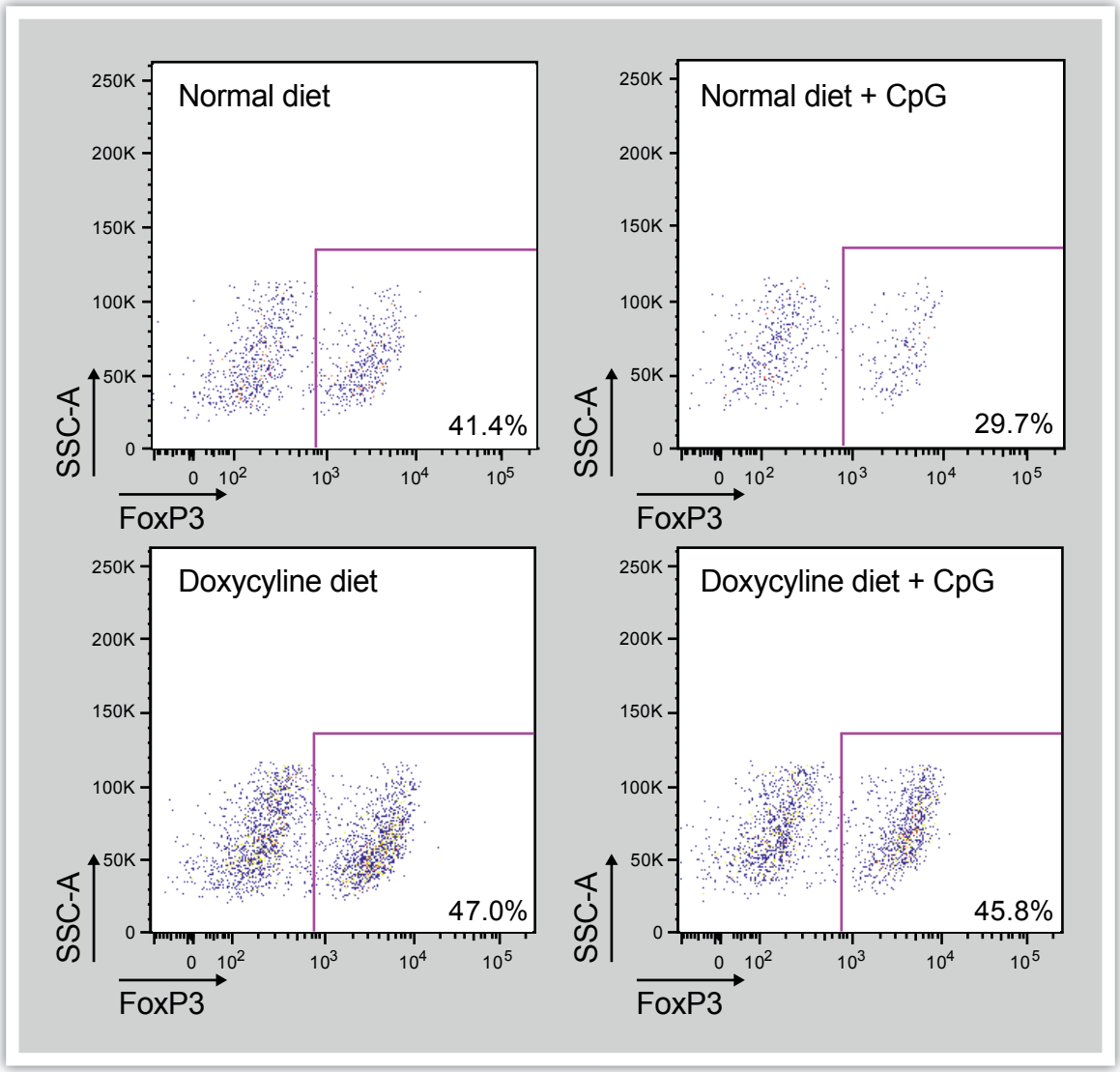

Figure 29: Intratumoral Treg levels of CpG and untreated mice bearing rtTA-CCL22-CT26 tumors. Mice with subcutaneous rtTA-CCL22-CT26 tumors were fed with a normal (n=28) or doxycycline-containing (25 mg/kg) diet (n=28). On day 21 after tumor induction both groups were either treated three times at a three-day interval with CpG or remained untreated. One day after the last injection, tumors were prepared and analyzed by FACS. The indicated numbers represent the percent of Tregs, defined as FOXP3+ cells, among CD3+CD4+ cells of the live gate. Shown is one representative FACS blot of each group.

3.3 Mouse models to verify the function of CCL22 in tumors

The experiments shown previously illustrated the impact of intratumoral CCL22 over-expression. For these experiments we used a tumor cell line with inducible CCL22 expression. However, as shown in part *3.1.2*, not the tumor cells are the main producer of CCL22 *in vivo*, but tumor-infiltrating DCs. To further investigate the impact of intratumoral CCL22, we decided to use

two different approaches. First, we generated a novel mouse line with DC specific CCL22 over-expression to verify the impact of increased DC-produced CCL22. Secondly, we used a newly generated CCL22 KO mouse line (National Institutes of Health) to investigate the effect of CCL22 depletion on tumor development and tumor growth.

3.3.1 Generation of a transgenic mouse with inducible DC-specific CCL22 expression

To generate a novel mouse line with inducible DC-specific CCL22 over-expression, two different mouse lines were needed, one mouse line transgenic for the construct CD11c-rtTA and one transgenic for TRE-CCL22. The CD11c-rtTA mouse was kindly provided by Dr. Leo Lefrancois (Connecticut, USA), and the TRE-CCL22 mouse was newly generated in cooperation with Dr. Marlon Schneider (Genzentrum, LMU).

In the CD11c-rtTA mouse CD11c regulates the expression of the tet-On advanced transactivator (rtTA). CD11c is a promoter sequence specifically active in dendritic cells. Thus, rtTA should be only expressed in DCs. In the TRE-CCL22 mouse the tetracycline response element (TRE) regulates the expression of CCL22. The activator element rtTA can bind the antibiotic doxycycline. The antibiotic binding leads to a conformation change of rtTA. This conformation change enables rtTA to bind to the promoter TRE which in turn is activated and initiates CCL22 expression. Hence, in a dendritic cell containing both constructs, CD11c-rtTA and TRE-CCL22, there are two possible scenarios. In the absence of doxycycline, TRE-mediated expression of CCL22 is blocked (*Figure 30*), whereas in the presence of doxycycline TRE activates expression of CCL22 (*Figure 31*). In all other cells CD11c is not active, and the activator rtTA is not expressed. Thus, in these cells CCL22 expression is not induced in the presence of doxycycline.

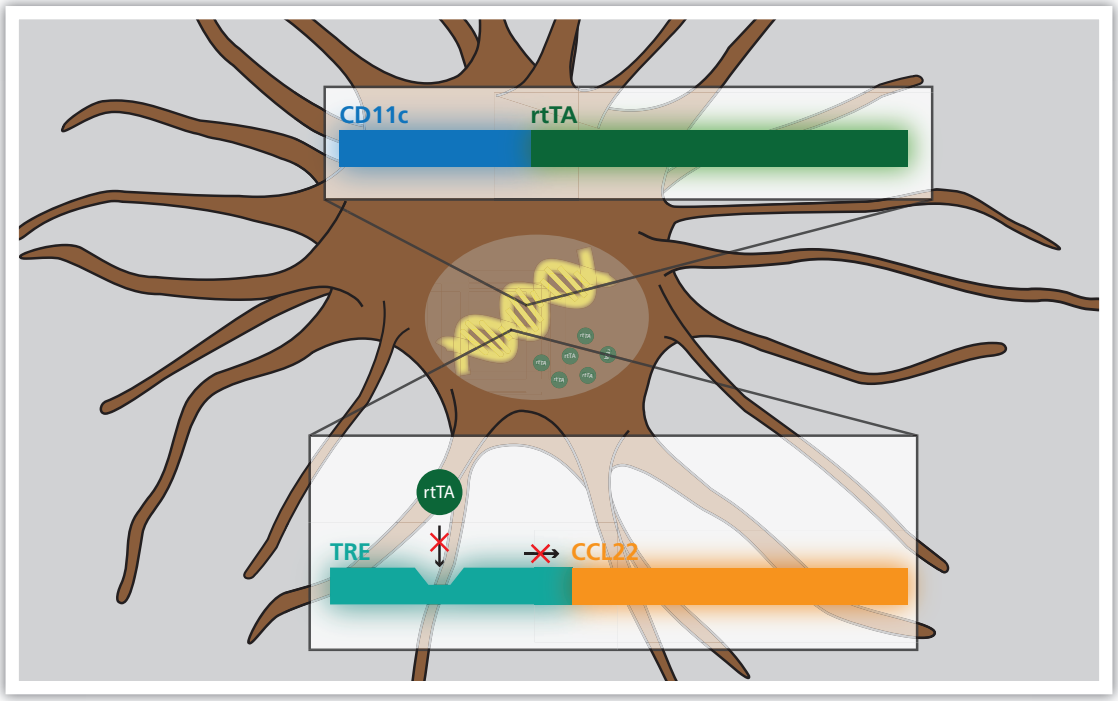

Figure 30: The CC11c-rtTA-TRE-CCL22 system in the absence of doxycycline. Shown is *a* DC bearing both constructs, CD11c-rtTA and TRE-CCL22. The expression of the activator element rtTA is mediated by the DC specific CD11c promoter. rtTA in turn activates the expression of the TRE regulated gene of interest (CCL22). However, in the absence of doxycycline the activator rtTA is unable to bind to TRE, and CCL22 expression is blocked.

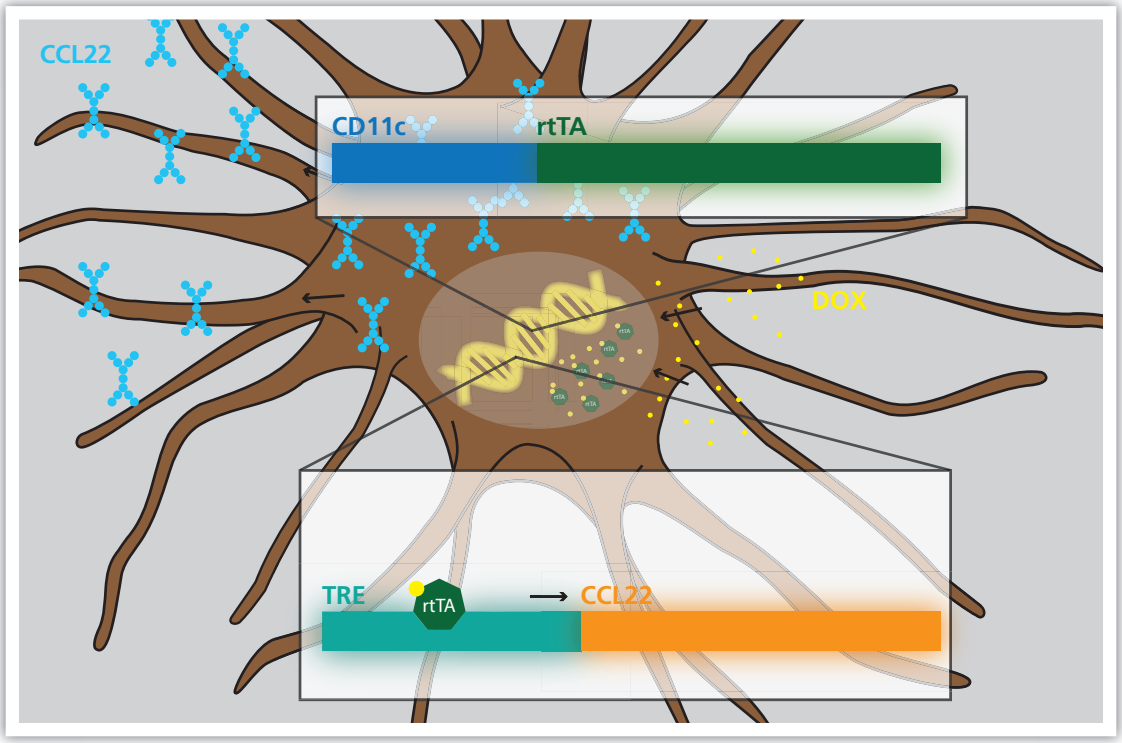

Figure 31: The CC11c-rtTA-TRE-CCL22 system in the presence of doxycycline. Doxycycline binds to rtTA and thereby facilitates a conformation change of the activator. This change enables rtTA to bind to TRE and activates DC-specific CCL22 over-expression.

TRE-Tight CCL22 Vector

The first step in establishing a doxycycline inducible CCL22 expression system was to integrate the cDNA sequence of murine CCL22 into a pTRE-Tight Vector provided by Clontech (Cat. # 631059). CCL22 was cloned downstream of the TRE promoter to enable TRE regulated expression of CCL22. We used the PCR primers CCL22-For-NotI and CCL22-Rev-SalI (for sequence see appendices *8.1*) for cloning the murine CCL22 cDNA into the pTRE-Tight vector. After positive clone selection via ampicillin and plasmid amplification, obtained plasmids were verified by sequencing. In all tested plasmids correct CCL22 cDNA integration was observed. Additionally, no mutations in CCL22 or the flanking region of CCL22 were detected (for sequencing data see appendices section *8.3*).

pTRE-Tight CCL22 transgenic mouse

The next step was the generation of a transgenic mouse. Mouse generation was done by Dr. Marlon Schneider (Genzentrum - LMU). The TRE-CCL22 segment was cut out of the pTRE-Tight-CCL22 vector by ApaLI digest. This segment was used for microinjection. In this procedure an elusion of the segment was injected into the pronuclei of fertilized eggs. Injection was done at the stage of development when mammalian ova have two pronuclei, one from each gamete, which will later fuse to form the diploid nucleus. The fertilized eggs were obtained from donor mice. After microinjection the eggs were transferred to the oviducts of pseudopregnant foster mothers. The offspring resulted from these injected eggs were screened for the transgenic TRE-CCL22 construct by PCR using the primer pair TRE-F/TRE-R (sequence: see appendices *8.1*). Overall, we identified one male mouse to carry the transgene. This founder animal was crossed with female CD11c-rtTA mice. The offspring were screened for both transgenes by PCR with the primer pairs TRE-F/TRE-R and rtTA-F/rtTA-R (sequence: see appendices *8.1*). Double positive mice are heterozygous for both, pTRE-CCL22 and CD11c-rtTA (CD11c-rtTA-CCL22 mice).

Characterization of the CD11c-rtTA-CCL22 mouse

After the identification of double transgenic mice, these mice were used for further characterization. To verify if the transgene was integrated correctly into the mouse genome, the transgenic sequence was analyzed by sequencing using the primer pTRE-Seq-For and pTRE-Seq-Rev. In all analyzed mice correct

TRE-CCL22 cDNA integration was observed. Only in the multiple cloning site downstream of the CCL22 sequence a base transition (C T) was detected. However, this point mutation does not affect the functionality of the TRE-CCL22 segment (for sequencing data see appendices section *8.4*). Next, we analyzed the expression of the rtTA transactivator in CD11c-rtTA-CCL22 mice RNA was isolated from splenocytes of wild-type and rtTA transgenic mice, transcribed in cDNA and used for qRT-PCR (probe-number and primer sequence: see appendices *8.2*). The PCR confirmed a high rtTA expression in all analyzed CD11c-rtTA-CCL22 mice compared to wild-type mice (*Figure 32*).

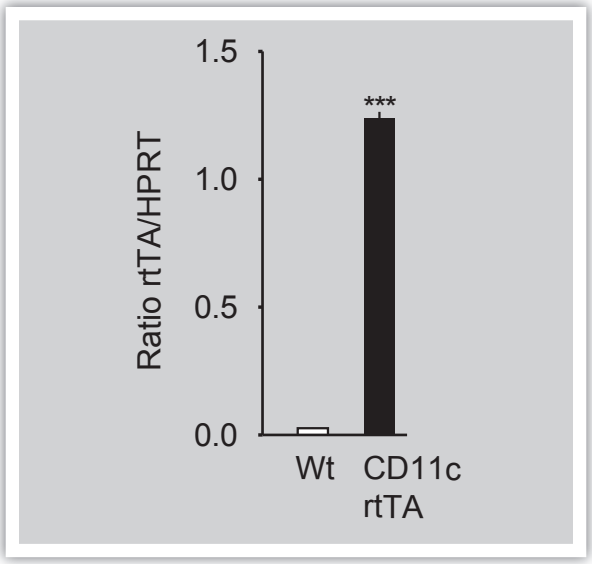

Figure 32: rtTA Expression level of splenocytes. Shown is the expression of rtTA in the spleen of two wild-type and two rtTA transgenic mice. The expression was measured by qRT-PCR using Roche probe number 80 and normalized with the ubiquitous expressed mRNA of HPRT. The representative data of two performed experiments are shown. Error bars indicate SEM. P value was calculated relative to wild-type mice (***$p < 0.001$*)*

Subsequently, the inducibility of CCL22 was checked. Therefor, an *in vitro* and an *in vivo* assay was performed. For the *in vitro* experiments spleens from wild-type, TRE-CCL22 and CD11c-rtTA-CCL22 mice were isolated. Whole splenocytes and sorted DCs were cultured both in the absence and in the presence of doxycycline. 48 hours later CCL22 levels were measured in the supernatant by ELISA. As expected no CCL22 induction was observed for splenocytes and CD11c-sorted DCs in wild-type and CCL22 transgenic mice. However, also in the CD11c-rtTA-CCL22 double transgenic mice no induction was detected in the supernatant of splenocytes and DCs alone *(Figure 33* and *Figure 34)*.

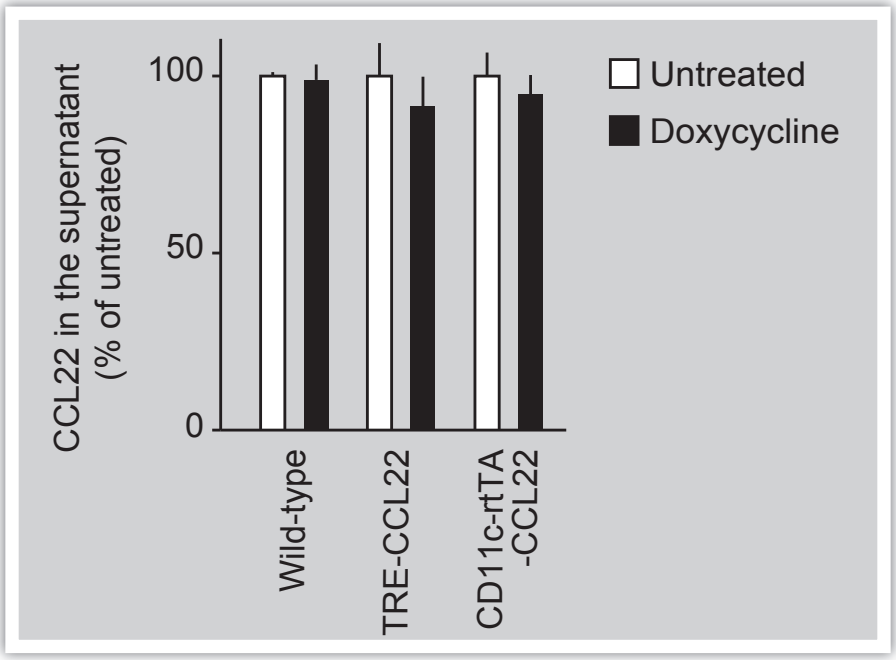

Figure 33: CCL22 expression in the supernatant of cultured splenocytes after 48 hours. The inducible CCL22 expression by doxycycline of wild-type, TRE-CCL22 transgenic and CD11c-rtTA-CCL22 double transgenic splenocytes was compared. For each group splenocytes were isolated from five mice and cultured in triplicates for 48 hours. In each case the expression level of the untreated condition was set to 100%, and the appropriate doxycycline-treated condition was set in relation to it. The experiment was repeated twice.

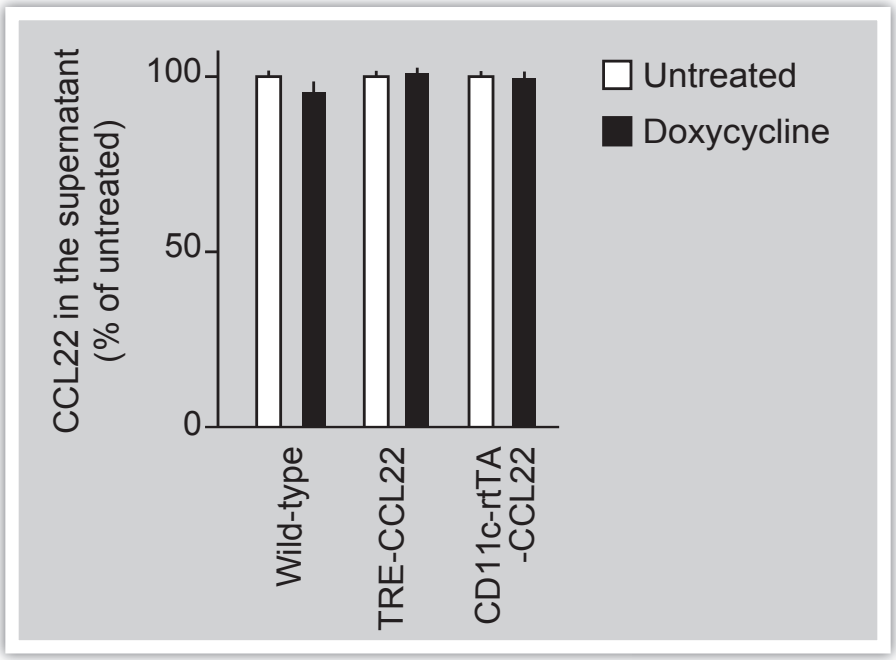

Figure 34: CCL22 expression in the supernatant of cultured DCs after 48 hours. The inducible CCL22 expression by doxycycline of wild-type, CCL22 transgenic and CD11c-rtTA-CCL22 double transgenic DCs was compared. DCs were isolated by sorting splenocytes for CD11c (purity >90). For every group DCs were isolated from three mice and cultured in triplicates for 48 hours. In each case the expression level of the untreated condition was set to 100%, and the appropriate doxycycline-treated condition was set in relation to it. The described experiment was repeated twice.

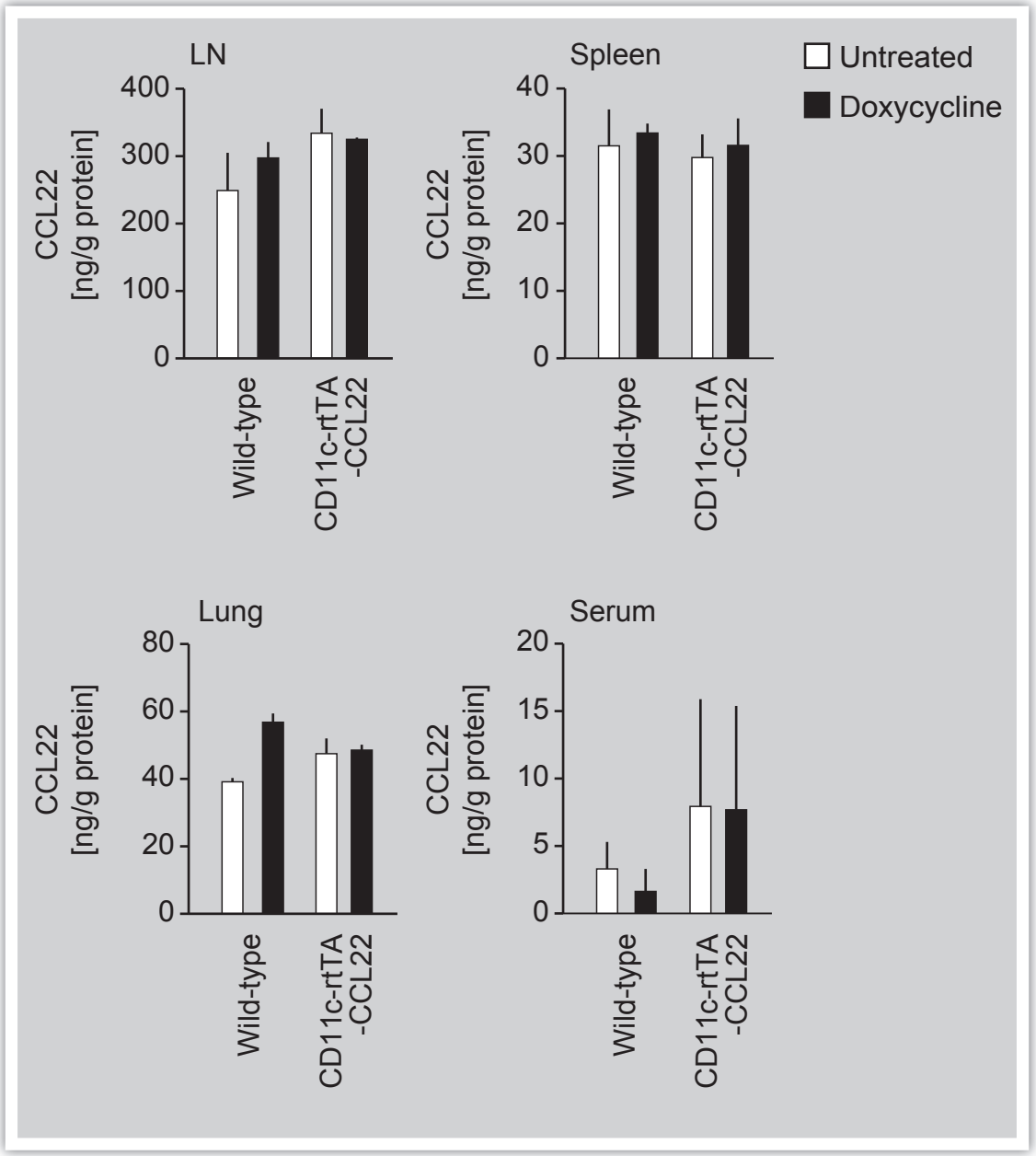

Figure 35: CCL22 expression level in lymph nodes, spleen, lung and serum of wild-type and CD11c-rtTA-CCL22 transgenic mice. To measure doxycycline-mediated CCL22 induction, both wild-type (n=8) and CD11c-rtTA-CCL22 transgenic mice (n=8) were separated into two groups. One group received doxycycline enriched diet (25 mg/kg) and the other group normal diet. Mice were sacrificed after one week, and chemokine levels were measured by ELISA. In each case the expression level of the untreated condition was set to 100%, and the appropriate doxycycline-treated condition was set in relation to it. The illustrated results were confirmed in two follow-up experiments.

For measuring CCL22 induction, *in vivo* wild-type and CD11c-rtTA-CCL22 transgenic mice were fed with a doxycycline-containing diet as well as a normal diet. After one week all mice were sacrificed, and the CCL22 levels in serum, lung, spleen and lymph nodes were measured by ELISA. In case of a functional CD11c-rtTA-CCL22 system double transgenic mice should show an induction

of CCL22 expression after doxycycline treatment. No induction in lung, spleen and lymph nodes was detectable (*Figure 35*).

Taking together the *in vitro* and *in vivo* data, both approved no functional CCL22 induction in double transgenic mice, the integrated TRE-CCL22 element seems not to be activated by doxycycline. Due to correct rtTA expression (*Figure 32*) and precise integration of the TRE-CCL22 sequence *(see appendices section 8.4)* the most likely reason for missing induction seems to be the integration site of the TRE-CCL22 element. As a result of random genomic integration of the transgene in the process of generating a transgenic mouse, the transgene can integrate into a silenced region of the mouse genome. To solve this problem, two more TRE-CCL22 transgenic mouse founder were generated. However, similar to the first founder, no CCL22 induction was observed. Therefore, we decided to simplify the transgenic approach. To circumvent the problems mentioned above, we intended to generate a new mouse line with DC specific CCL22 expression without inducibility.

3.3.2 Generation of a transgenic mouse with a stable non-inducible DC-specific CCL22 expression

Since the CD11c-rtTA-CCL22 mouse showed no inducible CCL22 over-expression, a new transgenic mouse approach was established. To simplify the tissue specific CCL22 expression system, we excluded the rtTA-dependent inducible expression system. Instead CCL22 should be expressed directly under the control of the DC-specific promoter CD11c. In such an expression system CCL22 is produced permanently and specifically by all CD11c+ DCs.

To achieve the DC specific CCL22 expression, we used a 5.5-kb fragment that contained the 5' region of the mouse CD11c gene (kindly provided by Dr. Thomas Brocker, Munich, Germany). The CD11c segment was cloned into a pBSbluescript vector that contained a rabbit beta-globin gene fragment. This fragment contained a multiple cloning site and provided the transgene with an intron and a polyadenylation signal. CCL22 was cloned into the multiple cloning site by using the restriction enzyme EcoRI. Therefore, CCL22 cDNA was amplified with the two PCR primers CCL22-EcoRI-for and CCL22-EcoRI-rev (for primer sequence see appendix *8.1*), cut with EcoRI and ligated with the EcoRI

digested pBSbluescript vector. After positive clone selection via ampicillin and plasmid amplification, obtained plasmids were verified by sequencing. In the plasmids of all tested clones CCL22 sequence was integrated correctly.

In a next step the functionality of the newly generated CD11c-CCL22 construct was verified *in vitro*. Therefore, we used the immortalized DC cell line DC2.4. Similar to primary DCs DC2.4 express high levels of CD11c (*Figure 36*). However, in contrast to primary DCs, this immortalized cell line lacks CCL22 production. Thus, this cell line is well suited to test the functionality of the CD11c-CCL22 fragment. We used Lipofectamine 2000 Transfection Reagent to transfect DC2.4. 24 hours post transfection CCL22 levels were measured in the supernatant of the cultured cells (*Figure 37*). Compared to untransfected cells we observed high CCL22 levels in the supernatant of CD11c-CCL22 transfected cells indicating that the new transgenic construct is functional in DCs.

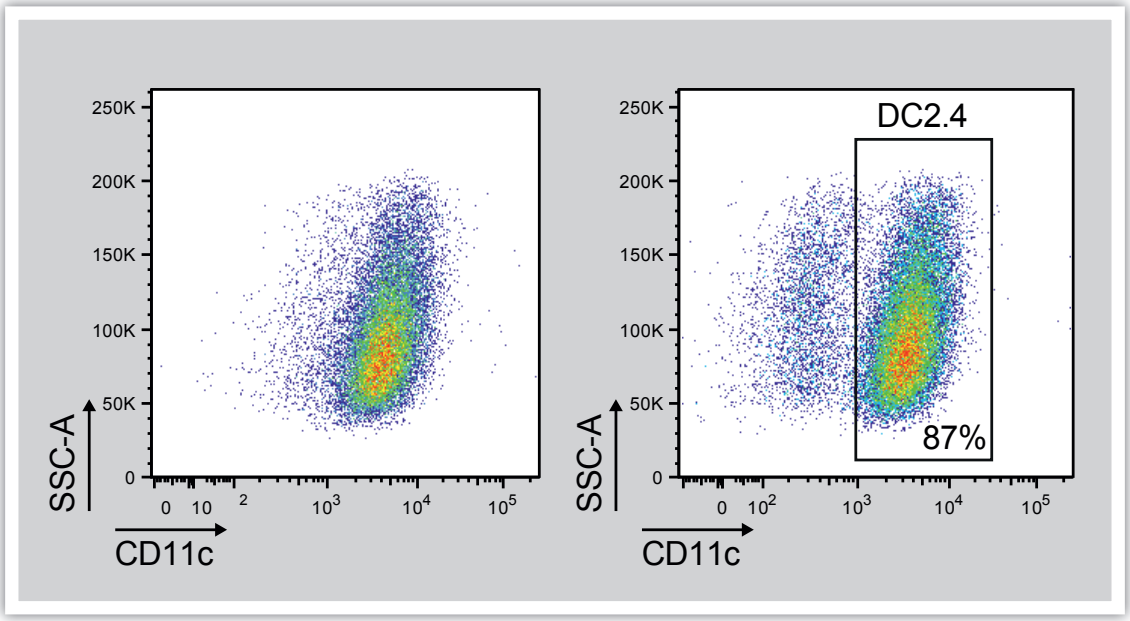

Figure 36: CD11c expression of DC2.4 cells. Left panel: CD11c-stained DC2.4 cells. Right panel: DC2.4 cells mixed with non-CD11c-expressing cells (here: Panc02 tumor cells) to exclude unspecific binding of the CD11c antibody. DC2.4 cells were mixed with Panc02 cells in a ratio of 10 to 1. 87% of the analyzed cells were positive for CD11c, reflecting the initial ratio of Panc02 and DC2.4 cells. Cells were analyzed in triplicates. Shown is one representative FACS blot of each condition.

Since the functionality of the CD11c-CCL22 construct was proved *in vitro*, we started to generate the CD11c-CCL22 transgenic mouse. Mouse generation by microinjection (as described above) was done by Dr. Marlon Schneider

(Genzentrum - LMU). The injected transgenic cassette was cut out of the pBSbluescript vector with the restriction enzymes NotI and XhoI resulting in a 6,5-kb long fragment. The generation of the CD11c-CCL22 transgenic mouse line is still in progress, and first offspring is expected at the beginning of next year (2013). After establishing the new mouse line and verifying DC specific CCL22 over-expression *in vivo,* these mice should be used for tumor experiments. Thereby, the impact of CCL22 on tumor development and tumor growth should be illustrated in a DC-specific setting.

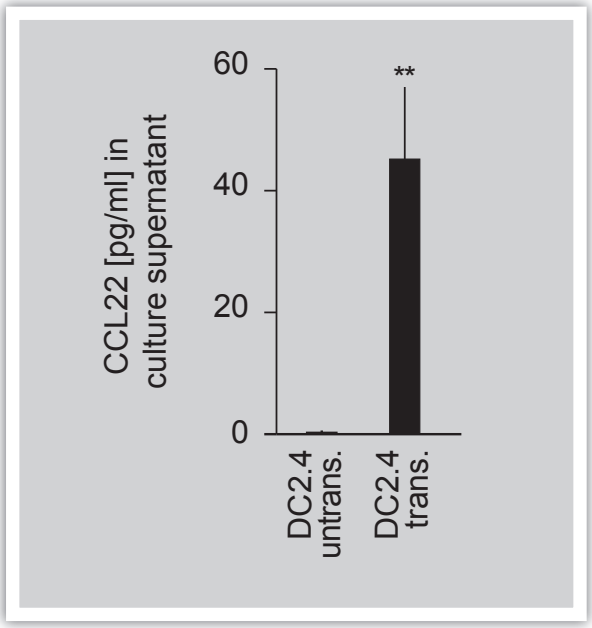

Figure 37: CCL22 expression of DC2.4 transfected cells. The CD11c-CCL22 construct was transiently integrated into DC2.4 cells. The plasmid integration was done by transfection with Lipofectamine 2000 Transfection Reagent. 24 hours before (= untransfected) and 24 hours after transfection the CCL22 levels in the cell culture supernatant of triplicates were measured via ELISA. Error bars indicate SEM. P value was calculated relative to untransfected cells (**$p < 0.01$).

3.3.3 CCL22 gene knockout mouse

Beside the tissue specific over-expression of CCL22 the role of this chemokine for tumor immunity should be verified by using a CCL22 gene knockout mouse (CCL22 KO). Therefore, we ordered a up to now undescribed CCL22 KO mouse from the NIH (National Institutes of Health) founded non-profit Knockout Mouse Project (www.komp.org). The CCL22 gene knockout was realized by replacing the CCL22 genomic coding region by homologous recombination. CCL22 was exchanged by a reporter (lacZ) plus selection (neomycin) fragment. Mice genotyping was done by PCR with two primer pairs, one primer

pair specific for the selection fragment (NeoinF and NeoinR) and one pair specific for the coding region of CCL22 (TDF and TDR; for primer sequences see appendix *8.1*). With these two primer pairs we were able to distinguish between wild-type, heterozygous and CCL22 KO homozygous mice.

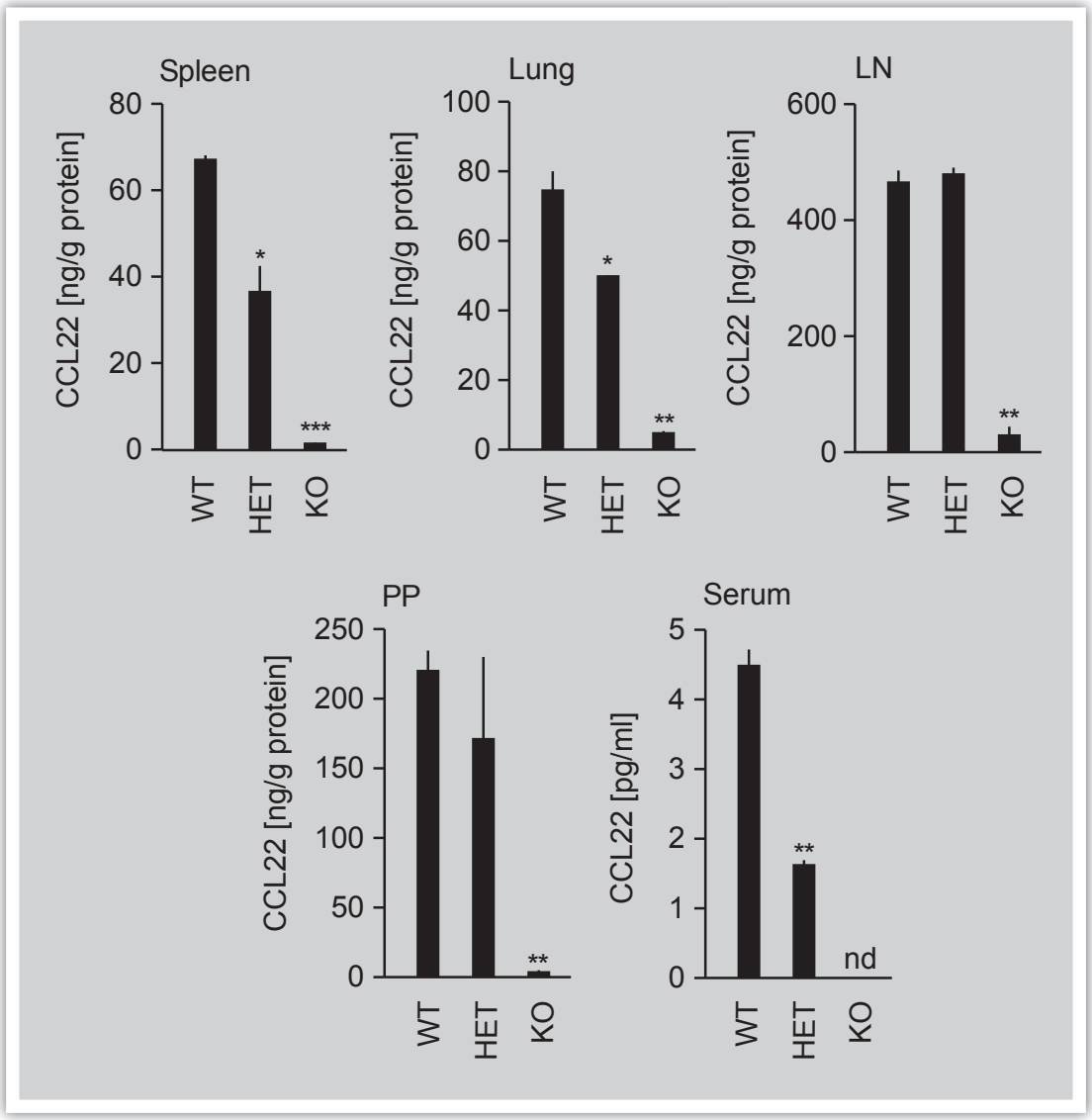

Figure 38: CCL22 levels in spleens, lungs, lymph nodes, peyer's patches and Sera of CCL22 KO mice. 6 week old wild-type (n=2), CCL22 KO heterozygous (n=2) and CCL22 KO homozygous mice (n=2) were sacrificed and spleen, lung, lymph nodes (LN), Peyer's patches (PP) and serum were obtained. The obtained organs were lysed, and CCL22 levels in the lysates and the sera were measured by ELISA. Shown are the representative results of two independent experiments. Error bars indicate SEM. P values were calculated relative to wild-type mice (**p < 0.01, ***p<0.001, nd indicates not detectable).

Since the CCL22 KO mouse line was newly generated, the first upcoming experiment was to verify the functionality of the CCL22 knockout. Therefore,

we dissected spleens, lungs, lymph nodes, Peyer's patches and sera from wild-type, CCL22 KO heterozygous and CCL22 KO homozygous mice. Subsequently, we measured CCL22 protein levels in organ lysates and sera by ELISA. Indeed, no CCL22 was detectable in all analyzed lysates and in the serum of CCL22 homozygous knockout mice.

In addition, a significant intermediate down-regulation in spleens, lungs and sera of heterozygous CCL22 KO mice compared to wild-type mice was observed (*Figure 38*). We also measured CCL17 levels in CCL22 KO mice by ELISA. Since CCL17 is the only CCR4 ligand apart from CCL22, we wanted to exclude that the lack of CCL22 in CCL22 KO mice is compensated via up-regulated CCL17 expression. However, no differences in CCL17 levels were observed between wild-type and CCL22 KO mice (data not shown). In summary, the newly generated CCL22 knockout mice completely lack CCL22 expression.

Since DCs are the main source of intratumoral CCL22, tumors from CCL22 KO mice are expected to lack CCL22. This in turn should lead to reduced amounts of tumor-infiltrating Tregs and thereby reduced tumor growth in CCL22 KO mice. However, the accuracy of this hypothesis needs to be verified in upcoming tumor experiments.

Discussion

4. Discussion

The mechanisms by which tumor cells create a suppressive environment to escape from an anti-tumor immune reaction are complex and poorly understood. However, recent studies have shown that recruitment of certain immune cells of the innate and adaptive immune system can help the tumor to establish an immunosuppressive milieu. In this context one very important cell type are regulatory T cells. Increased amounts of Tregs in cancer patients as well as the suppressive characteristics of Tregs support a role for these cells in cancer-induced immunosuppression.

Indeed, in the last decade several reports have associated high Treg tumor infiltration with increased tumor progression and decreased patient survival. In breast carcinoma high Treg tumor infiltration predicts aggressive tumor growth and poor patient survival (Bohling and Allison, 2008; Bates *et al.*, 2006). A negative impact of Tregs on patient survival is also reported for lung, pancreas, gastric, liver and ovarian carcinoma (Petersen *et al.*, 2006; Woo *et al.*, 2001; Liyanage *et al.*, 2002; Mizukami *et al.*, 2008; Hiraoka *et al.*, 2006; Kobayashi *et al.*, 2007; Gao *et al.*, 2007; Curiel *et al.*, 2004). Nevertheless, the effects of Tregs on tumor progression could vary in different tumor entities (Faget *et al.*, 2011). In B cell lymphoma or head and neck carcinoma higher Treg numbers correlate with better outcome for tumor patients (Tzankov *et al.*, 2008; Badoual *et al.*, 2006). Overall, in the majority of reports intratumoral Tregs are associated with a poor prognosis for cancer patients.

The trafficking of immune cells into the tumor tissue is regulated by the intratumoral expression of different chemokines. Identifying the chemokines involved in this trafficking is very important in order to establish targets for immunotherapy. Since the chemokine CCL22 is a potent attractor of Tregs, this chemokine could be involved in Treg tumor infiltration and thereby inducing intratumoral immunosuppression.

4.1 DCs are the main producer of intratumoral CCL22

We observed high levels of the chemokine CCL22 in tumor lysates of murine colon carcinoma, melanoma, mammary cancer and pancreatic cancer. In analogy to mice high CCL22 expression levels in several human tumors have been reported. For instance, immunohistochemical analyses of primary breast tumor sections revealed high intratumoral CCL22 levels in tumor patients (Anz *et al.*, 2011; Gobert *et al.*, 2009). Furthermore, high intratumoral CCL22 expression was observed in human Hodgkin lymphoma, B cell non-Hodgkin lymphoma, gastric cancer and ovarian carcinoma (Ishida *et al.*, 2006; Yang *et al.*, 2006; Mizukami *et al.*, 2008; Curiel *et al.*, 2004). Although many reports of intratumoral CCL22 expression can be found in the literature, there are still controversies about the cellular source of intratumoral CCL22. Several authors argue that tumor cells are the main source of intratumoral CCL22 in humans and mice. Only few reports convincingly identified tumor cells as CCL22 producers. Here, human breast cancer cells were shown to produce CCL22 *in vitro* and *in vivo* (Anz *et al.*, 2011; Faget *et al.*, 2011). However, in human breast cancer not only tumor cells but also DC-shaped infiltrating immune cells produce remarkable amounts of CCL22 (Anz *et al.*, 2011; Gobert *et al.*, 2009). In ovarian cancer tumor cells together with macrophages were hypothesized to be the source of intratumoral CCL22 (Curiel *et al.*, 2004).

In contrast to these reports we observed no CCL22 expression by tumor cell lines *in vitro*. It is reported that murine and human DCs are the most potent producers of CCL22 in healthy subjects (Tang and Cyster, 1999; Vulcano *et al.*, 2001). Additionally, beside other chemokines such as CCL16, CCL17, CCL18 and CX3CL1 intratumoral DCs can produce CCL22 (Raman *et al.*, 2007). Thus, we hypothesized that DCs could be the main producer of intratumoral CCL22. Indeed, we identified intratumoral murine DCs as the exclusive source of CCL22 in the tumor tissue. For our experiments we used CD11c as a DCs marker since CD11c is expressed on all defined DC subsets in mice. We observed very high CCL22 mRNA and protein expression levels in DC from freshly dissected tumors. In contrast, CCL22 was barely expressed in the DC-depleted fraction. After DC depletion no CCL22 production by tumor cells or other immune cells was detected in tumor single cell suspensions indicating that intratumoral DCs

are the exclusive CCL22 producers in murine cancer. Unlike previous reports our findings demonstrate that tumor cells do not produce CCL22. In this study we investigated the CCL22 expression profile of melanoma and pancreatic cancer. In other tumor types the situation could be different. In conclusion, our findings show that CCL22 expression by tumor cells is not a common characteristic of all tumor types, but rather an acquired property of certain tumor types such as breast cancer. Furthermore, DCs could have an important role in establishing an immunosuppressive tumor microenvironment and could serve as target for tumor immunotherapies.

4.2 CCL22 affects tumor growth and survival

As previously described, high intratumoral CCL22 expression is observed in many different tumor types in humans and in mice. According to this frequent occurrence of CCL22 in different types of tumors, we hypothesized that this chemokine could influence tumor development and growth. In healthy subjects CCL22 has been reported to be a very selective and potent Treg attractor (Iellem *et al.*, 2001). Consistent with these findings, the only known receptor for CCL22, which is CCR4, is highly expressed on Tregs compared to other T cell subtypes (Imai *et al.*, 1998). Thus, intratumoral CCL22 could be involved in Treg recruitment into the tumor tissue.

Indeed, in several publications a dependency between intratumoral CCL22 expression and Treg infiltration was observed. For instance, in a non-obese diabetic/severe combined immunodeficiency (NOD/SCID) mouse model human ovarian tumors which are known to express high levels of intratumoral CCL22 were highly infiltrated by adoptively transferred human Tregs. After treating these mice with an anti-CCL22 antibody, a significant decrease in Treg tumor infiltration was observed, whereas the migration of other T cell subtypes was not affected (Curiel *et al.*, 2004). In human gastric cancer samples flow cytometry analyses of single cells, derived from tumor tissues, revealed a significant correlation between the frequency of intratumoral CCL22 and tumor-infiltrating Tregs (Mizukami *et al.*, 2008).

We and other groups have observed high intratumoral levels of the potent Treg attractor CCL22 in several types of tumors. However, until now the impact of CCL22 expression on tumor growth and overall survival is completely unknown. In this study we used a novel generated murine tumor cell line with inducible intratumoral CCL22 expression to investigate the exclusive effect of CCL22 on tumor progression. With this rtTA-CCL22-CT26 tumor cell line we showed that an induced over-expression of CCL22 in the tumor tissue of tumor-bearing mice significantly promotes tumor growth. In addition, the overall survival of these mice was reduced compared to mice with low intratumoral CCL22 expression. Furthermore, presence of CCL22 allowed tumor development even if suboptimal doses of tumor cells were injected. Thus, we showed here for the first time a direct impact of intratumoral CCL22 on tumor development, growth and overall survival supporting a role for CCL22 in cancer-induced immunosuppression. These findings indicate that CCL22 could be a promising target for new anti-cancer drugs. Antagonizing CCL22 with antibodies or siRNA could have the potential to promote anti-tumor immunity.

4.3 IFN-α induces TLR-mediated CCL22 suppression

As described earlier, in previous studies done by Dr. David Anz we observed a significant suppression of intratumoral CCL22 after TLR treatment of tumor-bearing mice (unpublished data). We observed this suppressive effect in T-cell lymphoma, colon carcinoma, melanoma and pancreatic cancer with different TLR ligands such as CpG (TLR9), poly (I:C) (TLR3 and MDA-5) and R848 (TLR7). These findings indicate that intratumoral CCL22 regulation by TLR ligands is a general phenomenon and not specific for a certain TLR ligand or tumor entity. However, the precise impact of this regulation and the mechanism that induces CCL22 suppression are unclear.

In general, TLR ligand binding leads to TLR activation. Thereby, the expression of many different genes is induced in a complex signalling cascade. One very abundantly induced cytokine, especially after TLR3, 4, 7 or 9 and RLR activation, is IFN-α (Iwasaki *et al.*, 2004; Hertzog *et al.*; 2003). Strikingly,

we identified this cytokine to be the main mediator of TLR ligand-induced CCL22 suppression. We observed a highly suppressive effect of IFN-α on CCL22 secretion of freshly isolated intratumoral leukocytes. We saw the same effect after treating intratumoral DCs, the exclusive source of intratumoral CCL22 in murine melanoma and pancreatic cancer as shown above, with IFN-α indicating that IFN-α directly affects DCs. Additional to IFN-α we observed a significant CCL22 suppression after stimulating tumor-infiltrating immune cells with IL-10, IL-12 or IFN-γ. However, previous work done by Raffael Thaler (Department of Clinical Pharmacology, LMU) showed that the CpG-mediated suppression of CCL22 is not abolished in IL-10, IL-12 or IFN-γ knockout mice (unpublished data), indicating that these cytokines alone are not responsible for the TLR-induced suppression of CCL22.

In conclusion, our findings indicate that TLR stimulation initiates IFN-α expression by DCs themselves and other immune cells, and IFN-α in turn directly suppresses CCL22 secretion in intratumoral DCs. In addition to these *ex vivo* experiments we confirmed the impact of IFN-α on CCL22 suppression after TLR activation in IFNAR mice. In TLR ligand-treated IFNAR mice, which lack a functional type I interferon receptor, the effect of IFN-α was abrogated, and thereby also the suppression of intratumoral CCL22 was abolished. Indeed, the TLR ligand-induced decrease of intratumoral CCL22 expression was not only blocked in IFNAR mice, but even increased. As shown by Vulcano *et al.* and Penna *et al.* the stimulation with certain TLR ligands such as LPS could induce the CCL22 expression of *in vitro* differentiated DCs (Vulcano *et al.*, 2001; Penna *et al.*, 2002). In IFNAR mice this *in vitro* observation could be responsible for the measured increase of CCL22 expression after poly (I:C) treatment. Since the suppressive effect of IFN-α on CCL22 expression is abrogated in IFNAR mice, the impact of TLR-induced CCL22 induction seems to prevail in these mice. Due to limited available numbers of IFNAR mice we could verify the effect of only one TLR stimulus on CCL22 suppression in tumor-bearing IFNAR mice. Since we wanted to analyze the contribution of IFN-α to TLR-mediated CCL22 suppression we used poly (I:C), a TLR ligand that is known to induce strong IFN-α production in mice (Matsumoto and Seya 2008), for these limited experiments. However, the effect of CpG and other TLR ligands on

CCL22 suppression in IFNAR remains to be elucidated and should be verified in follow-up experiments.

In this study we have demonstrated for the first time that TLR-mediated CCL22 suppression is IFN-α-induced. The effects of IFN-α are very diverse. Initially discovered as an antiviral protein, many studies have revealed the impact of IFN-α in modulating the innate and adaptive immune reaction in response to a variety of pathogens (Theofilopoulos *et al.*, 2005). IFN-α can induce anti-angiogenesis, immune regulation, cell differentiation and apoptosis in different types of human tumors (Tarhini *et al.*, 2012; Kirkwood *et al.*, 2002). Especially DCs respond to IFN-α treatment. Several studies revealed an INF-α-promoting effect on the polarization, maturation, survival and antigen cross-presentation of DCs which in turn enhances anti-cancer therapy (Tarhini *et al.*, 2012; Kirkwood *et al.*, 2002; Wang *et al.*, 2007; Paquette *et al.*, 1998; Krown *et al.*, 1984). Minasian and others have revealed that IFN-α could have a beneficial effect in the therapy of human cancers such as renal cell cancer and melanoma (Minasian *et al.*, 1993; Kirkwood *et al.*, 2002; Takaoka *et al.*, 2003; Melichar *et al.*, 2012). Compatible with these reports our finding also indicates a pro-therapeutic effect of INF-α in tumor treatment. This aspect could be considered in order to find new fields of application and identifying appropriate cancer patient subsets for IFN-α treatment. Since only a very small cancer patient cohort profits of an INF-α therapy and so far a predictor of response has not been found CCL22 could possibly serve to select appropriate cancer patient subsets (Tarhini *et al.*, 2012; Kirkwood *et al.*, 2012). Our results imply that patients with high intratumoral CCL22 levels could have a higher benefit from IFN-α therapy. Thus, in this study we revealed new aspects for an IFN-α-mediated anti-cancer therapy.

4.4 CCL22 suppression is an important component of TLR-initiated tumor regression

In the past few years many new approaches for anti-cancer immunotherapy were developed, one of these are synthetic TLR ligands. With TLR ligands the innate immune system can be activated and the tumor-induced immune

suppression attenuated (Kanzler *et al.*, 2007). The TLR9 ligand CpG, for instance, reduces tumor growth and increases overall survival of tumor-bearing mice (Heckelsmiller *et al.*, 2002; Houot and Levy, 2009; Krieg, 2008). Beside the broadly described therapeutic effects and prospects of TLR ligands in literature the precise mechanisms that mediate TLR-induced anti-tumor immunity are still poorly understood. As described above we observed a significant suppression of intratumoral CCL22 after TLR treatment of tumor-bearing mice. In consideration of the tumor-growth-promoting effects of CCL22 we observed in this study, intratumoral CCL22 suppression could be an important component of TLR-initiated tumor regression.

In this study we were able to abolish the therapeutic effect of TLR treatment by preventing CpG-induced intratumoral CCL22 suppression. This was achieved by CCL22 over-expression in the tumor tissue of tumor-bearing mice. Thus, we demonstrated for the first time that CCL22 has a direct effect on TLR-mediated immunotherapy. According to our results, the suppression of CCL22 is therefore an important mechanism for TLR-induced tumor regression. Additionally, by counterbalancing the intratumoral suppression of CCL22 in TLR ligand-treated tumor-bearing mice, no decrease in intratumoral Treg levels was observed.

In previous experiments done by Dr. David Anz and Dr. Viktor Kölzer it was shown that TLR treatment not only reduces tumor-associated CCL22 levels, but also decreases the number of tumor-infiltrating Tregs (unpublished data). In addition, we and others observed a clear correlation between intratumoral CCL22 and Treg levels in the tumor tissue (Mizukami *et al.*, 2008). Furthermore, in several studies a promoting impact of tumor-associated Tregs on tumor progression has been reported. These findings indicate that intratumoral CCL22 mediates Treg tumor infiltration and thereby increases tumor progression. Thus, the benefit of TLR-induced CCL22 suppression is potentially mediated through an inhibition of Treg immigration into the tumor. *Figure 33* schematically illustrates the proposed mechanism of TLR ligand-induced tumor-associated CCL22 suppression and the assumed effects on tumor progression.

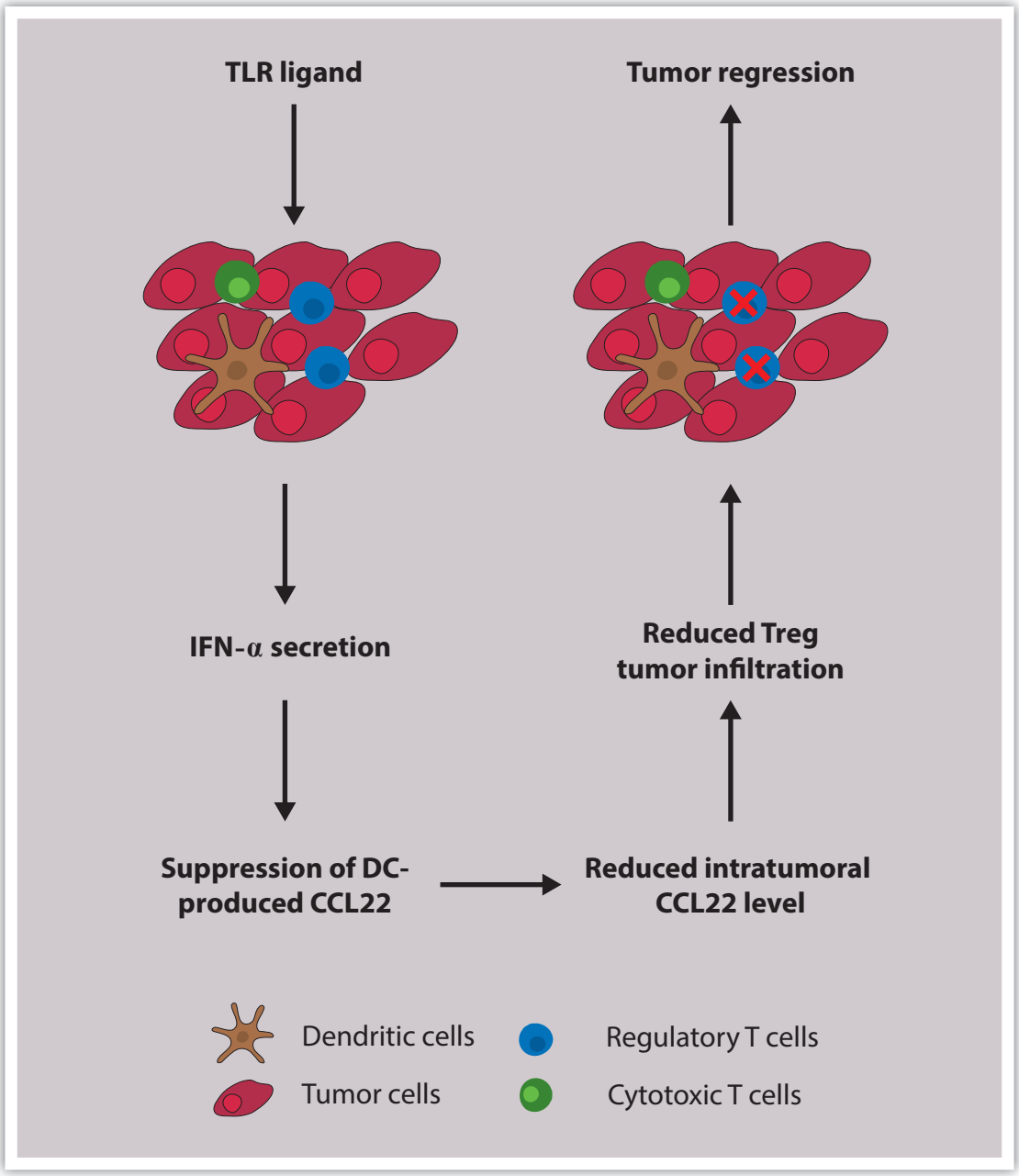

Figure 39: Overview of the proposed mechanisms in this study. This illustration shows the proposed mechanism of TLR ligand-mediated tumor regression. TLR stimulation activates IFN-α secretion by immune cells such as DCs. Via autocrine or paracrine signalling IFN-α suppresses CCL22 expression. This in turn blocks CCL22-mediated Treg recruitment into the tumor tissue. Thereby, the number of intratumoral Tregs is reduced, and Treg-induced immune suppression is abolished. Cytotoxic T cells are no longer suppressed and can actively kill tumor cells, whereby an anti-tumor immune reaction is induced.

4.5 CCL22 is a promising anti-tumor drug target

Manipulating the immune system has become a very promising approach for anti-tumor therapy in the last years. Many potential new targets have been

identified. However, new therapeutic approaches such as patient vaccination with tumor-specific antigens or adoptive T cell transfer of tumor antigen-specific cytotoxic T cells fail in the majority of cases to cure cancer patients due to tumor escape strategies. One of the major problems in this purpose is tumor-induced immune suppression. Therefore, circumventing this immune suppression is a very important step in achieving an efficient anti-tumor therapy. For this purpose Tregs seem to be a target with good prospects. These cells are known to mediate immune suppression and are associated with poor prognosis for cancer patients in many tumor entities. Indeed, in many experiments the therapeutic effects of Treg depletion or blockage in cancer patients have been confirmed. For instance, the depletion of Tregs by anti-CD25 depletion antibody enhanced a vaccine-mediated anti-tumor immunity in cancer patients (Dannull *et al.*, 2005; Onizuka *et al.*, 1999; Shimizu *et al.*, 1999). The dual use of CTLA-4 blocking antibody and CD25 depletion antibody also showed promising results for abolishing tumor-induced immune suppression (Sutmuller *et al.*, 2001). In patients with metastatic melanoma ipilimumab, a CTLA-4 blocking antibody, improved overall survival (Hodi *et al.*, 2011).

However, in these approaches not only intratumoral Tregs are depleted or blocked, but also all other Tregs which in turn often caused autoimmunity. In addition, Treg depletion always involves the depletion of other anti-tumor immunity promoting immune cells such as cytotoxic T lymphocytes since precise Treg surface marker are still missing. For instance, CD25 depletion antibody also depletes cytotoxic T lymphocytes which up-regulate CD25 after activation (Phan *et al.*, 2003; Jones *et al.*, 2002). To minimize side effects, new approaches must be investigated. One very promising alternative would be the blockade of intratumoral Treg infiltration. By blocking the infiltration of Tregs into the tumor, only the intratumoral immune suppressive effect of these cells would be abrogated and not their important function as suppressors of autoimmunity. In this study we showed that the chemokine CCL22 seems to have this potential. This chemokine is a very specific and potent Treg attractor (Iellem *et al.*, 2001). As shown above CCL22 is up-regulated in colon carcinoma, melanoma, mammary cancer and pancreatic cancer. Furthermore, high intratumoral CCL22 expression is associated with increased Treg tumor

infiltration (Mizukami *et al.*, 2008). In addition, we showed here for the first time that CCL22 can accelerate tumor growth and reduce overall survival in tumor-bearing mice.

Beside Treg recruitment to the tumor tissue, CCL22 could have additional unknown tumor-promoting effects. By blocking the function of this chemokine, these effects could be abrogated and anti-tumor immunity promoted. Therefore, the development of a CCL22 blocking antibody for further *in vivo* experiments will be the next step to verify this assumption. In addition, CCR4 and CCL22 KO mice could deliver further insights into the mechanism of CCL22-mediated Treg tumor infiltration and the tumor-promoting effect of CCL22. Since CCR4 is the exclusive receptor of CCL22 in CCR4 KO mice a CCL22-mediated cell migration is block. Thus, in these mice less Tregs should be present in the tumor tissue which in turn would confirm that CCL22 is involved in the attraction of Tregs into tumors. Furthermore, CCL22 KO mice could be used to analyze additional effects of CCL22 on tumor growth in more detail. We identified DCs and not tumor cells as the producer of intratumoral CCL22. Thus, in CCL22 KO mice no CCL22 should be expressed in the tumor tissue and therefore the tumor-promoting effect of CCL22 would be blocked. This in turn should result in a decrease of tumor growth. Since CCR4 and CCL22 KO mice as well as a CCL22 blocking antibody were not available until the end of my thesis these experiments still needs to be done. Taken together, the results of previous experiments and of this study illustrate that the chemokine CCL22 could be a promising target for anti-tumor therapy.

In conclusion, investigating the function of intratumoral CCL22 seems to have the potential to improve the outcome of current anti-tumor therapies. With the presented results we were able to gain new insights into this field and provided the basis for further experiments aiming to find new anti-cancer drugs.

Summary

5. Summary

An effective anti-cancer therapy requires that the tumor-induced immune suppressive environment is abolished. Without bypassing this suppressive milieu, most immunotherapies show only poor benefits for cancer patients. In order to escape from the host immune system, the tumor capitalizes on the protective immune mechanism of the host. One cell type involved in this process are regulatory T cells. Increased amounts of regulatory T cells in cancer patients as well as the suppressive characteristics of these cells support an important role for regulatory T cells in cancer-induced immunosuppression.

The aim of this study was to investigate the role of the chemokine CCL22 in tumor-induced immune suppression. In previous studies we demonstrated that in murine cancer high levels of CCL22 are expressed. Since CCL22 specifically attracts regulatory T cells, we hypothesized that intratumoral CCL22 expression is one of the mechanisms used by tumors to escape the host immune system.

In contrast to breast cancer in which CCL22 is expressed by tumor cells, we identified intratumoral dendritic cells as the main producers of tumor-associated CCL22 in melanoma and pancreatic cancer. By using a murine colon cancer tumor cell line with inducible CCL22 expression, a clear impact of intratumoral CCL22 on tumor genesis was observed. In mice tumor growth was increased and overall survival decreased after induction of intratumoral CCL22 indicating that high intratumoral CCL22 levels are associated with poor prognosis.

Treating tumor-bearing mice with immune activating Toll-like receptor (TLR) ligands reduces tumor growth and increases overall survival. In previous studies of our group it was shown that TLR activation suppresses intratumoral CCL22 expression. We demonstrated here for the first time that this TLR ligand-induced reduction of intratumoral CCL22 is mediated by IFN-α, a cytokine released by immune cells after TLR stimulation. Furthermore, when suppression of intratumoral CCL22 was counterbalanced by using a tumor

cell line with inducible CCL22 expression, the therapeutic benefit of TLR ligands in mice was abolished. In addition, the previously described reduction of intratumoral regulatory T cell numbers by TLR activation was reversed. These results indicate that TLR ligands lead to tumor regression at least partially by suppressing intratumoral CCL22 expression which in turn blocks the infiltration of immunosuppressive regulatory T cells into the tumor. Thus, CCL22 suppression is a crucial part of TLR-induced tumor regression.

In conclusion, this study illustrates the important role of CCL22 in tumor development and clinical outcome. CCL22 represents an essential chemokine in recruiting regulatory T cells into the tumor tissue and inducing an immune suppressive tumor environment. Thus, targeting this chemokine by treating cancer patients with IFN-α or CCL22-blocking antibody could be a promising approach for an efficient anti-cancer immunotherapy.

6. Zusammenfassung

Für eine effektive Anti-Tumor-Therapie ist es erforderlich das immunsuppressive Milieu des Tumors außer Kraft zu setzen. Ohne eine Aufhebung dieses suppressiven Milieus zeigen die meisten Immuntherapien nur geringe Erfolge in der Bekämpfung von Tumorerkrankungen. Um einer effektiven Immunreaktion zu entgehen, macht sich der Tumor bestimmte Schutzmechanismen des Immunsystems zunutze. Eine Zellart, die an diesem Prozess beteiligt ist, sind regulatorische T Zellen. Erhöhte Zahlen an regulatorischen T Zellen in Tumorpatienten, sowie die immunsuppressiven Eigenschaften dieser Zellen, deuten darauf hin, dass regulatorische T Zellen entscheidend zu der Etablierung eines immunsuppressiven Tumormileus beitragen.

Das Ziel dieser Doktorarbeit war es, den Einfluss des Chemokins CCL22 auf die tumor-induzierte Immunsuppression zu erforschen. In Vorarbeiten unserer Arbeitsgruppe konnten wir zeigen, dass in murinen Tumoren CCL22 in erhöhtem Maße exprimiert wird. Da CCL22 effektiv regulatorische T Zellen anlockt, vermuteten wir, dass die tumorassoziierte CCL22-Expression entscheidend an der Entstehung eines immunsuppressiven Tumormilieus beteiligt ist.

Im Gegensatz zu Brusttumoren, in denen die Tumorzellen selbst CCL22 produzieren, konnten wir im murinen Melanom und Pankreaskarzinom dendritische Zellen als die Hauptproduzenten von intratumoralem CCL22 identifizieren. Mit Hilfe einer murinen Kolontumorzelllinie, die induzierbar CCL22 produziert, wurde ein klarer Zusammenhang zwischen intratumoralem CCL22 und Tumorwachstum beobachtet. Nach Induktion der CCL22-Produktion war das Tumorwachstum in Mäusen beschleunigt und das Gesamtüberleben signifikant verringert. Diese Daten verdeutlichen, dass hohe CCL22 Konzentrationen im Tumor mit einer schlechten Prognose verbunden sind.

Eine Behandlung von tumor-tragenden Mäusen mit Toll-like-Rezeptor-Liganden, die eine aktivierende Wirkung auf das Immunsystem haben, führt zu einer Tumorregression und steigert das Gesamtüberleben der behandelten Mäuse. Frühere Experimente unserer Arbeitsgruppe demonstrierten, dass

TLR-Liganden die Expression von tumor-assoziiertem CCL22 supprimieren und die Infiltration von regulatorischen T Zellen in den Tumor reduzieren. In der vorliegenden Arbeit konnte erstmalig gezeigt werden, dass die TLR-Liganden-induzierte CCL22-Reduktion durch IFN-α, ein Zytokin, das Immunzellen nach TLR-Stimulation sezernieren, vermittelt wird. Durch die Verwendung von Tumorzellen mit induzierbarer CCL22-Expression konnte des Weiteren belegt werden, dass eine Aufhebung der TLR-vermittelten CCL22 Suppression den therapeutischen Effekt von TLR-Liganden abschwächt. Darüber hinaus wurde die TLR-induzierte Reduktion von tumorinfiltrierenden, regulatorischen T Zellen durch die Antagonisierung der CCL22-Suppression aufgehoben. Diese Ergebnisse deuten darauf hin, dass die TLR-Liganden-induzierte Tumorregression teilweise durch eine Suppression der intratumoralen CCL22 Expression vermittelt wird, die wiederum die Tumorinfiltration von immunsuppressiven, regulatorischen T Zellen verringert. Die Suppression von tumorassoziiertem CCL22 ist somit ein entscheidender Bestandteil der TLR-induzierten Tumorregression.

Die Erkenntnisse dieser Arbeit verdeutlichen die wichtige Rolle von CCL22 bei der Tumorentstehung sowie der Prognose von unterschiedlichen Tumorentitäten. CCL22 ist ein Chemokin, das entscheidend an der Rekrutierung von regulatorischen T Zellen in den Tumor und dadurch an der Etablierung eines immunsuppressiven Tumormilieus beteiligt ist. Aus diesem Grund könnten neue Therapieansätze, die spezifisch auf eine Regulierung von intratumoralem CCL22 ausgelegt sind, einen entscheidenden Beitrag im Kampf gegen Krebs leisten. Ein vielversprechender Ansatz ist somit zum Beispiel die Behandlung von Tumorpatienten mit IFN-α oder einem CCL22-blockierenden Antikörper.

References

7. References

Akira S, Uematsu S, Takeuchi O. (2006). Pathogen recognition and innate immunity. *Cell. 2006 Feb 24;124(4):783-801.*

Akira S, Takeda K. (2004). Toll-like receptor signalling. *Nat Rev Immunol. 2004 Jul;4(7):499-511.*

Alexopoulou L, Holt AC, Medzhitov R, Flavell RA. (2001). Recognition of double-stranded RNA and activation of NF-kappaB by Toll-like receptor 3. *Nature. 2001 Oct 18;413(6857):732-8.*

Allan SE, Crome SQ, Crellin NK, Passerini L, Steiner TS, Bacchetta R, Roncarolo MG, Levings MK. (2007). Activation-induced FOXP3 in human T effector cells does not suppress proliferation or cytokine production. *Int Immunol. 2007 Apr;19(4):345-54.*

Anz D, Eiber S, Scholz C, Endres S, Kirchner T, Bourquin C, Mayr D. (2011) In breast cancer, a high ratio of tumour-infiltrating intraepithelial CD8+ to FoxP3+ cells is characteristic for the medullary subtype. *Histopathology. 2011 Nov;59(5):965-74.*

Anz D, Koelzer VH, Moder S, Thaler R, Schwerd T, Lahl K, Sparwasser T, Besch R, Poeck H, Hornung V, Hartmann G, Rothenfusser S, Bourquin C, Endres S. (2010). Immunostimulatory RNA blocks suppression by regulatory T cells. *J Immunol. 2010 Jan 15;184(2):939-46.*

Anz D, Thaler R, Stephan N, Waibler Z, Trauscheid MJ, Scholz C, Kalinke U, Barchet W, Endres S, Bourquin C. (2009). Activation of melanoma differentiation-associated gene 5 causes rapid involution of the thymus. *J Immunol. 2009 May 15;182(10):6044-50.*

Badoual C, Hans S, Rodriguez J, Peyrard S, Klein C, Agueznay Nel H, Mosseri V, Laccourreye O, Bruneval P, Fridman WH, Brasnu DF, Tartour E. (2006). Prognostic value of tumor-infiltrating CD4+ T-cell subpopulations in head and neck cancers. *Clin Cancer Res. 2006 Jan 15;12(2):465-72.*

Bates GJ, Fox SB, Han C, Leek RD, Garcia JF, Harris AL, Banham AH. (2006). Quantification of regulatory T cells enables the identification of high-risk breast cancer patients and those at risk of late relapse. *J Clin Oncol. 2006 Dec 1;24(34):5373-80.*

Bennett CL, Christie J, Ramsdell F, Brunkow ME, Ferguson PJ, Whitesell L, Kelly TE, Saulsbury FT, Chance PF, Ochs HD. (2001). The immune dysregulation, polyendocrinopathy, enteropathy, X-linked syndrome (IPEX) is caused by mutations of FOXP3. *Nat Genet. 2001 Jan;27(1):20-1.*

Berger M, Ablasser A, Kim S, Bekeredjian-Ding I, Giese T, Endres S, Hornung V, Hartmann G. (2009). TLR8-driven IL-12-dependent reciprocal and synergistic activation of NK cells and monocytes by immunostimulatory RNA. *J Immunother. 2009; 32: 262-71.*

Betts GJ, Clarke SL, Richards HE, Godkin AJ, Gallimore AM. (2006). Regulating the immune response to tumours. *Adv Drug Deliv Rev. 2006 Oct 1;58(8):948-61.*

Bohling SD, Allison KH. (2008). Immunosuppressive regulatory T cells are associated with aggressive breast cancer phenotypes: a potential therapeutic target. *Mod Pathol. 2008 Dec;21(12):1527-32.*

Bonner JA, Harari PM, Giralt J, Cohen RB, Jones CU, Sur RK, Raben D, Baselga J, Spencer SA, Zhu J, Youssoufian H, Rowinsky EK, Ang KK. (2010). Radiotherapy plus cetuximab for locoregionally advanced head and neck cancer: 5-year survival data from a phase 3 randomised trial, and relation between cetuximab-induced rash and survival. *Lancet Oncol. 2010 Jan;11(1):21-8.*

Bourquin C, Schmidt L, Lanz AL, Storch B, Wurzenberger C, Anz D, Sandholzer N, Mocikat R, Berger M, Poeck H, Hartmann G, Hornung V, Endres S. (2009). Immunostimulatory RNA oligonucleotides induce an effective antitumoral NK cell response through the Toll-like receptor 7. *J Immunol. 2009; 183: 6078-86*.

Bourquin C, Schreiber S, Beck S, Hartmann G, Endres S. (2005). Immunotherapy with dendritic cells and CpG oligonucleotides can be combined with chemotherapy without loss of efficacy in a mouse model of colon cancer. *Int J Cancer. 2005; 188: 2790-5.*

Brunkow ME, Jeffery EW, Hjerrild KA, Paeper B, Clark LB, Yasayko SA, Wilkinson JE, Galas D, Ziegler SF, Ramsdell F. (2001). Disruption of a new forkhead/winged-helix protein, scurfin, results in the fatal lymphoproliferative disorder of the scurfy mouse. *Nat Genet. 2001 Jan;27(1):68-73.*

Bryda EC, Pearson M, Agca Y, Bauer BA. (2006). Method for detection and identification of multiple chromosomal integration sites in transgenic animals created with lentivirus. *Biotechniques. 2006 Dec;41(6):715-9.*

Burnet, F.M. (1970). The concept of immunological surveillance. Prog. Exp. *Tumor Res. 13, 1-27.*

Cederbom L, Hall H, Ivars F. (2000). CD4+CD25+ regulatory T cells down-regulate co-stimulatory molecules on antigen-presenting cells. *Eur J Immunol. 2000 Jun;30(6):1538-43.*

Chang YC, Madkan V, Cook-Norris R, Sra K, Tyring S. (2005). Current and potential uses of imiquimod. *South Med J. 2005 Sep;98(9):914-20.*

Coban C, Ishii KJ, Kawai T, Hemmi H, Sato S, Uematsu S, Yamamoto M, Takeuchi O, Itagaki S, Kumar N, Horii T, Akira S. (2005). Toll-like receptor 9 mediates innate immune activation by the malaria pigment hemozoin. *J Exp Med. 2005 Jan 3;201(1):19-25.*

Collison LW, Workman CJ, Kuo TT, Boyd K, Wang Y, Vignali KM, Cross R, Sehy D, Blumberg RS, Vignali DA. (2007). The inhibitory cytokine IL-35 contributes to regulatory T-cell function. *Nature. 2007 Nov 22;450(7169):566-9.*

Colombo MP, Piconese S. (2007). Regulatory-T-cell inhibition versus depletion: the right choice in cancer immunotherapy. *Nat Rev Cancer. 2007 Nov;7(11):880-7.*

Curiel TJ, Coukos G, Zou L, Alvarez X, Cheng P, Mottram P, Evdemon-Hogan M, Conejo-Garcia JR, Zhang L, Burow M, Zhu Y, Wei S, Kryczek I, Daniel B, Gordon A, Myers L, Lackner A, Disis ML, Knutson KL, Chen L, Zou W. (2004). Specific recruitment of regulatory T cells in ovarian carcinoma fosters immune privilege and predicts reduced survival. *Nat Med. 2004 Sep;10(9):942-9.*

Dannull J, Su Z, Rizzieri D, Yang BK, Coleman D, Yancey D, Zhang A, Dahm P, Chao N, Gilboa E, Vieweg J. (2005). Enhancement of vaccine-mediated antitumor immunity in cancer patients after depletion of regulatory T cells. *J Clin Invest. 2005 Dec;115(12):3623-33.*

Deaglio S, Dwyer KM, Gao W, Friedman D, Usheva A, Erat A, Chen JF, Enjyoji K, Linden J, Oukka M, Kuchroo VK, Strom TB, Robson SC. (2007). Adenosine generation catalyzed by CD39 and CD73 expressed on regulatory T cells mediates immune suppression. *J Exp Med. 2007 Jun 11;204(6):1257-65.*

Doyle S, Vaidya S, O'Connell R, Dadgostar H, Dempsey P, Wu T, Rao G, Sun R, Haberland M, Modlin R, Cheng G. (2002). IRF3 mediates a TLR3/TLR4-specific antiviral gene program. *Immunity. 2002 Sep;17(3):251-63.*

Dunn GP, Old LJ, Schreiber RD. (2004). The three Es of cancer immunoediting. *Annu Rev Immunol. 22, 329-360.*

Dunn GP, Bruce AT, Ikeda H, Old LJ, Schreiber RD. (2002). Cancer immunoediting: from immunosurveillance to tumor escape. *Nat Immunol. 3, 991-998.*

Euhus DM, Hudd C, LaRegina MC, Johnson FE. (1986). Tumor measurement in the nude mouse. *J Surg Oncol 1986, 31:229-234.*

Faget J, Biota C, Bachelot T, Gobert M, Treilleux I, Goutagny N, Durand I, Léon-Goddard S, Blay JY, Caux C, Ménétrier-Caux C. (2011). Early detection of tumor cells by innate immune cells leads to T(reg) recruitment through CCL22 production by tumor cells. *Cancer Res. 2011 Oct 1;71(19):6143-52.*

Fallarino F, Grohmann U, Hwang KW, Orabona C, Vacca C, Bianchi R, Belladonna ML, Fioretti MC, Alegre ML, Puccetti P. (2003). Modulation of tryptophan catabolism by regulatory T cells. *Nat Immunol. 2003 Dec;4(12):1206-12.*

Foss FM. (2000). DAB(389)IL-2 (ONTAK): a novel fusion toxin therapy for lymphoma. *Clin Lymphoma. 2000 Sep;1(2):110-6*

Gao Q, Qiu SJ, Fan J, Zhou J, Wang XY, Xiao YS, Xu Y, Li YW, Tang ZY. (2007). Intratumoral balance of regulatory and cytotoxic T cells is associated with prognosis of hepatocellular carcinoma after resection. *J Clin Oncol. 2007 Jun 20;25(18):2586-93.*

Gay NJ, Gangloff M, Weber AN. (2006). Toll-like receptors as molecular switches. *Nat Rev Immunol. 2006 Sep;6(9):693-8.*

Gitlin L, Barchet W, Gilfillan S, Cella M, Beutler B, Flavell RA, Diamond MS, Colonna M. (2006). Essential role of mda-5 in type I IFN responses to polyri boinosinic:polyribocytidylic acid and encephalomyocarditis picornavirus. *Proc Natl Acad Sci U S A. 2006 May 30;103(22):8459-64.*

Gobert M, Treilleux I, Bendriss-Vermare N, Bachelot T, Goddard-Leon S, Arfi V, Biota C, Doffin AC, Durand I, Olive D, Perez S, Pasqual N, Faure C, Ray-Coquard I, Puisieux A, Caux C, Blay JY, Ménétrier-Caux C. (2009). Regulatory T cells recruited through CCL22/CCR4 are selectively activated in lymphoid infiltrates surrounding primary breast tumors and lead to an adverse clinical outcome. *Cancer Res. 2009 Mar 1;69(5):2000-9.*

Godiska R, Chantry D, Raport CJ, Sozzani S, Allavena P, Leviten D, Mantovani A, Gray PW. (1997). Human macrophage-derived chemokine (MDC), a novel chemoattractant for monocytes, monocyte-derived dendritic cells, and natural killer cells. *J Exp Med. 1997 May 5;185(9):1595-604.*

Gossen M and Bujard H. (1992). Tight Control of Gene Expression in Mammalian Cells by Tetracycline Responsive Promoters. *Proc Natl Acad Sci. USA 89, 5547-5551.*

Grossman WJ, Verbsky JW, Tollefsen BL, Kemper C, Atkinson JP, Ley TJ. 2004. Differential expression of granzymes A and B in human cytotoxic lymphocyte subsets and T regulatory cells. *Blood. 2004 Nov 1;104(9):2840-8.*

Hara M, Kingsley CI, Niimi M, Read S, Turvey SE, Bushell AR, Morris PJ, Powrie F, Wood KJ. (2001). IL-10 is required for regulatory T cells to mediate tolerance to alloantigens in vivo. *J Immunol. 2001 Mar 15;166(6):3789-96.*

Haring JS, Badovinac VP, Harty JT. (2006). Inflaming the CD8+ T cell response. *Immunity. 2006; 25: 19-29.*

Hayashi F, Smith KD, Ozinsky A, Hawn TR, Yi EC, Goodlett DR, Eng JK, Akira S, Underhill DM, Aderem A. (2001). The innate immune response to bacterial flagellin is mediated by Toll-like receptor 5. *Nature. 2001 Apr 26;410(6832):1099-103.*

Heckelsmiller K, Rall K, Beck S, Schlamp A, Seiderer J, Jahrsdörfer B, Krug A, Rothenfusser S, Endres S, Hartmann G. (2002). Peritumoral CpG DNA elicits a coordinated response of CD8 T cells and innate effectors to cure established tumors in a murine colon carcinoma model. *J Immunol. 2002 Oct 1;169(7):3892-9.*

Heil F, Hemmi H, Hochrein H, Ampenberger F, Kirschning C, Akira S, Lipford G, Wagner H, Bauer S. (2004). Species-specific recognition of single-stranded RNA via toll-like receptor 7 and 8. *Science. 2004 Mar 5;303(5663):1526-9.*

Hemmi H, Takeuchi O, Kawai T, Kaisho T, Sato S, Sanjo H, Matsumoto M, Hoshino K, Wagner H, Takeda K, Akira S. (2000). A Toll-like receptor recognizes bacterial DNA. *Nature. 2000 Dec 7;408(6813):740-5.*

Hertzog PJ, O'Neill LA, Hamilton JA. (2003). The interferon in TLR signaling: more than just antiviral. *Trends Immunol. 2003 Oct;24(10):534-9*.

Hiraoka N, Onozato K, Kosuge T, Hirohashi S. (2006). Prevalence of FOXP3+ regulatory T cells increases during the progression of pancreatic ductal adenocarcinoma and its premalignant lesions. *Clin Cancer Res. 2006 Sep 15;12(18):5423-34.*

Hodi FS, O'Day SJ, McDermott DF, Weber RW, Sosman JA, Haanen JB, Gonzalez R, Robert C, Schadendorf D, Hassel JC, Akerley W, van den Eertwegh AJ, Lutzky J, Lorigan P, Vaubel JM, Linette GP, Hogg D, Ottensmeier CH, Lebbé C, Peschel C, Quirt I, Clark JI, Wolchok JD, Weber JS, Tian J, Yellin MJ, Nichol GM, Hoos A, Urba WJ. (2010). Improved survival with ipilimumab in patients with metastatic melanoma. *N Engl J Med. 2010 Aug 19;363(8):711-23.*

Hori S, Nomura T, Sakaguchi S. (2003). Control of regulatory T cell development by the transcription factor Foxp3. *Science. 2003 Feb 14;299(5609):1057-61.*

Houot R, Levy R. (2009). T-cell modulation combined with intratumoral CpG cures lymphoma in a mouse model without the need for chemotherapy. *Blood. 2009 Apr 9;113(15):3546-52.*

Huang CT, Workman CJ, Flies D, Pan X, Marson AL, Zhou G, Hipkiss EL, Ravi S, Kowalski J, Levitsky HI, Powell JD, Pardoll DM, Drake CG, Vignali DA. (2004). Role of LAG-3 in regulatory T cells. *Immunity. 2004 Oct;21(4):503-13.*

Iellem A, Mariani M, Lang R, Recalde H, Panina-Bordignon P, Sinigaglia F, D'Ambrosio D. (2001). Unique chemotactic response profile and specific

expression of chemokine receptors CCR4 and CCR8 by CD4(+)CD25(+) regulatory T cells. *J Exp Med. 2001 Sep 17;194(6):847-53.*

Imai T, Chantry D, Raport CJ, Wood CL, Nishimura M, Godiska R, Yoshie O, Gray PW. (1998). Macrophage-derived chemokine is a functional ligand for the CC chemokine receptor 4. *J Biol Chem. 1998 Jan 16;273(3):1764-8.*

Ishida T, Ishii T, Inagaki A, Yano H, Komatsu H, Iida S, Inagaki H, Ueda R. (2006). Specific recruitment of CC chemokine receptor 4-positive regulatory T cells in Hodgkin lymphoma fosters immune privilege. *Cancer Res. 2006 Jun 1;66(11):5716-22.*

Ishida T, Ueda R. (2006). *CCR4 as a novel molecular target for immunotherapy of cancer. Cancer Sci. 2006 Nov;97(11):1139-46.*

Iwasaki A, Medzhitov R. (2004). Toll-like receptor control of the adaptive immune responses. *Nat Immunol. 2004 Oc*t;5(10):987-95.

Jones E, Dahm-Vicker M, Simon AK, Green A, Powrie F, Cerundolo V, Gallimore A. (2002). Depletion of CD25+ regulatory cells results in suppression of melanoma growth and induction of autoreactivity in mice. *Cancer Immun. 2002 Feb 22;2:1.*

June CH (2007). Adoptive T cell therapy for cancer in the clinic. *J Clin Invest. 117 (6): 1466-76.*

Karapetis CS, Khambata-Ford S, Jonker DJ, O'Callaghan CJ, Tu D, Tebbutt NC, Simes RJ, Chalchal H, Shapiro JD, Robitaille S, Price TJ, Shepherd L, Au HJ, Langer C, Moore MJ, Zalcberg JR. (2008). K-ras mutations and benefit from cetuximab in advanced colorectal cancer. *N Engl J Med. 2008 Oct 23;359(17):1757-65.*

Kanzler H, Barrat FJ, Hessel EM, Coffman RL. (2007). Therapeutic targeting of innate immunity with Toll-like receptor agonists and antagonists. *Nat Med. 2007 May;13(5):552-9.*

Kawai T, Akira S. (2006). Innate immune recognition of viral infection. *Nat Immunol. 2006 Feb;7(2):131-7.*

Kirkwood JM, Butterfield LH, Tarhini AA, Zarour H, Kalinski P, Ferrone S. (2012). Immunotherapy of cancer in 2012. *CA Cancer J Clin. 2012 Sep-Oct;62(5):309-35.*

Kirkwood JM, Richards T, Zarour HM, Sosman J, Ernstoff M, Whiteside TL, Ibrahim J, Blum R, Wieand S, Mascari R. (2002). Immunomodulatory effects of high-dose and low-dose interferon alpha2b in patients with high-risk resected melanoma: the E2690 laboratory corollary of intergroup adjuvant trial E1690. *Cancer. 2002 Sep 1;95(5):1101-12.*

Knutson KL, Dang Y, Lu H, Lukas J, Almand B, Gad E, Azeke E, Disis ML. (2006). IL-2 immunotoxin therapy modulates tumor-associated regulatory T cells and leads to lasting immune-mediated rejection of breast cancers in neu-transgenic mice. *J Immunol. 2006 Jul 1;177(1):84-91.*

Kobayashi N, Hiraoka N, Yamagami W, Ojima H, Kanai Y, Kosuge T, Nakajima A, Hirohashi S. (2007). FOXP3+ regulatory T cells affect the development and progression of hepatocarcinogenesis. *Clin Cancer Res. 2007 Feb 1;13(3):902-11.*

Krieg AM. (2008). Toll-like receptor 9 (TLR9) agonists in the treatment of cancer. *Oncogene. 2008; 27: 161-7.*

Krown SE, Burk MW, Kirkwood JM, Kerr D, Morton DL, Oettgen HF. (1984). Human leukocyte (alpha) interferon in metastatic malignant melanoma: the American Cancer Society phase II trial. *Cancer Treat Rep. 1984 May;68(5):723-6.*

Kurt-Jones EA, Popova L, Kwinn L, Haynes LM, Jones LP, Tripp RA, Walsh EE, Freeman MW, Golenbock DT, Anderson LJ, Finberg RW. (2000). Pattern recognition receptors TLR4 and CD14 mediate response to respiratory syncytial virus. *Nat Immunol. 2000 Nov;1(5):398-401.*

Kwon YM, Ricke SC. (2000). Efficient amplification of multiple transposon-flanking sequences. *J Microbiol Methods. 2000 Aug;41(3):195-9.*

Lanzavecchia A, Sallusto F. (2000). Dynamics of T lymphocyte responses: intermediates, effectors, and memory cells. *Science. 2000 Oct 6;290(5489):92-7.*

Lemaitre B, Nicolas E, Michaut L, Reichhart JM, Hoffmann JA. (1997). The dorsoventral regulatory gene cassette spätzle/Toll/cactus controls the potent antifungal response in Drosophila adults. *Cell. 1996 Sep 20;86(6):973-83.*

Letterio JJ, Roberts AB. (1998). Regulation of immune responses by TGF-beta. *Annu Rev Immunol. 1998;16:137-61.*

Liyanage UK, Moore TT, Joo HG, Tanaka Y, Herrmann V, Doherty G, Drebin JA, Strasberg SM, Eberlein TJ, Goedegebuure PS, Linehan DC. (2002). Prevalence of regulatory T cells is increased in peripheral blood and tumor microenvironment of patients with pancreas or breast adenocarcinoma. *J Immunol. 2002 Sep 1;169(5):2756-61.*

Lund J, Sato A, Akira S, Medzhitov R, Iwasaki A. (2003). Toll-like receptor 9- mediated recognition of Herpes simplex virus-2 by plasmacytoid dendritic cells. *J Exp Med. 2003 Aug 4;198(3):513-20.*

Marley GM, Doyle LA, Ordóñez JV, Sisk A, Hussain A, Yen RW. (1989). Potentiation of interferon induction of class I major histocompatibility complex antigen expression by human tumor necrosis factor in small cell lung cancer cell lines. *Cancer Res. 1989 Nov 15;49(22):6232-6.*

Matsumoto M, Seya T. (2008). TLR3: interferon induction by double-stranded RNA including poly(I:C). *Adv Drug Deliv Rev. 2008 Apr 29;60(7):805-12.*

Mayordomo JI, Loftus DJ, Sakamoto H, De Cesare CM, Appasamy PM, Lotze MT, Storkus WJ, Appella E, DeLeo AB. (1996). Therapy of murine tumors with p53 wild-type and mutant sequence peptide-based vaccines. J *Exp Med. 1996 Apr 1;183(4):1357-65.*

Medzhitov R, Preston-Hurlburt P, Janeway CA Jr. (1997). A human homologue of the Drosophila Toll protein signals activation of adaptive immunity. *Nature. 1997 Jul 24;388(6640):394-7.*

Melichar B, Procházková-Študentová H, Vitásková D. (2012). Bevacizumab in combination with IFN-a in metastatic renal cell carcinoma: the AVOREN trial. *Expert Rev Anticancer Ther. 2012 Oct;12(10):1253-62.*

Meylan E, Tschopp J, Karin M. (2006). Intracellular pattern recognition receptors in the host response. *Nature. 2006 Jul 6;442(7098):39-44.*

Minasian LM, Motzer RJ, Gluck L, Mazumdar M, Vlamis V, Krown SE. (1993). Interferon alfa-2a in advanced renal cell carcinoma: treatment results and survival in 159 patients with long-term follow-up. *J Clin Oncol. 1993 Jul;11(7):1368-75.*

Mizukami Y, Kono K, Kawaguchi Y, Akaike H, Kamimura K, Sugai H, Fujii H. (2006). CCL17 and CCL22 chemokines within tumor microenvironment are related to accumulation of Foxp3+ regulatory T cells in gastric cancer. *Int J Cancer. 2008 May 15;122(10):2286-93.*

Moynagh PN. (2005). TLR signalling and activation of IRFs: revisiting old friends from the NF-kappaB pathway. *Trends Immunol. 2005 Sep;26(9):469-76.*

Müller U, Steinhoff U, Reis LF, Hemmi S, Pavlovic J, Zinkernagel RM, Aguet M. (1994). Functional role of type I and type II interferons in antiviral defense. *Science. 1994 Jun 24;264(5167):1918-21.*

Naito Y, Saito K, Shiiba K, Ohuchi A, Saigenji K, Nagura H, Ohtani H. (1998). CD8+ T cells infiltrated within cancer cell nests as a prognostic factor in human colorectal cancer. *Cancer Res. 1998 Aug 15;58(16):3491-4.*

Onizuka S, Tawara I, Shimizu J, Sakaguchi S, Fujita T, Nakayama E. (1999). Tumor rejection by in vivo administration of anti-CD25 (interleukin-2 receptor alpha) monoclonal antibody. *Cancer Res. 1999 Jul 1;59(13):3128-33.*

Ozinsky A, Underhill DM, Fontenot JD, Hajjar AM, Smith KD, Wilson CB, Schroeder L, Aderem A. (2000). The repertoire for pattern recognition of pathogens by the innate immune system is defined by cooperation between tolllike receptors. *Proc Natl Acad Sci USA. 2000 Dec 5;97(25):13766-71.*

Paquette RL, Hsu NC, Kiertscher SM, Park AN, Tran L, Roth MD, Glaspy JA. (1998). Interferon-alpha and granulocyte-macrophage colony-stimulating factor differentiate peripheral blood monocytes into potent antigen-presenting cells. *J Leukoc Biol. 1998 Sep;64(3):358-67.*

Penna G, Vulcano M, Sozzani S, Adorini L. (2002). Differential migration behavior and chemokine production by myeloid and plasmacytoid dendritic cells. *Hum Immunol. 2002 Dec;63(12):1164-71.*

Petersen RP, Campa MJ, Sperlazza J, Conlon D, Joshi MB, Harpole DH Jr, Patz EF Jr. (2006). Tumor infiltrating Foxp3+ regulatory T-cells are associated with recurrence in pathologic stage I NSCLC patients. *Cancer. 2006 Dec 15;107(12):2866-72.*

Phan GQ, Yang JC, Sherry RM, Hwu P, Topalian SL, Schwartzentruber DJ, Restifo NP, Haworth LR, Seipp CA, Freezer LJ, Morton KE, Mavroukakis SA, Duray PH, Steinberg SM, Allison JP, Davis TA, Rosenberg SA. (2003). Cancer regression and autoimmunity induced by cytotoxic T lymphocyte-associated antigen 4 blockade in patients with metastatic melanoma. *Proc Natl Acad Sci U S A. 2003 Jul 8;100(14):8372-7.*

Poeck H, Besch R, Maihoefer C, Renn M, Tormo D, Morskaya SS, Kirschnek S, Gaffal E, Landsberg J, Hellmuth J, Schmidt A, Anz D, Bscheider M, Schwerd T, Berking C, Bourquin C, Kalinke U, Kremmer E, Kato H, Akira S, Meyers R, Häcker G, Neuenhahn M, Busch D, Ruland J, Rothenfusser S, Prinz M, Hornung V, Endres S, Tüting T, Hartmann G. (2008). 5'-Triphosphate-siRNA: turning gene silencing and Rig-I activation against melanoma. *Nat Med. 2008 Nov;14(11):1256-63.*

Poltorak A, He X, Smirnova I, Liu MY, Van Huffel C, Du X, Birdwell D, Alejos E, Silva M, Galanos C, Freudenberg M, Ricciardi-Castagnoli P, Layton B, Beutler B. (1998). Defective LPS signaling in C3H/HeJ and C57BL/10ScCr mice: mutations in Tlr4 gene. *Science. 1998 Dec 11;282(5396):2085-8.*

Proost P, Struyf S, Schols D, Opdenakker G, Sozzani S, Allavena P, Mantovani A, Augustyns K, Bal G, Haemers A, Lambeir AM, Scharpé S, Van Damme J, De Meester I. (1999). Truncation of macrophage-derived chemokine by CD26/ dipeptidyl-peptidase IV beyond its predicted cleavage site affects chemotactic activity and CC chemokine receptor 4 interaction. *J Biol Chem. 1999 Feb 12;274(7):3988-93.*

Raman D, Baugher PJ, Thu YM, Richmond A. (2007). Role Of Chemokines In Tumor Growth. *Cancer Lett. 2007 October 28; 256(2): 137–165.*

Read S, Malmström V, Powrie F. (2000). Cytotoxic T lymphocyte-associated antigen 4 plays an essential role in the function of CD25(+)CD4(+) regulatory cells that control intestinal inflammation. *J Exp Med. 2000 Jul 17;192(2):295-302.*

Roach JC, Glusman G, Rowen L, Kaur A, Purcell MK, Smith KD, Hood LE, Aderem A. (2005). The evolution of vertebrate Toll-like receptors. *Proc Natl Acad Sci U S A. 2005 Jul 5;102(27):9577-82.*

Rosenberg SA, Yannelli JR, Yang JC, Topalian SL, Schwartzentruber DJ, Weber JS, Parkinson DR, Seipp CA, Einhorn JH, White DE. (1994). Treatment of patients with metastatic melanoma with autologous tumor-infiltrating lymphocytes and interleukin 2. *J Natl Cancer Inst. 1994 Aug 3;86(15):1159-66.*

Rossi D, Zlotnik A. (2000). The biology of chemokines and their receptors. *Annu Rev Immunol. 2000;18:217-42.*

Sakaguchi S. (2005). Naturally arising Foxp3-expressing CD25+CD4+ regulatory T cells in immunological tolerance to self and non-self. *Nat Immunol. 2005 Apr;6(4):345-52.*

Sallusto F, Palermo B, Lenig D, Miettinen M, Matikainen S, Julkunen I, Forster R, Burgstahler R, Lipp M, Lanzavecchia A. (1999). Distinct patterns and kinetics of chemokine production regulate dendritic cell function. *Eur J Immunol. 1999 May;29(5):1617-25.*

Savarin-Vuaillat C., Ransohoff RM. (2007). Chemokines and chemokine receptors in neurological disease: raise, retain, or reduce? *Neurotherapeutics. 2007 Oct;4(4):590-601.*

Schaniel C, Pardali E, Sallusto F, Speletas M, Ruedl C, Shimizu T, Seidl T, Andersson J, Melchers F, Rolink AG, Sideras P. (1998). Activated murine B lymphocytes and dendritic cells produce a novel CC chemokine which acts selectively on activated T cells. *J Exp Med. 1998 Aug 3;188(3):451-63.*

Schoenemeyer A, Barnes BJ, Mancl ME, Latz E, Goutagny N, Pitha PM, Fitzgerald KA, Golenbock DT. (2005). The interferon regulatory factor, IRF5, is a central mediator of toll-like receptor 7 signaling. *J Biol Chem. 2005 Apr 29;280(17):17005-12.*

Shankaran, V., Ikeda, H., Bruce, A.T., White, J.M., Swanson, P.E., Old, L.J., and Schreiber, R.D. (2001). IFNγ and lymphocytes prevent primary tumour development and shape tumour immunogenicity. *Nature. 410, 1107-1111.*

Shortman K, Heath WR. (2001). Immunity or tolerance? That is the question for dendritic cells. *Nat Immunol. 2001 Nov;2(11):988-9.*

Shimizu J, Yamazaki S, Sakaguchi S. (1999). Induction of tumor immunity by removing CD25+CD4+ T cells: a common basis between tumor immunity and autoimmunity. *J Immunol. 1999 Nov 15;163(10):5211-8.*

Sivori S, Falco M, Della Chiesa M, Carlomagno S, Vitale M, Moretta L, Moretta A. (2004). CpG and double-stranded RNA trigger human NK cells by Toll-like receptors: induction of cytokine release and cytotoxicity against tumors and dendritic cells. *Proc Natl Acad Sci U S A. 2004; 101: 10116-21.*

Speiser DE, Liénard D, Rufer N, Rubio-Godoy V, Rimoldi D, Lejeune F, Krieg AM, Cerottini JC, Romero P. (2005). Rapid and strong human CD8+ T cell responses to vaccination with peptide, IFA, and CpG oligodeoxynucleotide 7909. *J Clin Invest 2005; 115: 739-46.*

Suntharalingam G, Perry MR, Ward S, Brett SJ, Castello-Cortes A, Brunner MD, Panoskaltsis N. (2006). Cytokine storm in a phase 1 trial of the anti-CD28 monoclonal antibody TGN1412. *N Engl J Med. 2006 Sep 7;355(10):1018-28.*

Sutmuller RP, van Duivenvoorde LM, van Elsas A, Schumacher TN, Wildenberg ME, Allison JP, Toes RE, Offringa R, Melief CJ. (2001). Synergism of cytotoxic T lymphocyte-associated antigen 4 blockade and depletion of CD25(+) regulatory T cells in antitumor therapy reveals alternative pathways for suppression of autoreactive cytotoxic T lymphocyte responses. *J Exp Med. 2001 Sep 17;194(6):823-32.*

Tada T, Ohzeki S, Utsumi K, Takiuchi H, Muramatsu M, Li XF, Shimizu J, Fujiwara H, Hamaoka T. (1991). Transforming growth factor-beta-induced inhibition of T cell function. Susceptibility difference in T cells of various phenotypes and functions and its relevance to immunosuppression in the tumor-bearing state. *J Immunol. 1991 Feb 1;146(3):1077-82.*

Tanaka H, Tanaka J, Kjaergaard J, Shu S. (2002). Depletion of CD4+ CD25+ regulatory cells augments the generation of specific immune T cells in tumor-draining lymph nodes. *J Immunother. 2002 May-Jun;25(3):207-17.*

Tang HL, Cyster JG. (1999). Chemokine Up-regulation and activated T cell attraction by maturing dendritic cells. *Science. 1999 Apr 30;284(5415):819-22.*

Takaoka A, Hayakawa S, Yanai H, Stoiber D, Negishi H, Kikuchi H, Sasaki S, Imai K, Shibue T, Honda K, Taniguchi T. (2003). Integration of interferon-alpha/beta signalling to p53 responses in tumour suppression and antiviral defence. *Nature. 2003 Jul 31;424(6948):516-23.*

Takaoka A, Taniguchi T. (2003). New aspects of IFN-alpha/beta signalling in immunity, oncogenesis and bone metabolism. *Cancer Sci. 2003 May;94(5):405-11.* Takaoka A, Taniguchi T. (2003). New aspects of IFN-alpha/beta signalling in immunity, oncogenesis and bone metabolism. *Cancer Sci. 2003 May;94(5):405-11.*

Takeuchi O, Kawai T, Mühlradt PF, Morr M, Radolf JD, Zychlinsky A, Takeda K, Akira S. (2001). Discrimination of bacterial lipoproteins by Toll-like receptor 6. *Int Immunol. 2001 Jul;13(7):933-40.*

Tarhini AA, Gogas H, Kirkwood JM. (2012). IFN-alpha in the treatment of melanoma. *J Immunol. 2012 Oct 15;189(8):3789-93.*

Theofilopoulos AN, Baccala R, Beutler B, Kono DH. (2005). Type I interferons (alpha/beta) in immunity and autoimmunity. *Annu Rev Immunol. 2005;23:307-36.*

Thornton AM, Shevach EM. (1998) CD4+CD25+ immunoregulatory T cells suppress polyclonal T cell activation in vitro by inhibiting interleukin 2 production. *J Exp Med. 1998 Jul 20;188(2):287-96.*

Tormo D, Ferrer A, Bosch P, Gaffal E, Basner-Tschakarjan E, Wenzel J, Tüting T. (2006). Therapeutic efficacy of antigen-specific vaccination and toll-like receptor stimulation against established transplanted and autochthonous melanoma in mice. *Cancer Res. 2006 May 15;66(10):5427-35.*

Tzankov A, Meier C, Hirschmann P, Went P, Pileri SA, Dirnhofer S. (2008). Correlation of high numbers of intratumoral FOXP3+ regulatory T cells with improved survival in germinal center-like diffuse large B-cell lymphoma, follicular lymphoma and classical Hodgkin's lymphoma. *Haematologica. 2008 Feb;93(2):193-200.*

van Maren WW, Jacobs JF, de Vries IJ, Nierkens S, Adema GJ. (2008). Toll-like receptor signalling on Tregs: to suppress or not to suppress? *Immunology. 2008; 124: 445-52.*

van Seters M, van Beurden M, ten Kate FJ, Beckmann I, Ewing PC, Eijkemans MJ, Kagie MJ, Meijer CJ, Aaronson NK, Kleinjan A, Heijmans-Antonissen C, Zijlstra FJ, Burger MP, Helmerhorst TJ. (2008). Treatment of vulvar intraepithelial neoplasia with topical imiquimod. *N Engl J Med. 2008 Apr 3;358(14):1465-73.*

Vogelstein B, and Gillespie D. (1979). Preparative and Analytical Purification of DNA from Agarose. *Proc Natl Acad Sci USA 76, 615-619.*

Vollmer J, Krieg AM. (2009). Immunotherapeutic applications of CpG oligodeoxynucleotide TLR9 agonists. *Adv Drug Deliv Rev 2009; 61: 195-204.*

Vulcano M, Albanesi C, Stoppacciaro A, Bagnati R, D'Amico G, Struyf S, Transidico P, Bonecchi R, Del Prete A, Allavena P, Ruco LP, Chiabrando C, Girolomoni G, Mantovani A, Sozzani S. (2001). Dendritic cells as a major source of macrophage-derived chemokine/CCL22 in vitro and in vivo. *Eur J Immunol. 2001 Mar;31(3):812-22.*

Wang W, Edington HD, Rao UN, Jukic DM, Land SR, Ferrone S, Kirkwood JM. (2007). Modulation of signal transducers and activators of transcription 1 and 3 signaling in melanoma by high-dose IFNalpha2b. *Clin Cancer Res. 2007 Mar 1;13(5):1523-31.*

Weber JS, Zarour H, Redman B, Trefzer U, O'Day S, van den Eertwegh AJ, Marshall E, Wagner S. (2009). Randomized phase 2/3 trial of CpG oligodeoxynucleotide PF-3512676 alone or with dacarbazine for patients with unresectable stage III and IV melanoma. *Cancer. 2009 Sep 1;115(17):3944-54*.

Williamson NA, Rossjohn J, Purcell AW. (2006). Tumors reveal their secrets to cytotoxic T cells. *Proc Natl Acad Sci U S A. 2006 Oct 3;103(40):14649-50.*

Woo EY, Chu CS, Goletz TJ, Schlienger K, Yeh H, Coukos G, Rubin SC, Kaiser LR, June CH. (2001). Regulatory CD4(+)CD25(+) T cells in tumors from patients with early-stage non-small cell lung cancer and late-stage ovarian cancer. *Cancer Res. 2001 Jun 15;61(12):4766-72.*

Yang ZZ, Novak AJ, Stenson MJ, Witzig TE, Ansell SM. (2006). Intratumoral CD4+CD25+ regulatory T-cell-mediated suppression of infiltrating CD4+ T cells in B-cell non-Hodgkin lymphoma. *Blood. 2006 May 1;107(9):3639-46.*

Yarovinsky F, Zhang D, Andersen JF, Bannenberg GL, Serhan CN, Hayden MS, Hieny S, Sutterwala FS, Flavell RA, Ghosh S, Sher A. (2005). TLR11 activation of dendritic cells by a protozoan profilin-like protein. *Science. 2005 Jun 10;308(5728):1626-9.*

Yu P, Lee Y, Liu W, Krausz T, Chong A, Schreiber H, Fu YX. (2005). Intratumor depletion of CD4+ cells unmasks tumor immunogenicity leading to the rejection of late-stage tumors. *J Exp Med. 2005 Mar 7;201(5):779-91.*

Zhou G, Drake CG, Levitsky HI. (2006). Amplification of tumor-specific regulatory T cells following therapeutic cancer vaccines. *Blood. 2006 Jan 15;107(2):628-36.*

Zlotnik A, Yoshie O. (2000). Chemokines: a new classification system and their role in immunity. *Immunity. 2000 Feb;12(2):121-7.*

Appendices

8. Appendices

8.1 PCR primer list

All primers were obtained from Metabion (Planegg, Germany) or Eurofins MWG (Ebersberg, Germany).

CCL22-For-EcoRI	5′-ATTAGAATTCATGGCTACCCTGCG-3′
CCL22-For-EcoRI	5′-ATTAGAATTCCTAGGACAGTTTATG-3′
CCL22-For-NotI	5′-ATT AGC GGC CGC ATG GCT ACC CTG CGT GTC-3′
CCL22-Rev-SalI	5′-ATT AGT CGA CCT AGG ACA GTT TAT GGA GTA G-3′
pTRE-Seq-For	5′-AGG CGT ATC ACG AGG CCC TTT CGT-3′
pTRE-Seq-Rev	5′-TAT TAC CGC CTT TGA GTG AGC TGA-3′
pTRE-tight-Rev	5′-CGC CTT TGA GTC AGC TGA TAC CGC TCG CCG-3′
TRE-F	5′-TAG GCG TGT ACG GTG GGA G-3′
TRE-R	5′-CTC TAC AAA TGT GGT ATG GC-3′
rtTA-F	5′-CAA TCG AGA TGC TGG ACA GG-3′
rtTA-R	5′-CAG CAG GCA GCA TAT CAA GG-3′
TDF	5′-GCCCTTAGTAGTGTCTGCTTTC-3′
TDR	5′-GCTCCTTGTTAGCAAGTCAGC-3′
NeoinF	5′-TTCGGCTATGACTGGGCACAACAG-3′
NeoinR	5′-TACTTTCTCGGCAGGAGCAAGGTG-3′

8.2 Quantitative real-time PCR primer list

All primers were obtained from Metabion (Planegg, Germany) or Eurofins MWG (Ebersberg, Germany). Primers and probes were designed by using the online Roche Assay Design Center.

RT-PCR-CCL22-For	5′-TCT TGC TGT GGC AAT TCA GA-3′
RT-PCR-CCL22-Rev	5′-GAG GGT GAC GGA TGT AGT CC-3′
Roche Probe for CCL22	#84
RT-PCR-CD11c-For	5′-ATG GAG CCT CAA GAC AGG AC-3′
RT-PCR-CD11c-Rev	5′-GGA TCT GGG ATG CTG AAA TC-3′
Roche Probe for CD11c	#20

RT-PCR-rtTA-For	5′-CTT TTC GGC CTG GAA CTA ATC-3′
RT-PCR-rtTA-Rev	5′-GCC GCT TTC GCA CTT TAG-3′
Roche Probe for rtTA	#80
RT-PCR-HPRT-For	5′-GGA GCG GTA GCA CCT CCT-3′
RT-PCR-HPRT-Rev	5′-CTG GTT CAT CAT CGC TAA TCA C-3′
Roche Probe for HPRT	#69

8.3 Sequencing data of pTRE-Tight CCL22 vector

Primer for Sequencing: pTRE-Seq-Rev; CCL22 sequence is shown in blue letters.

Clone 1

5′-CGTTTTCTGGGTGAGGCAAAAAAACAGAGCCAAATGCGCAAAAACGATA-
AGGGGCGGACACCGAATGGTGGATTACTCCATACTCTCCGTTTTCAATATT-
TATTGAAGCATTTATCAGGCTTATTGTCTCCATGAGCGGATACATATTT-
GAATGTATTTAGAAAAAATAAACAAATAGGGGTTCCGCGCACATTTCCCC-
GAAAAGTGCCACCTGACGTCTAAGAAACCATTATTATCATGACATTAACCTATA-
AAAATAGGCGTATCACGAGGCCCTTTCGTCTTCACTCGAGTTTACTCCCTAT-
CAGTGATAGAGAACGTATGTCGAGTTTACTCCCTATCAGTGATAGAGA-
ACGATGTCGAGTTTACTCCCTATCAGTGATAGAGAACGTATGTCGAGTT-
TACTCCCTATCAGTGATAGAGAACGTATGTCGAGTTTACTCCCTATCAGT-
GATAGAGAACGTATGTCGAGTTTATCCCTATCAGTGATAGAGAACGTATGTC-
GAGTTTACTCCCTATCAGTGATAGAGAACGTATGTCGAGGTAGGCGTGTACG-
GTGGGAGGCCTATATAAGCAGAGCTCGTTTAGTGAACCGTCAGATCGCCTG-
GAGAATTCGAGCTCGGTACCCGGGGATCCTCTAGTCAGCTGACGCGTGCTAGC-
GCGGCCGCATGGCTACCCTGCGTGTCCCACTCCTGGTGGCTCTCGTCCTTCTT-
GCTGTGGCAATTCAGACCTCTGATGCAGGTCCCTATGGTGCCAATGTGGAAGA-
CAGTATCTGCTGCCAGGACTACATCCGTCACCCTCTGCCATCACGTTTAGT-
GAAGGAGTTCTTCTGGACCTCAAAATCCTGCCGCAAGCCTGGCGTTGTTTT-
GATAACCGTCAAGAACCGAGATATCTGTGCCGATCCCAGGCAGGTCTGGGT-
GAAGAAGCTACTCCATAAACTGTCCTAGGTCGACGATATCTCTAGAGGATCATA-
ATCAGCCATACCACATTTGTAGAGGTTTTACTTGCTTTAAAAAACCTCCCA-
CACCTCCCCCTGAACCTGAAACATAAAATGAATGCAATTGTTGTTGTTAACTT-
GTTTATTGCAGCTTATAATGGTTACAAATAAAGCAATAGCATCACAAATTTCA-
CAAATAAAGCATTTTTTTCACTGCCTCGAGCTTCCTCGCTCACTGACTCGCTGC-
GCTCGTCGTCGCTGCGGCAGACCGG-3′

Clone 2

5’-CAGGGCGTTTTTCTGGTGAGGCAAAAATACGGAAGGCAAATGCG-
CAAAAGAATACGGCGACACGTAATGTGATACTCATACTCTCTTTTGCAC-
TATATTGAGCAATTTATCAAGGCTAATGTCTCATGAGCGGATACATATTC-
GATGTATTTAGAAAAATAAACAAATAGGGGTTCCGCGCACATTTCCCC-
GAAAAGTGCCACCTGACGTCTAAGAAAGCCATTATTATCATGACATTA-
ACCTATAAAAATAGGCGTATCACGAGGCCCTTTCGTCTTCACTCGAGTT-
TACTCCCTATCAGTGATAGAGAACGTATGTCGAGTTTACTCCCTATCAGT-
GATAGAGAACGATGTCGAGTTTACTCCCTATCAGTGATAGAGAACGTATGTC-
GAGTTTACTCCCTATCAGTGATAGAGAACGTATGTCGAGTTTACTCCCTATCAGT-
GATAGAGAACGTATGTCGAGTTTATCCCTATCAGTGATAGAGAACGTATGTC-
GAGTTTACTCCCTATCAGTGATAGAGAACGTATGTCGAGGTAGGCGTGTACG-
GTGGGAGGCCTATATAAGCAGAGCTCGTTTAGTGAACCGTCAGATCGCCTG-
GAGAATTCGAGCTCGGTACCCGGGGATCCTCTAGTCAGCTGACGCGTGCTAGC-
GCGGCCGCATGGCTACCCTGCGTGTCCCACTCCTGGTGGCTCTCGTCCTTCTT-
GCTGTGGCAATTCAGACCTCTGATGCAGGTCCCTATGGTGCCAATGTGGAAGA-
CAGTATCTGCTGCCAGGACTACATCCGTCACCCTCTGCCATCACGTTTAGT-
GAAGGAGTTCTTCTGGACCTCAAAATCCTGCCGCAAGCCTGGCGTTGTTTT-
GATAACCGTCAAGAACCGAGATATCTGTGCCGATCCCAGGCAGGTCTGGGT-
GAAGAAGCTACTCCATAAACTGTCCTAGGTCGACGATATCTCTAGAGGATCATA-
ATCAGCCATACCACATTTGTAGAGGTTTTACTTGCTTTAAAAAACCTCCCA-
CACCTCCCCCTGAACCTGAAACATAAAATGAATGCAATTGTTGTTGTTAACTT-
GTTTATTGCAGCTTATAATGGTTACAAATAAAGCAATAGCATCACAAATTTCA-
CAAATAAAGCATTTTTTTCACTGCCTCGAGCTTCCTCGCTCACTGACTCGCTGC-
GCTCGTCGTACGCTGCGGCAGACCGT-3’

8.4 Sequencing data of pTRE-CCL22 mouse

Primer for Sequencing: pTRE-Seq-Rev; TRE promoter sequence is shown in green letters, CCL22 sequence in light blue letters, MCS in black letters and SV40polyA sequence in blue letters. The observed transition point mutation (C ▯ T) is part of the MCS and is indicated by a red letter.

pTRE-CCL22 mouse

5’-CTCGAGTTTACTCCCTATCAGTGATAGAGAACGTATGTCGAGTTTACTCCCTAT-
CAGTGATAGAGAACGATGTCGAGTTTACTCCCTATCAGTGATAGAGAACGTAT-

GTCGAGTTTACTCCCTATCAGTGATAGAGAACGTATGTCGAGTTTACTCCCTAT-
CAGTGATAGAGAACGTATGTCGAGTTTATCCCTATCAGTGATAGAGAACGTAT-
GTCGAGTTTACTCCCTATCAGTGATAGAGAACGTATGTCGAGGTAGGCGTGTAC-
GGTGGGAGGCCTATATAAGCAGAGCTCGTTTAGTGAACCGTCAGATCGCCTG-
GAGAATTCGAGCTCGGTACCCGGGGATCCTCTAGTCAGCTGACGCGTGCTAGC-
GCGGCCGCATGGCTACCCTGCGTGTCCCACTCCTGGTGGCTCTCGTCCTTCTT-
GCTGTGGCAATTCAGACCTCTGATGCAGGTCCCTATGGTGCCAATGTGGAAGA-
CAGTATCTGCTGCCAGGACTACATCCGTCACCCTCTGCCATCACGTTTAGT-
GAAGGAGTTCTTCTGGACCTCAAAATCCTGCCGCAAGCCTGGCGTTGTTTT-
GATAACCGTCAAGAACCGAGATATCTGTGCCGATCCCAGGCAGGTCTGGGT-
GAAGAAGCTACTCCATAAACTGTCCTAGGTCGACGATAT **T** TCTAGAGGAT-
CATAATCAGCCATACCACATTTGTAGAGGTTTTACTTGCTTTAAAAAACCTCCCA-
CACCTCCCCCTGAACCTGAAACATAAAATGAATGCAATTGTTGTTGTTAACTT-
GTTTATTGCAGCTTATAATGGTTACAAATAAAGCAATAGCATCACAAATTTCA-
CAAATAAAGCATTTTTTTCACTGCCTCGAGCTTCCTCGCTCACT-3’

8.5 Abbreviations

A

APC	Antigen-presenting cell
aa	Amino acid

B

bp	Base pairs
BrdU	5’-Bromo-2’-deoxyuridine

C

CCL	Chemokine (C-C motif) ligand
CCR	Chemokine receptor
cDNA	Copy-desoxyribonucleic acid
CpG	Oligonucleotide with cytosine-(phosphate)-guanine motifs
CTLA-4	T lymphocyte-associated antigen 4

D

cDC	Conventional dendritic cell
DC	Dendritic cell
DMEM	Dulbecco's modified Eagle´s medium
DMSO	Dimethyl sulfoxide
DNA	Desoxyribonucleid acid
ds	Double-stranded
pDC	Plasmacytoid dendritic cell

E

EDTA	Ethylenediamine-tetraacetic acid
EGFR	Epidermal growth factor receptors
ELISA	Enzyme-linked immunosorbent assay

F

FACS	Fluorescent-activated cell sorting
FCS	Fetal calf serum

FITC	Fluorescein isocyanate
FOXP3	Forkhead box p3
FSC	Forward scatter

G

GITR	Glucocorticoid-induced TNF receptor family-related gene

H

HET	Heterogenous
HPRT	Hypoxanthine-guanine phosphoribosyltransferase
HRP	Horseradish peroxidase

I

IFN-α	Interferon-alpha
IFN-β	Interferon-beta
IFN-γ	Interferon-gamma
IFNAR	Interferon-receptor-type-1
IL	Interleukin
ip	Intraperitoneally
IRF	IFN regulatory factor

K

kb	Kilo base pairs
KO	Knockout

L

LacZ	β-Galactosidase Enzym
LAG-3	Lymphocyte activation gene-3
LN	Lymph node
LPS	Lipopolysaccharid

M

MACS	Magnetic-activated cell sorting
MAP	Activation of mitogen-activated protein

MCS	Multiple cloning site
MDA-5	Melanoma differentiation associated gene 5
MHC	Major histocompatibility complex
mRNA	Messenger ribonucleic acid
MyD88	Myeloid differentiation primary response gene 88

N

nd	Not determined
NEAA	Non-essential amino acids
NF-κB	Nuclear factor-κB
NK cell	Natural killer cell
NKT cells	Natural killer T cell
ns	Not significant

O

OD	Optical density

P

PAMP	Pathogen-associated molecular pattern
PBS	Dulbecco's Phosphate buffered saline
PCR	Polymerase chain reaction
PE	Phycoerythrin
PerCP	Peridinin chlorophyll protein
PP	Peyer's patches
PFA	Paraformaldehyde
PRR	Pattern-recognition receptor

Q

qRT-PCR	Quantitative real-time PCR

R

RCC	Renal cell carcinoma
RIG-I	Retinoic acid-inducible gene-I
RLR	RIG-I-like receptors

RPMI	Roswell Park Memorial Institute
RNA	Ribonucleic acid
RT	Room temperature

S

sc	Subcutaneous
SEM	Standard error of the mean
ss	Single-stranded
SSC	Sideward scatter

T

Teff	T effector cell
TGF-β	Transforming growth factor-beta
TH cell	T-helper cell
TIR	Toll/IL-1 receptor
TIRAP	TIR domain-containing adapter molecule
TLR	Toll-like receptors
TMB	Tetramethylbenzidin
TNF	Tumor necrosis factor
TRAM	TRIF-related adapter molecule
Treg	Regulatory T cell
TRIF	TIR-containing adapter inducing IFN-α

V

VLE	Very low endotoxin

W

wt	Wild-type

8.6 Publications

8.6.1 Original publications

Zoglmeier C, Bauer H, Nörenberg D, Wedekind G, Bittner P, Sandholzer N, **Rapp M**, Anz D, Endres S, Bourquin C. (2011). CpG blocks immunosuppression by myeloid-derived suppressor cells in tumor-bearing mice. *Clin Cancer Res. 2011 Apr 1;17(7):1765-75.*

Anz D, Mueller W, Golic M, Kunz WG, **Rapp M**, Koelzer VH, Ellermeier J, Ellwart JW, Schnurr M, Bourquin C, Endres S. (2011). CD103 is a hallmark of tumor-infiltrating regulatory T cells. *Int J Cancer. 2011 Nov 15;129(10):2417-26.*

Anz D*, **Rapp M***, Eiber S, Koelzer VH, Thaler R, Haubner S, Nagel S, Golic M, Bauernfeind F, Wurzenberger C, Radtke-Schuller S, Noessner E, Hornung V, Scholz C, Mayr D, Rothenfusser S, Endres S, Bourquin C. Suppression of CCL22 by Toll-like receptor agonists inhibits cancer growth in a type I interferon dependent manner. Manuscript in preparation 2013.
*Anz D. and Rapp M. contributed equally to this work.

8.6.2 Oral presentations

Rapp M. A novel doxycycline inducible chemokine over-expressing tumor model. 5th Annual Retreat, Graduiertenkolleg 1202, Sylvensteinsee, Germany, 2010

Rapp M. CCL22 - a potential mediator in tumor-induced immunosuppression 6th Annual Retreat, Graduiertenkolleg 1202, Schloss Fürstenried, Germany, 2011

Rapp M. TLR agonists prevent Treg infiltration of tumors by specifically inhibiting migration of regulatory T cells. LMU-Harvard Young Scientists' Forum, München, Germany, 2011

Rapp M. Suppression of CCL22 by TLR agonists inhibits cancer growth in a type I interferon dependent manner. 7th Annual Retreat, Graduiertenkolleg 1202, Frauenchiemsee, Germany, 2012

8.6.3 Poster presentations

Anz D, **Rapp M**, Scholz C, Endres S, Kirchner T, Bourquin C, Mayr D. In breast cancer a high ratio of tumor-infi ltrating intraepithelial CD8+ to FoxP3+ cells is unique for the medullary subtype. World Immune regulation Meeting IV, Davos, Switzerland, 2010

Anz D, Mueller W, Golic M, Kunz WG, **Rapp M**, Koelzer VH, Ellermeier J, Ellwart JW, Schnurr M, Bourquin C, Endres S. CD103 is a hallmark of tumor-infiltrating regulatory T cells. World Immune regulation Meeting V, Davos, Switzerland, 2010

Wiedemann G, **Rapp M**, Kriegl L, Mayr D, De Toni E, Gülberg V, Endres S, Anz D. Regulatory T cell-attracting chemokines in hepatocellular carcinoma. Falk symposium, Hamburg, Germany, 2012

Rapp M, Haubner S, Nagel S, Wiedemann G, Mayr D, Eiber S, Rothenfusser S, Bourquin C, Endres S, Anz D. CCL22 in murine and human tumors is derived from tumor-infi ltrating macrophages and dendritic cells. China Tregs 2012 Conference, Shanghai, China, 2012

8.7 Acknowledgements

First I would like to thank Prof. Dr. med. Stefan Endres for giving me the opportunity of working in the Division of Clinical Pharmacology as a member of the Graduiertenkolleg "Oligonukleotide in Zellbiologie und Therapie".

I also would like to gratefully and sincerely thank Dr. med. David Anz and Prof. Dr. med. Dr. rer. nat. Carole Bourquin for providing me with such an interesting research project and letting me participate in planning and implementation. Their constant personal encouragement and scientific input were truly inspiring.

Last but not least, I thank my fellow doctoral students and co-workers for all their help and support during the last three year.